1-1-2008

A novel RGBW pixel for LED displays

Neveen Shlayan
University of Nevada, Las Vegas

A NOVEL RGBW PIXEL FOR

LED DISPLAYS

by

Neveen Shlayan

Bachelor of Science
University of Nevada, Las Vegas
2006

A thesis submitted in partial fulfillment
of the requirements for the

Master of Science Degree in Electrical and Computer Engineering
Department of Electrical and Computer Engineering
Howard R. Hughes College of Engineering

Graduate College
University of Nevada, Las Vegas
December 2008

INFORMATION TO USERS

The quality of this reproduction is dependent upon the quality of the copy submitted. Broken or indistinct print, colored or poor quality illustrations and photographs, print bleed-through, substandard margins, and improper alignment can adversely affect reproduction.

In the unlikely event that the author did not send a complete manuscript and there are missing pages, these will be noted. Also, if unauthorized copyright material had to be removed, a note will indicate the deletion.

ProQuest LLC
789 E. Eisenhower Parkway
PO Box 1346
Ann Arbor, MI 48106-1346

UNLV
UNIVERSITY OF NEVADA LAS VEGAS

Thesis Approval

The Graduate College
University of Nevada, Las Vegas

November 10, 20 08

The Thesis prepared by

Neveen Shlayan

Entitled

A Novel RGBW Pixel for LED Displays

is approved in partial fulfillment of the requirements for the degree of

Master of Science in Electrical Engineering

Examination Committee Chair

Dean of the Graduate College

Examination Committee Member

Examination Committee Member

Graduate College Faculty Representative

ABSTRACT

A Novel RGBW Pixel for LED Displays

by

Neveen Shlayan

Dr. Rama Venkat, Examination Committee Chair
Professor of Electrical Engineering
University of Nevada, Las Vegas

In this work, a novel pixel configuration RGBW, consisting of red (R), green (G), blue (B), and white (W) LEDs, is employed and investigated for color generation. Energy consumption and various hues of new pixels are compared to standard pixels consisting of RGB LEDs. Human perception experiments are conducted in order to study the perceptual difference between the two architectures when the same colors are generated using RGBW vs. RGB. Power measurements for an 8x8 pixel LED display has demonstrated up to 49% power savings for gray scale, over 30% power savings for low saturated colors, and up to 12% for high saturated colors using RGBW as an alternative. Furthermore, human perception studies has shown that vast majority of test subjects could not distinguish between most colors displayed using RGB and RGBW showing that RGBW is an excellent substitute for RGB. Statistics has shown that 44% of test subjects found the colors in gray scale to be the same, whereas 82% and 95% of test subject found low saturated colors and high saturated colors, respectively, to be identical.

TABLE OF CONTENTS

LIST OF FIGURES

LIST OF TABLES

ACKNOWLEDGMENTS

I would like to acknowledge my advisor and committee chair, Dr. Rama Venkat, for his thesis guidance, the technical and editorial help and for being devoted to his students. I would also like to thank, Dr. Paolo Ginobbi, for the practical teaching and training of concepts and hardware implementation of the project. In addition, I would like to thank Dr. Ashok Singh for the statistical counseling and help. I would like to acknowledge, Dr. Emma Regentova and Dr. Mohamed Trabia, for being members in my committee. Last but not least, I would like to acknowledge TecnoVision for providing the LED Display and the Department of Energy support under grant # RF-06-PRD-001 (7156APP131).

CHAPTER 1

INTRODUCTION

Every year, the display industry introduces many innovations to improve quality and economy of displays. The factors, which contribute to the superiority of various displays, are: response time, size, weight, viewing angle, brightness, screen life, and power consumption. The current market places very high expectations in terms of the quality of the display. The limitations of the liquid crystal display (LCD), size and brightness, and that of the Plasma display, image retention and size [1] render them unsuitable for certain applications such as billboards and entertainment displays [2,3,4]. LED displays, which are perfect fit for such applications, just like any other technology have some issues, such as cost, power consumption, and achromatic point (AP) maintenance.

LEDs are semiconductor devices that are capable of fast switching with the addition of appropriate electronics [5]. Different types of LED displays were initially introduced in the early 70s such as LED array with silicon micro reflector and integrated circuits for driving LEDs. The reflector is formed on a silicon wafer by anisotropic chemical etching. LEDs on the unit are arrayed in a matrix structure and the brightness is controlled by the pulse width of the current into the LEDs [6]. In the other type of display, the LED chips are mounted on the driving circuits that allow holding and controlling of the selected LED currents. Integrated circuit drivers are superior in brightness to the silicon micro

reflector displays and therefore are still used for the current LED display technologies.

In the early seventies, when LED displays were first originated, red was the only color available. By the late seventies, the color variety became wider to include green, yellow, orange and red [7]. Solid state has witnessed significant advancements to improve LED's brightness by up to 40% per year [7]. Shuji Nakamura of Nichia Corporation of Japan demonstrated the first high-brightness blue LED based on InGaN which quickly led to the development of the first white LED, which is basically a blue LED with a phosphors coating to produce a white light. The mixture of yellow and blue lights produces a white light.

Advancements of LED technology tremendously improved LED display technology. The fact that obtaining light of the colors red, green, and blue was feasible, LED displays went through a revolutionary phase. RGB are monochromatic colors or centered about a single wavelength with a small bandwidth. The mixture of the three lights with the different possible intensities for each light results in a forth unique color perceptible to the human eye. The possible range of colors that can be produced using RGB is called the color gamut. Thus, LED display technology uses RGB LEDs to form a pixel in order to produce any color in the gamut. The LEDs in the display are connected to an integrated driver chip that controls each and every LED individually and hence the pixel.

In LEDs, colors are produced by a recombination process where electrons and holes are recombined. As a result, the electron falls into a lower energy level and the excess energy is released in a form of photons with a certain wavelength which determines the color to be perceived after the emission. This process is power consuming. There are many factors that affect the efficiency of LEDs such as the wavelength of the emitted

photon and the human visual perception. The human eye, for example, is more sensitive to green in day vision than red and blue. It is, however, more sensitive to blue in night vision. Taking these factors into consideration, efficiency of LED displays could be further improved.

Since LED's I-V characteristics are not identical due to manufacturing imperfections, usage, weather conditions, and heat dissipation, it is a challenge to maintain a uniform color throughout the display throughout its life time. The difference between the colors becomes more noticeable in gray scale or, in other words, when LEDs are at equal intensity. This may be noticed as different shades of the color displayed or as spots of discoloration at random locations on the display.

High cost is one of the disadvantages in LED displays due to the expensive process used. Thus, maintenance costs are one of the major issues of LED displays. Therefore, one of the purposes of this work is to increase the life time of LED displays as much as possible in order to avoid these maintenance costs.

The three major drawbacks identified in the current RGB LED display technology are: power consumption, degradation of display, and cost. In order to address these three issues, a new pixel architecture including a white LED in the traditional RGB LEDs configuration is proposed. A 5"x5" board containing RGBW LEDs placed in a square configuration is used for the investigation.

In chapter 2, a survey of different types of display technologies and the current state of the art advancements are presented. Theoretical foundation of this work is presented in chapter 3. Chapter 4 presents the design of the front end software and hardware. The proposed technology is introduced and discussed theoretically as well. Results and

discussions of human experiment and energy measurements are in chapter 5. Then conclusions and recommendations are in chapter 6.

CHAPTER 2

DIFFERENT DISPLAY TECHNOLOGIES

In this chapter, different display technologies with state of the art technological developments are presented. A detailed survey of LED technology and recent trends are also presented.

2.1 Liquid Crystal Display (LCD)

LCDs have come into prominence in the last few years because of their low power consumption and picture quality. LCDs are power efficient since they either reflect or transmit light efficiently [8]. Therefore, LCDs are very suitable for battery-powered electronics such as: cell phones, ipods, laptops, calculators, and digital watches.

In LCDs, every pixel is composed of a cell between two glass plates coated with a conductive material as shown in figure 2.1. The light utilized by the LCD display goes through a polarizer before going through the cell. The cell is basically filled with liquid crystal material which is a phase of matter over a certain temperature range. At the lowest end of the range, the material becomes crystalline with a set of optical and electrical properties; whereas, at the upper end of the range, this material becomes clear liquid with a different set of electrical and optical properties. However, within this range the material combines some of the optical properties of solids with the fluidity of liquids [8]. One of

the most important characteristic of the liquid crystal material is the rod shape of its molecule. These rods can take a certain orientation with respect to each other and to the surface of the cell. The most widely used orientation in LCD technology is twisted nematic. In nematic ordering, all the rod shaped molecules (directors) are parallel to each other. The direction of this ordering can be changed by applying an electric field to the liquid crystal material. A schematic Diagram illustrating the operation of an LCD cell is shown in Figures 2.1 a and b.

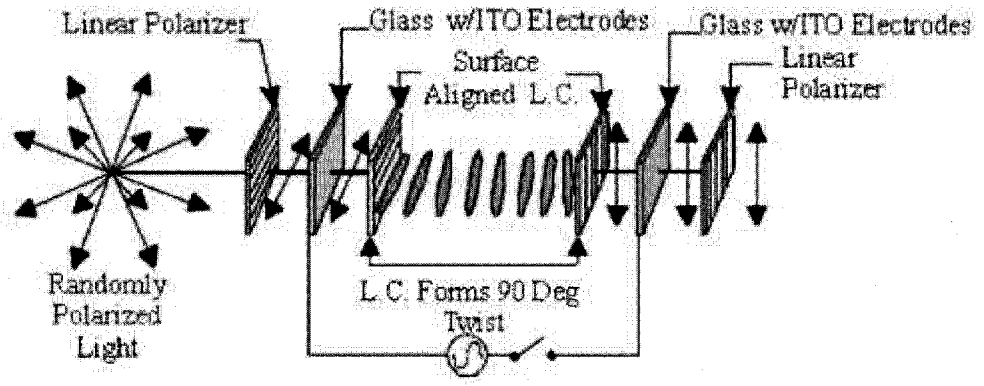

(a)

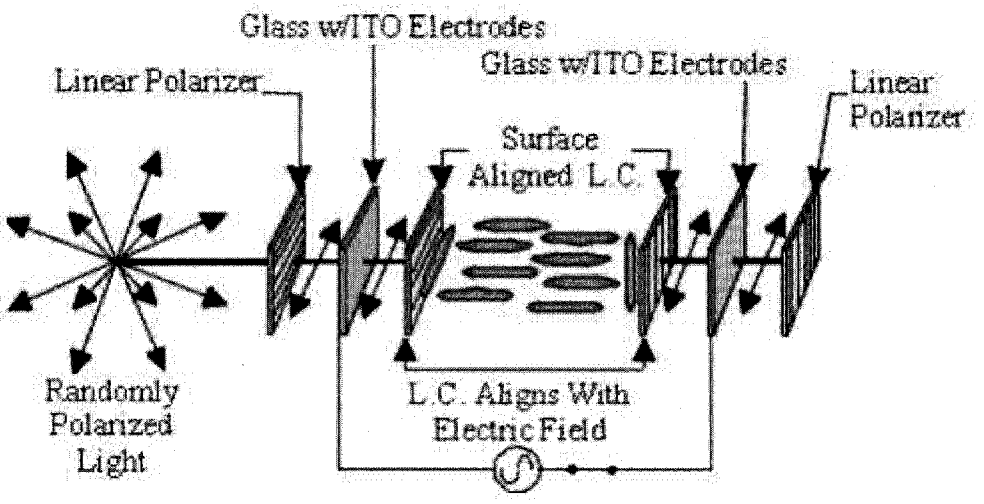

(b)

Figure 2.1 A schematic diagram showing a liquid crystal cell in the (a) off state (b) on state [9].

There are two types of LCDs: reflective and transmissive. The first of which utilizes front illumination. Most displays of the reflective type use ambient light with provision for secondary illumination such as an incandescent lamp or LED when ambient light becomes insufficient. On the other hand, the transmissive type requires rear illumination.

There are two types of architectures for LCD displays: passive matrix and active matrix. In passive-matrix addressed topology, each row or column of the display has a single electrical circuit. The pixels are addressed one at a time by row and column addresses. The pixel must retain its state between refreshes without the benefit of a steady electrical charge. This becomes less feasible as the number of pixels increases, since the response time will increase as well, resulting in a poor contrast which is typical of passive-matrix addressed LCDs.

Active matrix architecture results from adding a matrix of thin film transistors (TFT) to the polarizing and color filters. Each pixel is controlled by a single transistor. A schematic diagram showing the TFT active matrix array is shown in Figure 2.2. When a row line is activated, all the columns connect to the pixels in the selected row driving the appropriate voltage while the rest of the rows are electrically isolated which reduces cross talk. The row lines are activated in sequence during the refresh period in order to charge the capacitors that belong to each pixel with the desired amount given by the column voltage [10]. This method has largely improved the quality of LCD displays guaranteeing a brighter and sharper image than passive matrix. Most importantly, active matrix has significantly improved the response time.

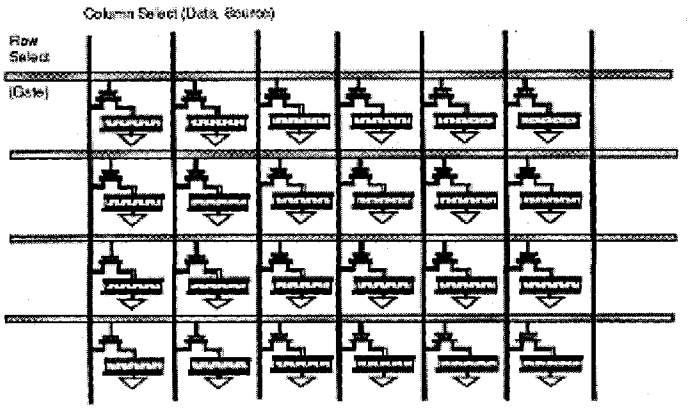

Figure 2.2. A schematic diagram showing simple TFT Active Matrix Array [11]

TFT technology, however, is very complex and the cost increases rapidly with increasing the area of the matrix [10]. Another disadvantage of TFT displays is that the transistor blocks part of the light-path which limits the resolution which requires a brighter backlight [10].

LCD technology, however, has its drawbacks such as low contrast ratio, image scaling, ghosting (resulting from low response time), limited viewing angle, fragile, and dead pixels. This limits their usage to certain application such as billboards. LCD displays are equipped with an illuminator called a backlight system disposed at the rear surface. Thus, the amount of light from the backlight which transmits through the liquid crystal panel is controlled by the liquid crystal panel in order to realize images, which makes it more challenging to obtain dark colors. Low contrast ratio is a result of the unwanted light leakage in dark areas and passive full-on backlight control [12]. LCD screens can only display native resolution which is the number of pixels in every vertical and horizontal line that make up the LCD matrix. Changing the resolution settings of the

display will cause it to use a reduced visible area of the screen or to extrapolate in which multiple pixels are blended together. This can result in a fuzzy image [13].

In an LCD, there are two different time responses describing two different transitions. Rising time response, which is the amount of time required to turn on the cell from an off-state and falling time response, which is the amount of time required to turn off the cell from an on-state. Rising time is much smaller than falling time. Thus, a blurring action will occur on bright moving images on black background or in other words ghosting effect.

Images in LCDs are produced by having a film that will turn on the desired shade of color when a current is applied to the pixel. This color can only be accurately represented when viewed straight on which could be problematic. The color tends to wash out when viewed further away from a perpendicular viewing angle [13].

2.1.1 Recent Trends in LCD Technology

LCD monitors are very desirable in the current market especially for applications like computer monitors, portable electronics, laptops, etc. Thus, recent market has been witnessing many competitors such as Gateway, Samsung, Dell, and Lenovo attempting to come up with the best LCD in the market by improving viewing angle, contrast ratio, resolution, and size.

Gateway has recently launched their XHD3000 monitor. It offers a wide-range of connectivity options along with bright picture and an up-scaler [14]. Then Samsung's brand new 743B offers a 1280x1024 resolution, fast 5ms response time and a 7000:1 contrast ratio [14]. Dell has recently developed an award winning LCD monitor sandwiched between layers of clear glass are significant advancements in LCD display;

protruding elegantly from the rear of the monitor are minimal speaker housings. All of the electronic wiring for the capacitive touch controls, digital camera, and the speakers has visible wire traces [15]. Lenovo has produced a 22" LCD monitor that offers a 1920 x 1200 native resolution [14].

2.2 Plasma Display

Plasma technology was invented at the University of Illinois in 1964 by Donald Bitzer, H. Gene Slottow, and graduate student Robert Willson [16]. Larry Weber developed the first prototype of a 60-inch plasma display that combines many of the industry's desirable features such as large size, high definition, and thickness.

Plasma has many characteristics that increased the demand for plasma technology in the display industry especially home entertainment. Plasma displays are bright, have a wide viewing angle, have a wide color gamut, and can be produced in large sizes, up to 150 inches diagonally [17]. Compared to the LCD, plasma displays have a better low luminance black level. The total thickness of a plasma display, including electronics, is less than 4 inches; the display panel by itself is only about 2.5 inches thick [17]. Power consumption differs with the brightness level of the image displayed, with bright scenes drawing significantly more power than darker ones. Nominal power rating is typically 400 watts for a 50-inch screen. Newer models (after 2006) consume 220 to 310 watts for a 50-inch display. The lifetime of the latest generation of plasma displays is estimated at 60,000 hours of actual display time [17].

Plasma displays are based on light generation. When an electrical current passes through gas, the electrons acquire a high kinetic energy, and when they collide with the

gas atoms, they transfer their kinetic energy to the atoms exciting them into energy levels above their ground state. Either direct or alternating currents can be used in order to generate an internal electric field. A plasma element is composed of a gas cavity with transparent electrodes on the outside of the containing dielectric layer as shown in Figure 2.3. The gas is normally neon that is electrically turned into plasma which, then, excites the phosphors to emit white light.

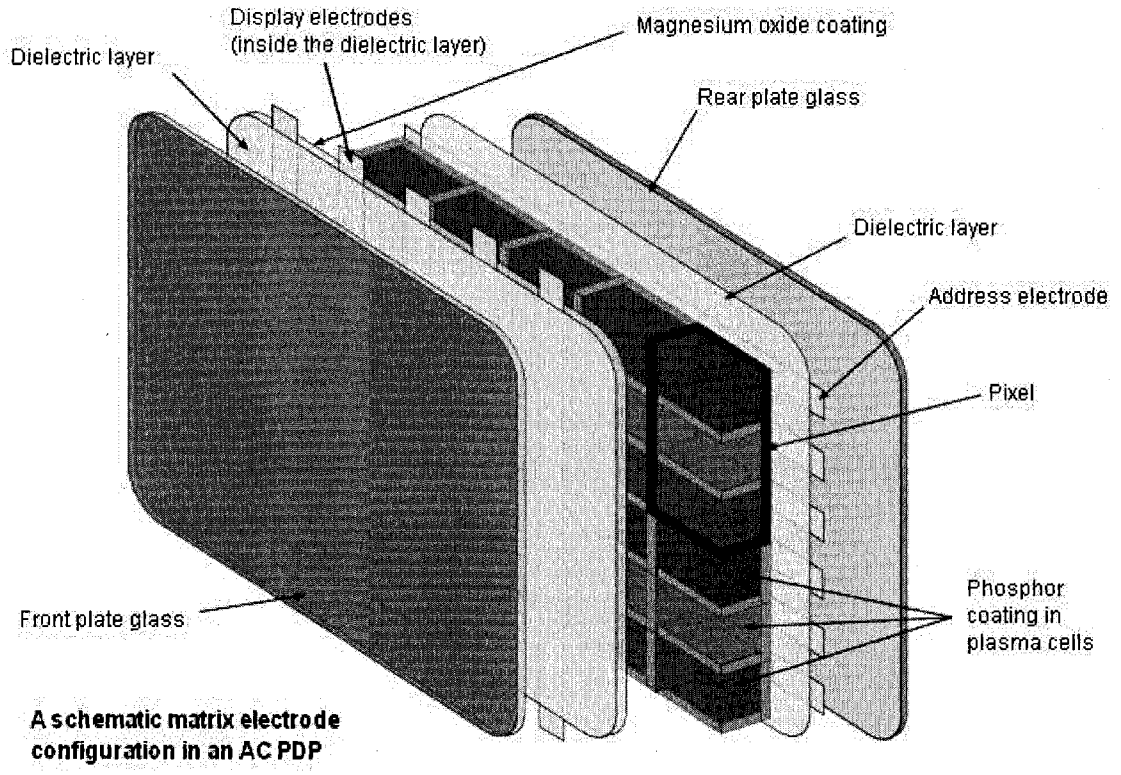

Figure 2.3. A schematic diagram showing a composition of plasma display panel [17]

The driving circuitry of the plasma display technology has been a major issue due to its complexity. To drive a plasma display, the driving circuit must apply high voltage and

high frequency pulses to the scan electrodes [18]. The address-electrodes are located under the cells perpendicular to the X and Y electrodes. A schematic diagram showing the 3-electrods of AC plasma display is shown in Figure 2.4. As mentioned, cells in a plasma display emit visible lights via a plasma discharge induced by a pseudo square alternating electric field applied between the X and Y electrodes [19]. For charging the panel capacitance and supporting the plasma discharge, a large amount of displacement and discharge current is required. Hence, it is necessary to use the switches that can cope with high peak and root mean square (RMS) currents, which means a high cost driving system [19].

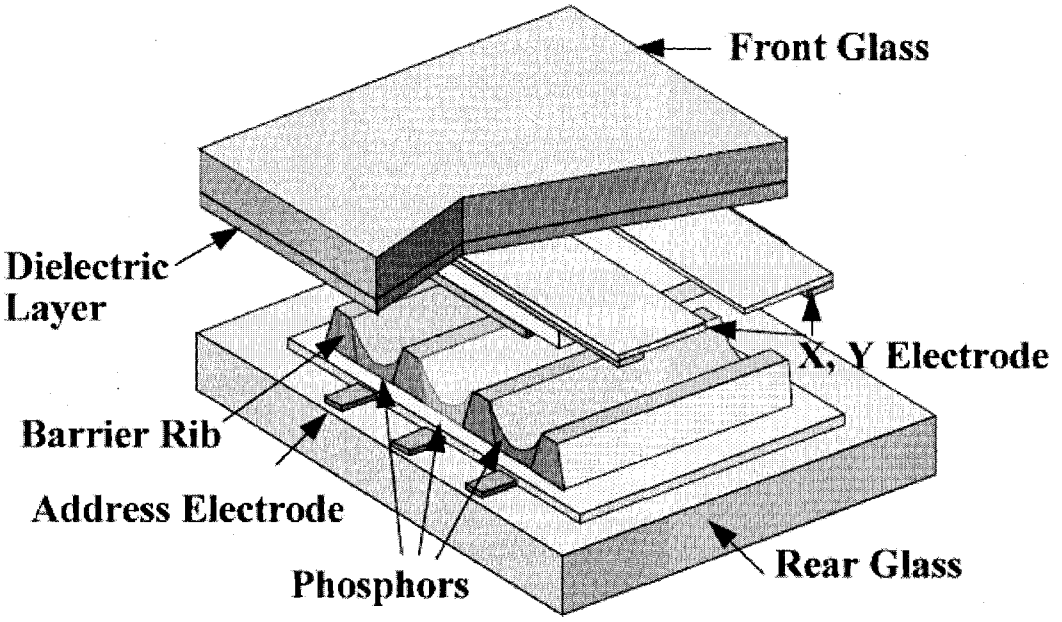

Figure 2.4. A schematic diagram showing the structure of the three-electrode AC plasma display [19].

Address Display period Separation (ADS) scheme as illustrated in Figure 5 that is a commonly used driving method for commercialized plasma display TV sets. In the ADS scheme, there are 9–11 subfields in one TV field of 1/60 or 1/50 second, and one subfield is divided into three operational periods such as reset, scan (or address), and sustain. Since the ADS scheme requires three different operations, conventional plasma display panel (PDP) schemes have three different circuit blocks corresponding to each operation [19]. For the sustain operation, a half bridge structure with energy recovery circuits (ERC) of the Weber type, which is based on an LC series resonance between an inductor and a panel capacitor, is typically used [19]. The ramp reset is widely adopted, which initializes RGB cells to have the same wall charge conditions by a weak gas regardless of the previous on/off state of cells. In the address period, scanning pulses from scan ICs are sequentially applied to the Y electrodes, and data pulses are given to the cells to be addressed while the scan switch Ysc is turned on to offer a negative scan voltage [19]. A circuit schematic for the panel driving system is shown in Figure 2.5.

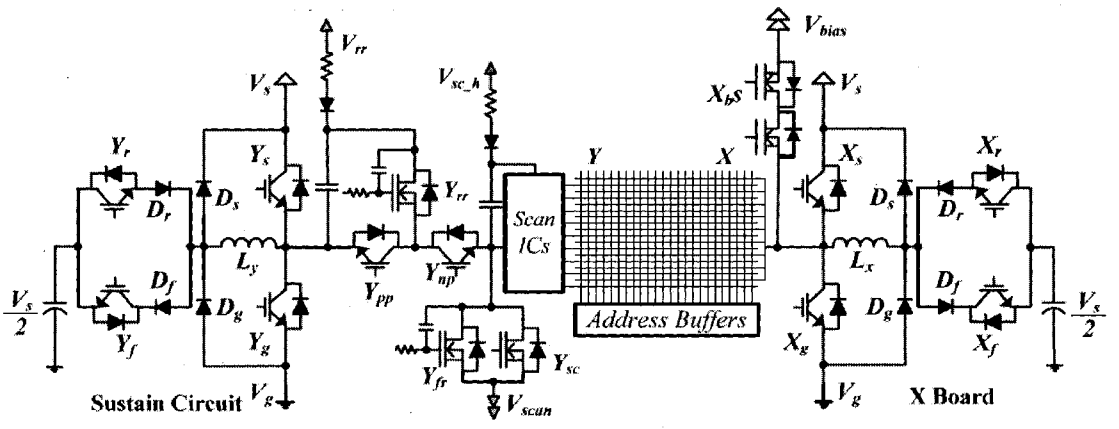

Figure 2.5. A schematic showing a PDP driving system [19].

Advantages of plasma display technology are the possibility of producing very large and thin screen, and very bright image and a wide viewing angle. Contrast ratios for plasma displays are as high as 30,000:1, which is a significant advantage of plasma technology over most other display technologies other than LED [19]. However, just like any other technology, plasma display technology has its challenges. Each cell on a plasma display has to be precharged before it is illuminated so that the cell would respond quickly enough. Due to precharging, the cells cannot achieve a true black [19]. Also, with phosphor-based electronic displays, the phosphor compounds, which emit the light, lose their capacity to emit light with use, which causes burn in [19]. When a group of pixels are run at high brightness for an extended period of time, a charge build-up in the pixel structure occurs, which results in a ghost image [19].

2.2.1 Current Trends in Plasma Technology

The size of plasma display has been one of the key advantages that attract electronic consumers to them. However, the complex and expensive circuitry that is involved in this technology is a major downside. Thus, most recent researchers and plasma manufacturers have been focused on reducing this aspect of plasma displays. Pioneer, Samsung and Panasonic have recently come up with the latest plasma display technology. Pioneer has developed a 50-inch plasma TV. The KURO PDP-5010FD is the best in cinematic image quality. The colors are rich and well-saturated, with great black levels [20]. The Pioneer TV is also packed with features, and an anti-glare screen coating helps reduce shine. The big downside is cost compared to other plasma TV sets [20]. The latest Samsung's 50-inch plasma HDTV has a great blend of image quality and value. Colors in Samsung PN50A550 are very accurate, and video processing is one of the best. However, Top

rated Pioneer and Panasonic plasma TVs have slightly deeper blacks [20]. Like most plasma TVs, the Samsung PN50A550 has a reflective screen, but reports say that glare is worse than most, which could pose a problem in bright rooms [20]. Panasonic's best 46-inch plasma TV when it comes to color accuracy, shadow detail and screen uniformity rank among the best [20].

2.3 LED Displays

In LED displays every pixel consists of three LEDs that are of the colors red, green, and blue, normally formed in a shape of a square as shown in Figure 2.6.a. These pixels are spaced evenly apart and are measured from center to center for absolute pixel resolution. There are two types of LED panels conventional, and surface mounted device panel (SMD) panels. Conventional panels use discrete LEDs (individually mounted LEDs) and are usually used for outdoor displays and sometimes indoor. Most indoor screens on the market are built using SMD technology that has a minimum brightness of 600 candelas per square meter. SMD technology is currently reaching the outdoor market as well, but under high ambient-brightness conditions, higher brightness may be required for visibility. Minimum of 2,000cd/m^2 is required in most for outdoor use; however, higher brightness is recommended up to 5,000cd/m^2 since they cope better with direct sunlight on the screen. An SMD pixel also consists of red, green, and blue diodes mounted on a chipset, which is then, mounted on the driver PC board as shown in Figure 2.6.a and 2.6.b. The individual diodes are very small and are set very close together. The difference is that the maximum viewing distance is reduced by 25% from the discrete LED display with the same resolution [21].

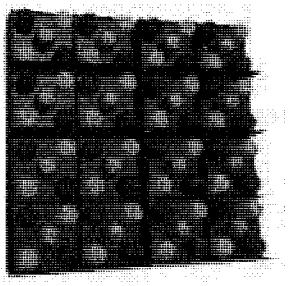

(a)

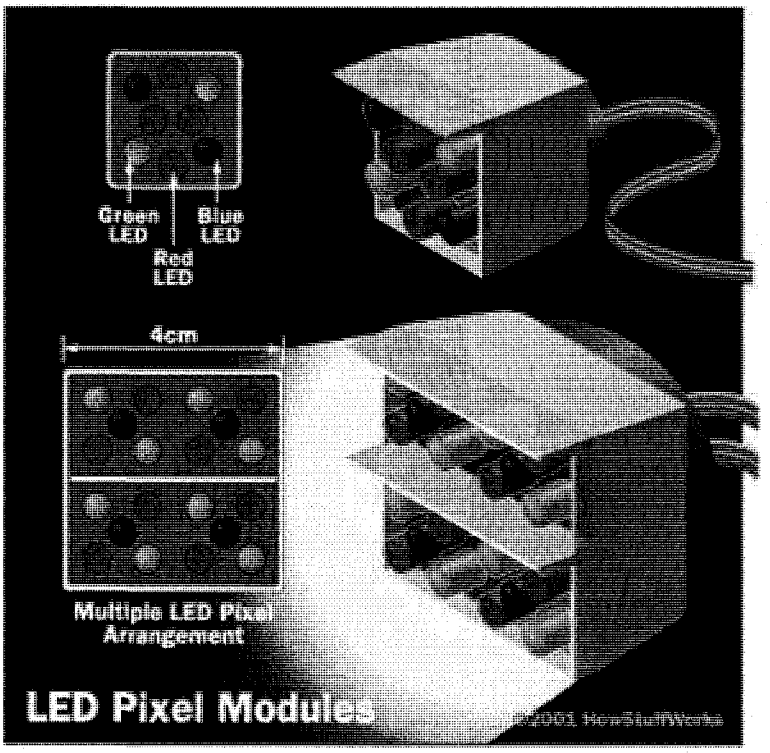

(b)

Figure 2.6 A schematic picture showing (a) 4x4 LED display matrix (b) LED pixel Modules [22].

The first recorded flat panel LED television screen was developed in 1977 by J. P. Mitchell in 1977 [21]. The modular, scalable display array was initially enabled by hundreds of MV50 LEDs and a newly available TTL (transistor transistor logic) memory

addressing circuit from National Semiconductor [21]. In Anaheim May 1978, at the 29th Engineering Exposition organized by the Science Service in Washington D.C. the 1/4 inch thin flat panel prototype was displayed and a related scientific paper was presented. However, efficient blue LEDs were missing in order to develop a color display which they did not emerge until the early 1990s completing the desired RGB color triad [21]. In the 1990s, LEDs with high brightness colors progressively developed allowing new innovations for such as huge video displays for billboards and stadiums [21].

Using LEDs for displays has many advantages. LEDs can emit light of an intended color, which is more efficient and less costly than the use of color filters that traditional lighting methods require. In order to display a moving image frequent on-off cycling is required; LEDs are ideal for use in such applications because of the fast response time of LEDs. LEDs have a very fast response time which is its advantage over other display technologies such as LCD and Plasma. LEDs light up very quickly. A typical red LED will achieve full brightness in microseconds. LEDs can be dimmed very easily either by Pulse width modulation or lowering the forward current. Saving power or achieving an apparent higher brightness for a given power input is also feasible when pulse width or duty cycle modulated. Furthermore, LEDs mostly fail by dimming over time, rather than the abrupt burn out of incandescent bulbs. LEDs can have a relatively long useful life estimated to be 35,000 to 50,000 hours where fluorescent tubes, typically, are rated at about 30,000 hours, and incandescent light bulbs at 1,000–2,000 hours [21]. LEDs, being solid state components, are difficult to damage with external shock. They can also be very small and are easily mounted onto printed circuit boards.

On the other hand, LED displays are currently more expensive than most

conventional lighting technologies. Most of its expense partially stems from the relatively low lumen output and the drive circuitry and power supplies needed. LED performance largely depends on the ambient temperature of the operating environment. Over driving the LED in high ambient temperatures may result in overheating of the LED package, eventually leading to device failure [21]. Adequate heat sinking is required to maintain long life [21]. Since white LEDs emit much more blue light than conventional outdoor light sources such as high pressure sodium lamps, the strong wavelength dependence of Rayleigh scattering means that LEDs can cause more light pollution than other light sources. It is, therefore, very important that LEDs are fully shielded when used outdoors [21].

LEDs have become very popular in certain applications such as display boards because they offer significant advantages in brightness, energy efficiency and product lifetime over traditional illumination choices.

2.3.1 Recent Developments in LED Displays

LED display industry has started in the early 1990s and has rapidly and steadily developed. Each year, the LED display market shows a growth of 15-20% [23]. There is a high demand for LED displays especially for outdoor screens such as sign displays and billboards, and also for indoor screens. With the improving LED technology, LED displays have developed to meet high industry standards when it comes to color variability, quality, viewing angle, resolution, etc. Therefore, competitors have found it very critical to introduce more features that extend even beyond high image quality. For example, LED display market is headed towards mobile displays in some companies such as YESCO and GOVISION. Water proof and flexible LED displays are being produced

by Shenzhen Cheng Guangxing Industrial Development Co. and BaoChengXin Opto-electronic Technologies Co. Technology developments of LED screen in the near future will target many issues such as improvement of performance indexes color, brightness, angle of view, etc. of LED screen, development of color and gray degree control, improving color regenerating ability and visual quality of a full color screen, and constant current driving control technology. Development of the system technology will also be a target for future developments such as applying automatic checking and remote control [23]. Improving the product structure technique is also vital for instance LED's level, heat dissipation and protection degree. Definitely, there is always room for improving the overall stability and reliability of the display [23].

CHAPTER 3

UNDERSTANDING COLORS

3.1 Definitions of Basic Colorimetric Concepts

Psychological concepts related to color perception as defined by the authors in [24]:

Light:	is a facet of radiant energy of which a human observer is responsive through the visual sensations that occur from the incentive of the retina of the eye by the radiant energy.
Color:	is an aspect of visual perception by which an observer may differentiate between identical structure shapes, which may be a result of variations in the spectral composition of the radiant energy concerned in the observation.
Hue:	is the feature of a color perception.
Saturation:	is the feature of a color perception determining the degree of its difference from the monochromatic color perception most resembling it.
Chromaticness:	is the feature of a color perception composed of the features hue and saturation.
Brightness:	is the feature of a color perception ranging from very dim or black to very bright.

Lightness: is the feature of a color perception ranging for light diffusing objects from black to white.

Psychophysical Concepts Related to Color-Matching as defined by the authors in [24]:

Color stimulus: is radiant energy of given intensity and spectral composition, producing a sensation of color when entering the eye.

Spectrum color: is the color of monochromatic light, light of a single frequency.

Achromatic color: is a color of a light chosen because it usually yields an achromatic color perception under the desired observing conditions.

Primary colors: are the colors of three reference lights. The additive mixture of such colors produces nearly all other colors in the color gamut visible to the human eye.

Tristimulus values: are the relative amounts of the three reference lights required to give by a linear combination a match with the color or light considered.

Color–matching functions: are the tristimulus values, with respect to three primary colors, of monochromatic lights of equal radiant energy, regarded as functions of the wavelength that depend on the human eye sensitivity.

Chromaticity coordinates: are the ratios of each tristimulus value needed to produce a certain desired color by a linear combination.

Dominant wavelength: is the wavelength of the spectrum color that, when additively mixed in suitable magnitudes with a specified achromatic color, yields a match with the color considered.

Basic photometric concepts and units as defined by the authors in [24]:

Luminous flux: is the magnitude derived from radiant flux by evaluating the radiant energy according to the human eye sensitivity which is determined by its action upon a selective receptor in the eye, the spectral sensitivity of which is defined by a standard relative luminous efficiency function.

Lumen (lm): the unit of luminous flux is defined by the luminous flux emitted within unit solid angle by a point source having a uniform luminous intensity of one candela.

Luminous intensity: is the proportion of the luminous flux emitted by a point source in an infinitesimal cone containing the given direction, by the solid angle of that cone.

Candela (cd): the unit of luminous intensity.

3.2 The Eye and Perception

The external stimulus is the visible radiant flux incident on the eye. The ability of the human eye to distinguish colors is based on the varying sensitivity of different cells in the retina (rods and cones) to different wavelengths of visible light.

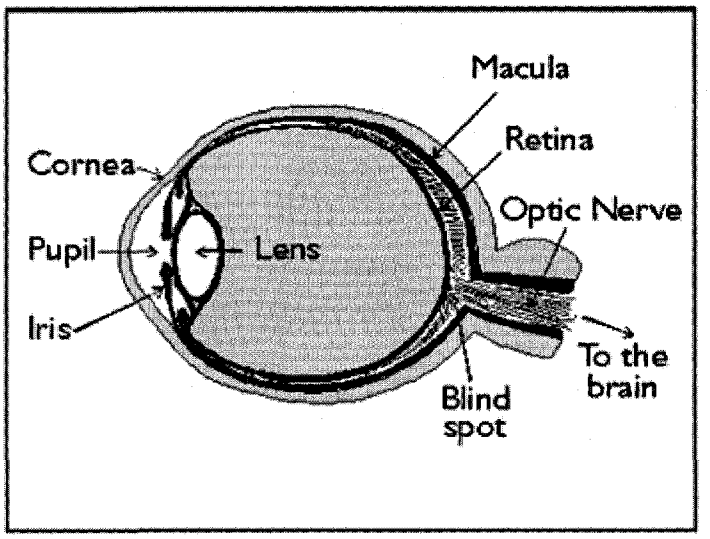

Figure 3.1. A schematic diagram showing different parts of the eye [25].

The vision is an optical process up to a certain point, the critical point. This point is reached when the radiant flux, originated from the external stimulus, is absorbed by the light sensitive visual pigments of the retinal end organs the rods and the cones [24]. The internal stimulus is defined as the quality and intensity of the radiant flux at each point occupied by a visual pigment.

There are two different sensors in the retina: the cones which are sensitive to the colors concentrated in the fovea (macula), as shown in Figure 1, and the rods which are sensitive to low levels of light. Cones are coated with pigments that are sensitive to different wavelengths. There are about seven million cones in every eye; each of which is connected with single neuron. However, rods are grouped in bunches and every bunch is connected to a neuron. There are about 120 million Rods in each eye. A schematic diagram in Figure 3.2 pictorially depicts the nature of the retina.

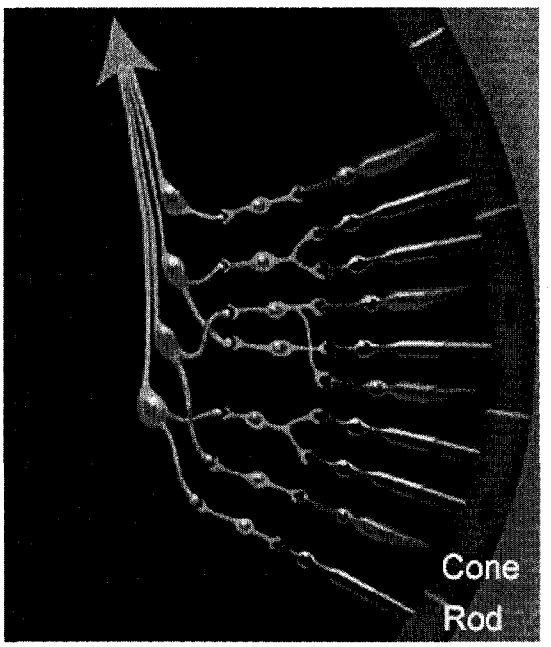

Figure 3.2. A schematic diagram showing rods and cones [26]

No matter how complex light is, the composition of wavelengths is reduced to three color components by the eye which are red, green and blue. For each location in the visual field, the three types of cones yield three signals based on the extent to which each is stimulated. These values are called tristimulus values. The "green" and "red" cones are mostly packed into the fovea centralis. Approximately, 64% of the cones are sensitive to red, 32% green sensitive, and about 2% are blue sensitive [24]. The "blue" cones have the highest sensitivity and are mostly found outside the fovea. A schematic diagram shoeing response of the retina versus wavelength of light is shown in figure 3.3. These curves are obtained by measurement of the absorption by the cones, but the relative heights for the three types are set equal for lack of detailed data. There are fewer blue cones, but the blue sensitivity is comparable to the others, so there must be some boosting mechanism [24]. In the final overall visual perception, the three colors appear comparable. Light may be

precisely characterized by giving the power of the light at each wavelength in the visible spectrum, and this function is called the spectral power distribution (SPD).

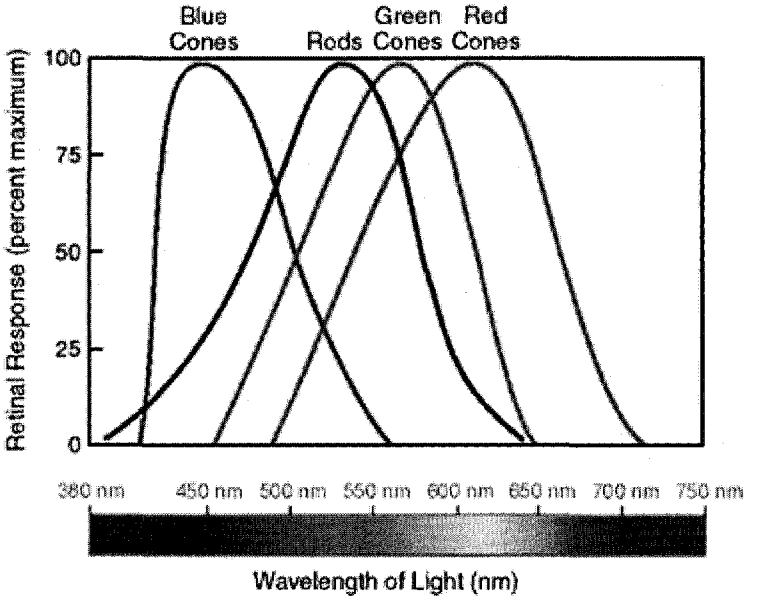

Figure 3.3. A schematic diagram showing the different response curves for cones and rods [27].

3.2.1 Photoptic and Scotoptic Vision

Scotopic vision is the eye's nighttime sensitivity; at night the vision shifts toward the blue end of the visible light. It is at its peak at 507 nm and falls to 10^{-4} at 340 and 670 nm as shown in figure3.4. The eye's daytime sensitivity is called photopic vision which shifts toward the green end of the visible light with a peak at 555 nm. It falls to 10^{-4} at 380 and 750 nm. In other words, human vision is more sensitive to blue at night; where it is more sensitive to green in day vision.

The scotopic vision is primarily rod vision, and the photopic vision includes the cones. The response curve of the eye, shown in Figure 3.4, together with the spectral power distribution of a luminous object determines the perceived color of the object. The curves represent the spectral luminous efficacy for human vision. The lumen is defined such that the peak of the photopic vision curve has a luminous efficacy of 683 lumens/watt. The efficacy of the scotopic vision equals the efficacy of the photopic value at 555 nm [27]. This was done by taking a person with normal vision, and having them compare the brightness of monochromatic light at 555 nm, where the eye is most sensitive, with the brightness of another monochromatic source of differing wavelength. To achieve a balance, the brightness of the 555 nm source was reduced until the observer felt that the two sources were equal in brightness. The fraction by which the 555 nm source is reduced measures the observer's sensitivity to the second wavelength [27].

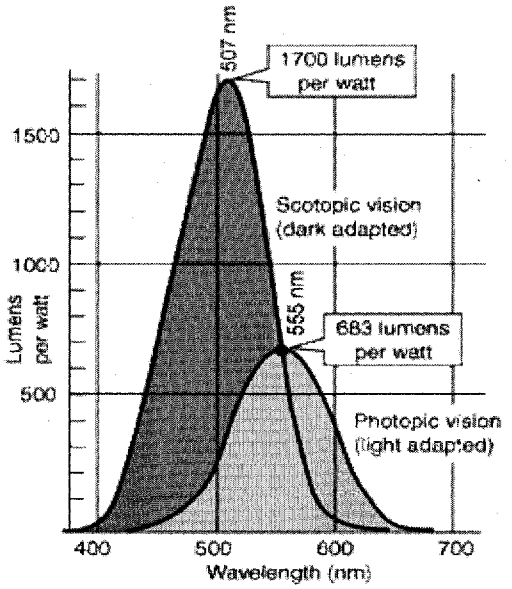

Figure 3.4. A schematic diagram of the spectral luminous efficacy for human vision [27]

3.3 The Nature of Color

Color is a visual perceptual property that steams from the spectrum of light, which is the distribution of light energy versus wavelength, interacting with the light receptors of the eye that is featured by spectral sensitivities [28]. Visible light is when the wavelength is within the visible spectrum which is the range of wavelengths humans can perceive, approximately from 380 nm to 740 nm. Table 1 shows the colors that can be produced by visible light of a single wavelength only, the pure spectral or monochromatic colors. Different light sources emit light at many different wavelengths; a source's spectrum represents the intensity distribution at each wavelength. The spectrum of light arriving at the eye from a given direction determines the color sensation in that direction.

Table 3.1. The colors of the visible light spectrum [26]

Color	**Wavelength Interval**	**Frequency Interval**
Red	700-630 nm	430-480 THz
Orange	630-590 nm	480-510 THz
Yellow	590-560 nm	510-540 THz
Green	560-490 nm	540-610 THz
Blue	490-450 nm	610-670 THz
Violet	450-400 nm	670-750 THz

A common list identifying six main bands: red, orange, yellow, green, blue, and violet; their wavelengths and frequencies are presented in Table 3.1. Newton's conception included a seventh color, indigo, between blue and violet. The intensity of a spectral color may alter its perception considerably; for example, a low-intensity orange-yellow is

brown, and a low-intensity yellow-green is olive-green.

3.4 Color Interpreted by the Brain

3.4.1 Reproduction of Colors

Light sources are either monochromatic or mixtures of various wavelengths of light. Some monochromatic colors can be reproduced as combination of other light sources. Orange, for instance, is a monochromatic color that is also obtained as a combination of red and green light. In Newton's experiment [29], he investigated what happens when mirrors are placed so as to superimpose on a white screen, two beams of monochromatic light from different regions of the spectrum. He found that a different third color was seen. This intermingled light was not monochromatic, because Newton found that when it passed through another prism two beams emerged with the two original monochromatic colors. From these observations Newton deduced that the notion of color applies to the perception we have, not to the light itself [29]. Two different light spectra which have the same effect on the three color receptors in the human eye will be perceived as the same color. This is exemplified by the white light that is emitted by fluorescent lamps, which typically has a spectrum consisting of a few narrow bands, while daylight has a continuous spectrum but human beings perceive them as very similar. The human eye cannot tell the difference between such light spectra just by looking into the light source, although reflected colors from objects can look different, because the absorption behavior of the object may be different for different parts of the spectrum.

3.4.2 Luminous Flux

Luminous flux is a weighted average of the Radiant Flux in the visible spectrum. It is a weighted average since the human eye responds unequally (it has different sensitivity) to the different visible wavelengths [24]. For conversion of Radiant Flux to Luminous Flux at any wavelength a weighing factor (V_λ) has to be taken into consideration; this weighing factor is the luminance efficacy, which is the response of the eye as a function of frequency. Further discussion is in section 3.3.

3.4.3 Matching Function

Given that Q is the vector representing a particular color and R, G, and B are the unit vectors representing three fixed primaries, then the vector equation

$$Q = RR + GG + BB \tag{3.4.1}$$

states that the given color is matched by a linear combination of quantities R, G, B of the respective primaries [29]. The scalar multipliers *R, G,* and *B* are the tristimulus values of the given color with respect to the set of primaries R, G, and B. This three dimensional vector space is called the *RGB* tristimulus space. Given that P_λ is the spectral energy distribution of color Q, then Q can be considered as an additive mixture of colors whose corresponding stimuli are the monochromatic components P_λ of the original stimulus out of which the color Q is composed. If $R_\lambda\, d\lambda$, $G_\lambda\, d\lambda$, and $B_\lambda\, d\lambda$ are the tristimulus values of $Q_\lambda\, d\lambda$ and *R, G, B* are those of Q, then [24]

$$Q = \int_\lambda Q_\lambda\, d\lambda \tag{3.4.2}$$

and

$$R=\int_\lambda R_\lambda \, d\lambda, \quad G=\int_\lambda G_\lambda \, d\lambda, \quad B=\int_\lambda B_\lambda \, d\lambda \tag{3.4.3}$$

Using Equation 3.4.2 and 3.4.3, Equation 3.4.1 can be written as

$$Q = \int_\lambda Q_\lambda \, d\lambda = R \int_\lambda R_\lambda \, d\lambda + G \int_\lambda G_\lambda \, d\lambda + B \int_\lambda B_\lambda \, d\lambda \tag{3.4.4}$$

Given that $\bar{q}_\lambda$ is the tristimulus value of spectrum for the color Q, one can conclude that the corresponding stimuli are monochromatic and contain the same constant radiant flux. These values are denoted by $\bar{r}_\lambda$, $\bar{g}_\lambda$, $\bar{b}_\lambda$ which represent the color matching properties of the human eye in the particular primary system, R, G, B, and are called color matching functions as shown in Figure 3.5. Therefore, the set of equations in (3.4.2) and (3.4.3) above can be rewritten as follows:

$$Q=\int_\lambda P_\lambda \, \bar{q}_\lambda \, d\lambda \tag{3.4.5}$$

$$R=\int_\lambda P_\lambda \, \bar{r}_\lambda \, d\lambda, \quad G=\int_\lambda P_\lambda \, \bar{g}_\lambda \, d\lambda, \quad B=\int_\lambda P_\lambda \bar{b}_\lambda \, d\lambda \tag{3.4.6}$$

This implies that the tristimulus values *R, G, B*, the coefficients of the unit vectors R, G, B in the linear equation (3.4.1), can be represented as the multiplication of two amounts the spectral energy distribution and the matching function which adapts the radiant flux observed by the human eye to the corresponding, wave length dependent, luminance flux. In other words, *R, G*, and *B* are the weighted average of the spectral energy distribution. Thus, Q is the summation of the product of those weighted averages

by the RGB unit vectors.

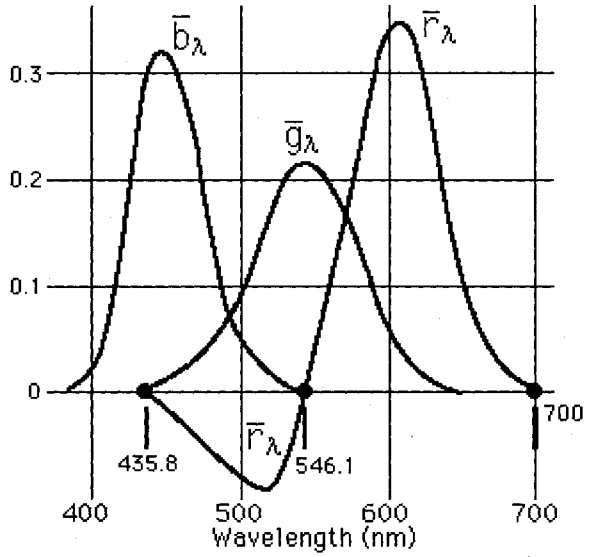

Figure 3.5 Color- matching functions, $\bar{r}_\lambda$, $\bar{g}_\lambda$, $\bar{b}_\lambda$ in the primary system R, G, B [27].

The color matching functions are based on 3 laws, Grassmann's laws of additive color mixture (1853), which state [29]:

1. Any four colors Q, R, G, and B are always linearly dependent. In other words, the following relationship must hold

$$QQ+RR+GG+BB = 0$$

where the scalar multipliers, *Q, R, G, B* are not all 0.

2. The color of a mixture of colors Q and Q_1 is the same as that of a mixture Q and Q_2, if Q_1 matches Q_2, although the spectral energy distributions $\{P_{1\lambda}\, d\lambda\}$ and $\{P_{2\lambda}\, d\lambda\}$ of the color stimuli corresponding, respectively, to Q_1 and Q_2 may be different.

3. A continuous change in the spectral energy distribution $\{P_\lambda\ d\lambda\}$ of the color stimulus of color Q results in a continuous change of Q.

3.5 Color Spaces

A color space is a notation, by which we can quantify colors. There are many different color spaces that are used for different applications specifically in image processing. The choice of a color space can be a very important decision, which can largely influence the results of the processing [30]. Color spaces can be categorized in 3 different categories: human visual system (HVS) based color spaces, Application specific color spaces, and CIE color spaces.

3.5.1 HVS Color Spaces

The HVS based color spaces fall under three categories: the RGB color spaces, the opponent colors theory based color spaces, and the phenomenal color spaces. The RGB color space is the first attempt to simulate light in the human eye based on the HVS. The color is described with three components: R, G and B. The value of these components is the sum of the respective sensitivity functions S_λ and the light spectrums $R_\lambda\ d\lambda$, $G_\lambda\ d\lambda$, and $B_\lambda\ d\lambda$.

$$R=\int_\lambda S_\lambda R_\lambda\, d\lambda, \quad G=\int_\lambda S_\lambda G_\lambda\, d\lambda, \quad B=\int_\lambda S_\lambda B_\lambda\, d\lambda \tag{3.5.1}$$

The RGB color space is device dependent since the RGB values depend on the specific sensitivity function. Capturing, printing, and displaying devices are based on the RGB color space.

The German physiologist Ewald Hering proposed the opponent colors theory in the

late 19th century [30]. He noted that certain hues were never perceived to occur together; for example, reddish-green or yellowish-blue are not visually possible, while all other combinations are possible such as bluish-green or reddish-yellow. Researchers found out that there is a layer in the HVS that converts the RGB values from the cones into an opponent color vector. This vector has an achromatic component White-Black (WhBl) and two chromatic components Red-Green (RG) and Yellow-Blue (YeB) [30]. The transformation between RGB values and RG, YeR, and WhBl is done according to the following model:

$$RG = R - G$$

$$YeB = 2B - R - G$$

$$WhBl = R + G + B \tag{3.5.2}$$

Isaac Newton [24] arranged colors in a circle, called the Newton's color circle, which belongs to the phenomenal color spaces. This uses the attributes of hue and saturation for describing colors as shown in Figure 3.6, where the hue is represented by the angle, saturation by the radius, and value or luminance by the hypotenuse formed by the line that extends on the surface of the cone from zero brightness, the pointy part of the cone. Naturally, the human brain tends to organize colors by hue, saturation and brightness. This is the mind's representation of colors - the highest level in human visual processing [30]. Hue is the attribute which tells us whether the color is red, green, yellow, blue, purple, etc which is represented by the angle. Saturation is the level of non-whiteness which is represented by the radial length of the point from the center. Brightness is a measure of the intensity of light which is represented by the tangent of the cone. The Munsell color space is a phenomenal color space and an atlas of 1500 systematically

ordered color samples. These samples are chosen in such a way that the steps are perceptually equal [30].

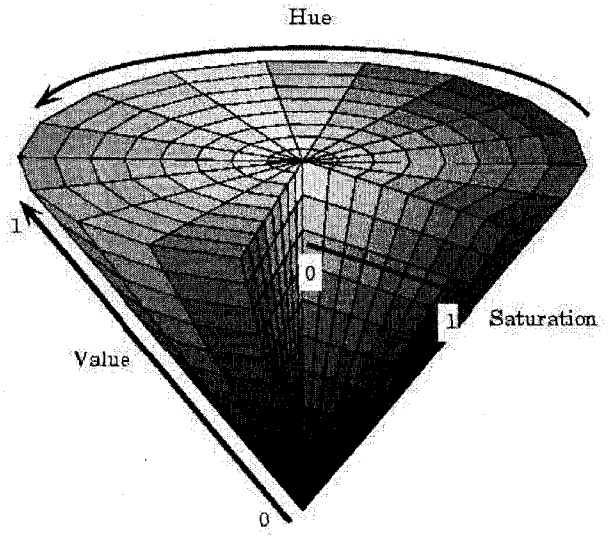

Figure 3.6 A schematic diagram representing the phenomenal color space [31]

HSV (hue, saturation, and value) color spaces are also phenomenal color spaces. They are a linear transformation from the RGB space. There are many of HSV spaces defined in literature [30]. In the following, one of the models used for HSV transformation is described below:

Saturation is presented as:

$$S = \frac{\max(R,G,B) - \min(R,G,B)}{\max(R,G,B)} \tag{3.5.3}$$

Value is defined as:

$$V = \max(R,G,B) \tag{3.5.4}$$

Hue is defined as:

$$H = 5 + B' \quad when \quad \mathrm{R} = \max(R,G,B), G = \min(R,\ G,B\ )$$

$$H = 1 - G' \quad when \quad R = \max(R,G,B), G \neq \min(R, G,B)$$

$$H = R' + 1 \quad when \quad G = \max(R,G,B), B = \min(R,G,B)$$

$$H = 3 - B' \quad when \quad G = \max(R,G,B), B \neq \min(R, G,B)$$

$$H = 3 + G' \quad when \quad B = \max(R,G,B)$$

$$H = 5 - R' \text{ otherwise} \tag{3.5.5}$$

where

$$R' = \frac{\max(R,G,B) - R}{\max(R,G,B) - \min(R,G,B)}$$

$$G' = \frac{\max(R,G,B) - G}{\max(R,G,B) - \min(R,G,B)}$$

$$B' = \frac{\max(R,G,B) - B}{\max(R,G,B) - \min(R,G,B)}$$

then H is converted to degrees by multiplying by 60.

Phenomenal color spaces do not take into account the human perception. There is also a bad correlation between the computed and the perceived lightness [30]. Thus, using phenomenal color spaces becomes inaccurate in many applications.

3.5.2 Application Specific Color Spaces

The two main applications, where the usage of color spaces is essential, are printing and television. In printing, subtractive mixing of colors is used, which is a way to produce colors by selectively removing a portion of the visual spectrum. The CMY (Cyan Magenta Yellow) color space is a subtractive color space and is mainly used in printing

applications [30]. It is perceptually non-linear. The three components represent three reflection filters. There is also the CMYK color space, where the fourth component K represents the amount of black ink [30]. There are two types of transformation to the CMYK color space, a simple one and a more complicated one that uses complicated polynomial arithmetic or three-dimensional interpolations of lookup tables.

Simple transformation from RGB to CMY color space is given by:

$$C = 1 - R$$

$$M = 1 - G$$

$$Y = 1 - B \tag{3.5.6}$$

Transformation from $C'\ M'\ Y'$ to the *CMYK* color space is given by:

$$K = \min\ (C, M, Y)$$

$$C = \frac{(C' - K')}{(1 - K')}$$

$$M = \frac{(M' - K')}{(1 - K')}$$

$$Y = \frac{(Y' - K')}{(1 - K')} \tag{3.5.7}$$

The YUV color space is one of the color spaces used for TV application. The RGB signals are encoded in the YUV space with the following equations:

$$Y = 0.299R + 0.587G + 0.114B$$

$$U = -0.147R - 0.289G + 0.437B = 0.493\ (B - Y)$$

$$V = 0.615R - 0.515G - 0.1B = 0.877\ (R - Y) \tag{3.5.8}$$

The YUV space can be transformed in a phenomenal color space, with Y representing

the V (value) component, as:

$$H_{UV} = \tan^{-1}\left(\frac{V}{U}\right)$$
$$S_{UV} = \sqrt{U^2 + V^2} \tag{3.5.9}$$

3.5.3 The CIE Color Spaces

The CIE, the international Commission on Illumination, laid down the CIE 1931 standard colorimetric observer in 1931. This is the data on the ideal observer on which all colorimetric is based [30]. As shown in equation 3.4.1, colors can be expressed as vectors that are geometrically represented as a three-dimensional vector space where R, G, and B are the axis, color of vector Q is a point with the coordinates of *R*, *G*, and *B* [24]. The unit plane that satisfies the condition R+G+B = 1 is considered as the two dimensional (r, g) chromaticity diagram as shown in Figure 3.7.

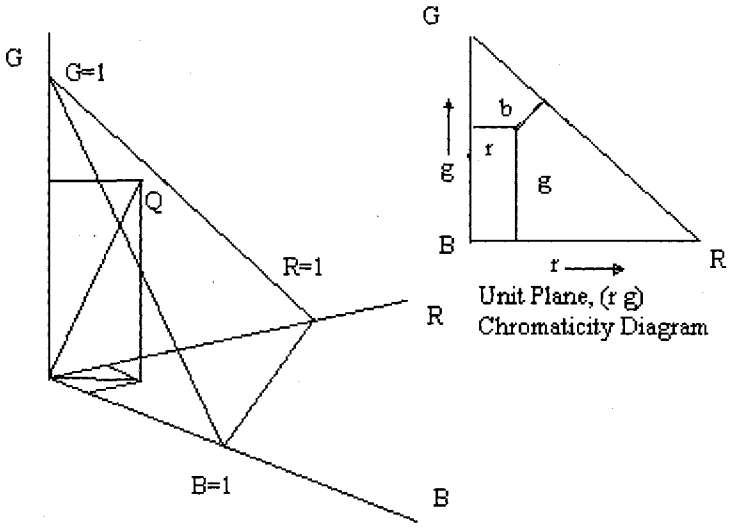

Figure 3.7 A schematic diagram showing the three-dimensional RGB vector space and the (r g) chromaticity diagram.

The following set of equations is used for the transformation of the tristimulus values

R, G, B to the chromaticity coordinates r, g, b:

$$r = \frac{R}{R+G+B},$$
$$g = \frac{G}{R+G+B}, \tag{3.5.10}$$
$$b = \frac{B}{R+G+B},$$

The CIE standardized the XYZ values as tristimulus values that can describe any color that can be perceived by an average human observer. This color space is defined by the color matching functions $\bar{x}_\lambda, \bar{y}_\lambda, \bar{z}_\lambda$ [24]. These values, which were experimentally obtained, are tabulated with the corresponding chromaticity coordinates $x_\lambda, y_\lambda, z_\lambda$. The CIE color space chromaticity presented in Figure 3.8 is showing the color gamut for the (x y) chromaticity coordinates; the wavelengths are denoted by the values surrounding the color gamut.

The tristimulus values X, Y, and Z are obtained by the summation of the spectral distribution of its radiant flux $\{P_\lambda\, d\lambda\}$ as shown in the following equations:

$$X = k\sum_{\lambda} P_\lambda \bar{x}_\lambda \Delta\lambda$$
$$Y = k\sum_{\lambda} P_\lambda \bar{y}_\lambda \Delta\lambda$$
$$Z = k\sum_{\lambda} P_\lambda \bar{z}_\lambda \Delta\lambda \tag{3.5.11}$$

where the color matching functions $\bar{x}_\lambda, \bar{y}_\lambda, \bar{z}_\lambda$ are obtained from the tabulated data, and k is a normalizing factor. After obtaining the tristimulus values, the chromaticity coordinates are obtained by using the following equations:

$$x = \frac{X}{X+Y+Z}$$

$$y = \frac{Y}{X + Y + Z}$$

$$z = \frac{Z}{X + Y + Z} \tag{3.5.12}$$

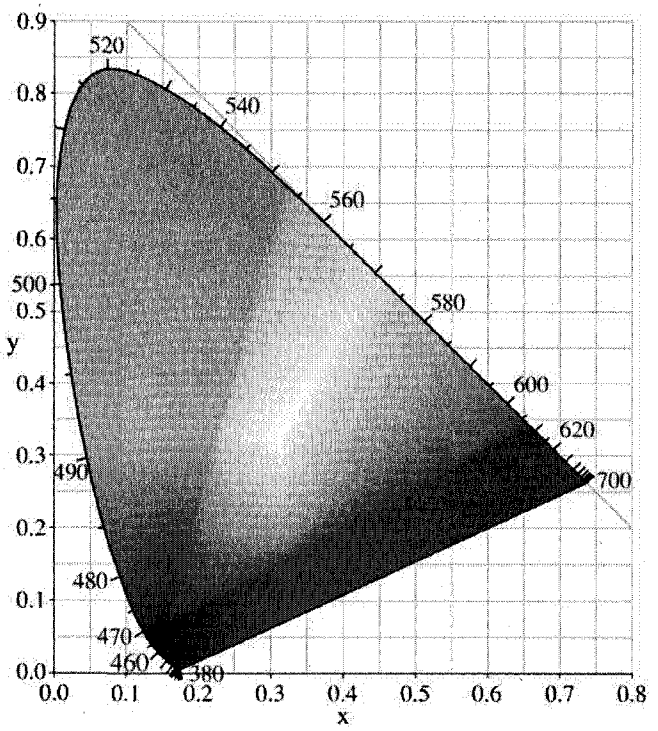

Figure 3.8 The CIE 1931 color space (x y)chromaticity diagram [27]

For any given stimulus, the transformation between r, g, b and x, y, z is given by the following set of equations:

$$x = \frac{0.49r + 0.31g + 0.2b}{0.66697r + 1.1324g + 1.20063b},$$

$$y = \frac{0.17697r + 0.8124g + 0.01063b}{0.66697r + 1.1324g + 1.20063b}, \tag{3.5.13}$$

$$z = \frac{0.0r + 0.01g + 0.99b}{0.66697r + 1.1324g + 1.20063b},$$

In 1976, the CIE introduced the color spaces CIELUV and CIELAB. Perceptual uniformity is what distinguishes the CIELUV and CIELAB color spaces. Thus, any change in value corresponds approximately to the same perceptual difference over any part of the space [30]. The CIELUV space was specifically designed for emissive colors that are found in various applications such as photography or computer graphics rendering program. For the 'a' value, CIELAB uses a red/green axis and a blue/yellow axis for the 'b' value [32]. This model is very similar to the way the human optic system works. CIELUV uses chromaticity (saturation) for the 'u' value and hue angle for the 'v' value. The CIELUV space uses the CIE 1976 $(u' v')$ chromaticity diagram, shown in Figure 3.9, where L, U, V are the tristimulus values that correspond to the $(u' v')$ coordinates; however, CIELAB uses a modification of Adam's chromatic-value diagram, as shown in Figure 3.10, where L, A, B are the tristimulus values that correspond to the $(a^* b^*)$ coordinates [32].

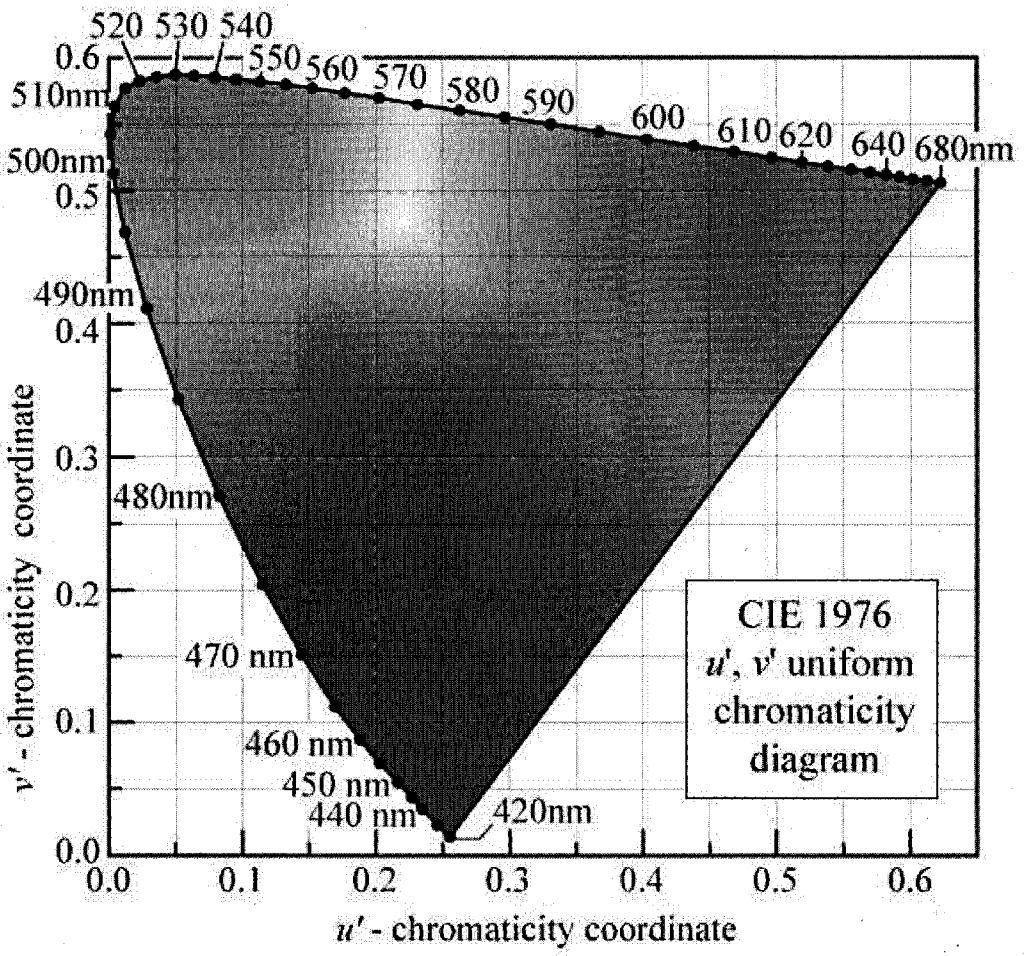

Figure 3.9 The CIE 1976 color space (u' v') chromaticity diagram [28].

In the CIELAB model presented in Figure 3.10, differences in colors perceived, correspond to measured linear colorimetric distances. The 'a' axis extends from green (-a) to red (+a) and the 'b' axis from blue (-b) to yellow (+b). The brightness (L) increases from the bottom to the top of the spherical model [33].

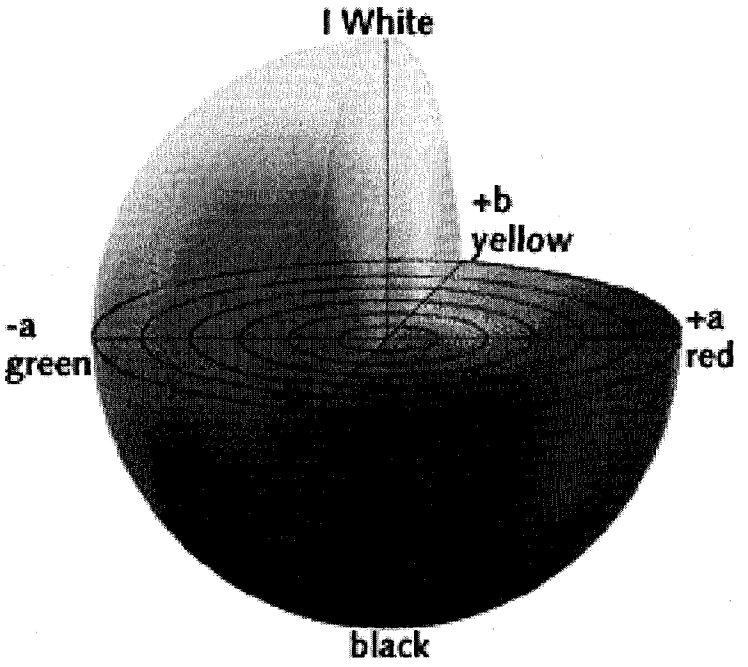

Figure 3.10 The CIELAB chromaticity diagram ($a^* b^*$) plane [33].

The transformation from CIE XYZ to CIELUV is performed with the following equations

For $\frac{Y}{Y_n} > 0.01$

$$L^* = 116\left(\frac{Y}{Y_n}\right)^{\frac{1}{3}} - 16$$

$$u^* = 13L^*\left(u' - u'_n\right) \qquad (3.5.14)$$

$$v^* = 13L^*\left(v' - v'_n\right)$$

else

$$L^* = 903.3\left(\frac{Y}{Y_n}\right) \tag{3.5.15}$$

where

$$u' = \frac{4X}{X + 15Y + 3Z}$$

$$u'_n = \frac{4X_n}{X_n + 15Y_n + 3Z_n} \tag{3.5.16}$$

$$v' = \frac{9Y}{X + 15Y + 3Z}$$

$$v'_n = \frac{9Y_n}{X_n + 15Y_n + 3Z_n}$$

The transformation from CIE XYZ to CIELAB is performed with the following equations

$$L^* = 116\left(\frac{Y}{Y_n}\right)^{\frac{1}{3}} - 16$$

$$a^* = 500\left[\left(\frac{X}{X_n}\right)^{\frac{1}{3}} - \left(\frac{Y}{Y_n}\right)^{\frac{1}{3}}\right] \tag{3.5.17}$$

$$b^* = 200\left[\left(\frac{Y}{Y_n}\right)^{\frac{1}{3}} - \left(\frac{Z}{Z_n}\right)^{\frac{1}{3}}\right]$$

where L^* is the lightness scale, which depends only on Y the luminance value, for both color spaces CIELUV and CIELAB; The tristimulus values X_n, Y_n, Z_n are those of the nominally white object-color stimulus [30].

CHAPTER 4

THEORETICAL AND PRACTICAL MODELING OF RGBW PIXEL BASED LED DISPLAY

4.1 Introduction of the New Pixel with a White LED

Even though, the rapid development in solid state technology has witnessed advancements in high power LED obtaining on average 150 lumen/ Watt [34], efficiency of LED displays could be further improved by introducing a white LED to the pixel. In addition, the introduction of the white LED is expected to improve picture quality of LED displays. There are several approaches using LEDs to achieve white light. One approach is to use a blue or UV LED to excite one or more phosphors to produce white light [35] [36]. Another approach is to use RGB LEDs to give white light. A key challenge for RGB LEDs is to maintain the desired white point within acceptable tolerances. This arises from the significant spread in lumen output and wavelength of manufactured LEDs, and the changes in LED characteristics that occur with temperature and time. Maintaining the desired white point can only be achieved with feedback schemes to control the relative contributions of red, green, and blue to the white light [36]. This paper focuses on the first method of white light generation in which a blue LED is used. The traditional method of using LED light source composed of RGB LEDs is modified to include a white LED. The white LED will be turned on to the level

of the appropriate luminance when all three RGB are turned on in order to produce a certain color. The luminance of the white LED will be decided based on the minimum luminance flux (which takes into account human eye response) of the RGB and tristimulus values, which are the amounts of the reference lights necessary for the additive mixture to provide a close match to the light considered [24].

By introducing the white LED into the pixel, usage of the green LED will be reduced, which is the least efficient. Also, usage of red and blue LEDs will be reduced which results in a life expectancy increase of the display on an average. Moreover, less complicated feedback control schemes for RGB LEDs will be needed in order to maintain achromatic point (AP) since pure white light is used to achieve the white point resulting in more uniform white color point integration with the added benefits of a less complicated control circuitry. Based on a theoretical modeling and test measurements (using a prototype) for the new suggested method (RGBW), the advantages compared to the RGB LED display technology will be demonstrated.

4.2 Issues with RGB

Although RGB has the benefit of color variability, it also has some challenging issues such as: Color instability due to temperature changes and the variability in light output of nominally identical LEDs by over a factor of two, and the wavelength can vary by many nanometers due to aging differently and initial spread in the performance of the LEDs [36]. A study on thermal effects on RGB LED characteristics was reported in [35]. The study in [35] shows a 10% decrease in light output for every 100C increase in temperature for AlInGaP red LED 5% for InGaN green LED and 2% for InGaN blue

LED. It is also shown that as temperature increases the LED shifts towards longer wavelength. In [36], minimum perceptible-color-difference (MPCD) as an outcome of changes in light output of the individual LEDs, due to aging or manufacturing inconsistency, was studied and reported. Results show the calculated shift in the (u, v) color coordinates as a result of a change in the flux of the red, green, or blue LEDs.

4.3 Theoretical Analysis of the New RGBW Pixel

In this study, the classical pixel RGB is modified to include a white LED. In a frame, some pixels will have a certain intensity of white. In other words, certain hues can be modeled as the addition of a certain amount of white and some intensities of two of the three colors, R, G and B. For every pixel that has some amount of white in it, or the color is not fully saturated; the maximum luminance flux of white of the color is supplied using the white LED in order to retain the saturation level required. In the process, the intensity of one of the three colors will be completely eliminated and the two others will be reduced in intensity. Figure 4.1 schematically demonstrates the process of conversion from RGB to RGBW through an example, where the source data is chosen to be R = 75, G = 90, and B = 45. First, the three data sources are compared in order to distinguish the source with the minimum intensity out of RGB which in this case is B. Then, the value of the minimum intensity will be deducted from all three sources so R would take the value 30, G = 45, and B = 0. Finally, this value will be supplied to the W which becomes 45. As shown in the example in figure 4.1, the converted data will consist of four data sources, RGB and W.

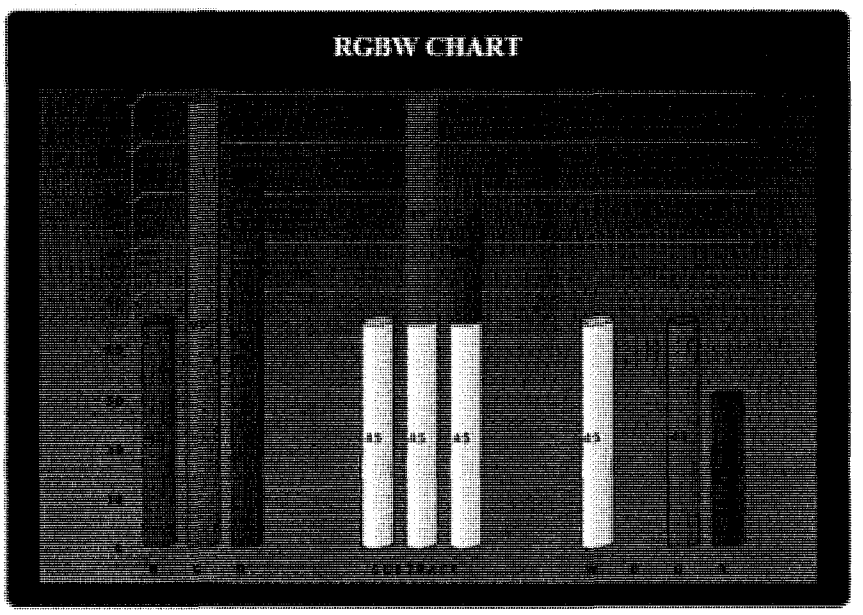

Figure 4.1 RGBW chart. Y axis represents 255 different possible levels of digital color intensities that correspond to an eight bit data bus for each color. (a) Intensity levels for RGB in a pixel (b) Identified intensity of white in the pixel (c) B completely eliminated, white LED introduced and R and G reduced.

The combination of light wavelengths to produce a given perceived color is not unique. The white intensity in a certain color affects its saturation [24]. In other words, a perfectly saturated color is missing the element of white; therefore, only monochromatic and dual chromatic colors can be perfectly saturated. That given, it is concluded that by eliminating the white component, the hue will not change but its saturation level will, which could be compensated by adding a white light from any other light source such as a white LED. The human eye can not distinguish between similar hues that are produced by different components of light wavelengths; however, it may affect the way colors of objects are perceived by the human eye if these light sources are used for ambient lighting purposes. Since this project is only concerned with display systems, one can

conclude that using the white LED in order to display colors in such systems will not affect the colors perceived by the observers.

The following analysis theoretically demonstrates that the hue from RGBW and RGB will be the same. Using equation 4.1, the new color, Cnew, after reducing the intensities of R, G and B by x, is given by:

$$\text{Cnew} = (R\text{-x})\,\text{R} + (B\text{-x})\text{B} + (G\text{-x})\,\text{G}$$

$$= (R\text{R}+B\text{B}+G\text{G}) - \text{x}(\text{R}+\text{G}+\text{B}) = \text{C} - \text{xW} \qquad (4.1)$$

Note that the rewritten equation 4.2 has two components on the right hand side. The first term corresponds to the old color with the original intensities of the R, G and B and the second term corresponds to the amount of white intensity, which was removed from the pixel by reducing intensities of R, G and B by x. The calculations above show that the process of reducing an x amount of luminance from every RGB LED is equivalent to the process of reducing the same amount of white light.

Considering the HSV system, one can also show that the hue can be maintained when comparing the traditional pixel to the new RGBW pixel set up. Using the set of equations 3.5.5 in order to determine the hue, all sub-pixel combinations can be taken into account as follows:

When R is maximum and G is minimum, H_{new} is given by:

$$H_{new} = 5 + \frac{(R-G)-(B-G)}{(R-G)-(G-G)} = 5 + \frac{R-B}{R-G} = H_{old} \qquad (4.2.a)$$

When R is maximum and G is not minimum, H_{new} is given by:

$$H_{new} = 1 - \frac{(R-B)-(G-B)}{(R-B)-(B-B)} = 1 - \frac{R-G}{R-B} = H_{old} \qquad (4.2.b)$$

When G is maximum and B is minimum, H_{new} is given by:

$$H_{new} = 1 + \frac{(G-B)-(R-B)}{(G-B)-(B-B)} = 1 + \frac{G-R}{G-B} = H_{old} \tag{4.2.c}$$

When G is maximum and B is not minimum, H_{new} is given by:

$$H_{new} = 3 - \frac{(G-R)-(B-R)}{(G-R)-(R-R)} = 3 - \frac{G-B}{G-R} = H_{old} \tag{4.2.d}$$

When B is maximum, H_{new} is given by:

$$H_{new} = 3 + \frac{(B-\min)-(G-\min)}{(B-\min)-(\min-\min)} = 3 + \frac{B-G}{B-\min} = H_{old} \tag{4.2.e}$$

where H_{new} is the hue obtained from the new RGBW pixel and H_{old} is the hue obtained from the traditional RGB pixel. Equations 4.2.a-4.2.e clearly show that the hues H_{new} (RGBW) and H_{old} are the same. Using equation 3.5.3, the saturation of the new pixel is found to be 1, which means it is fully saturated since the element of the white is removed. However, the saturation level can be individually controlled by the white LED to match the saturation of the old pixel. The value, as stated in equation 3.5.4, is the maximum component among RGB which in the new pixel configuration that value will be reduced by the minimum amount among RGB, which can also be compensated by the value of the white.

4.4 The RGBW LED Display Prototype and Driver

4.4.1 Hardware

An 8X8 pixel block display prototype is developed; each pixel consists of RGBW LEDs placed in a square configuration as shown in Figure 4.2. LEDs are driven by LED

drivers. Each driver drives eight LEDs. The display block has eight parallel inputs, which implies that every four drivers are serially connected (red and white are serially connected, green and blue are serially connected). The prototype is driven by an FPGA.

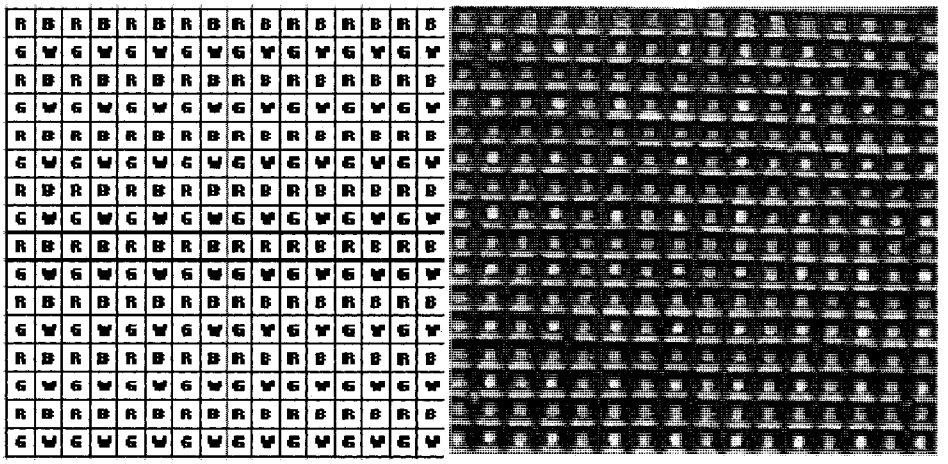

Figure 4.2 A schematic diagram showing the square pixel configuration with RGB and W LEDs used for this research and the prototype from TecnoVision.

4.4.2 The LED Driver

The STP08CDC596 chip is An 8-bit constant current LED sink driver with full outputs detection and is used for driving the LEDs that compose the pixels of the display. Key features as listed in the data sheet of the LED driver chip are [37]:

- 8 constant current output channels
- Adjustable output current through one external resistor
- Open and short line, short to GND, short to V-LED supply error detection
- Serial data in/parallel data out
- Serial out change state on the falling edges of clock

- Output current: 20-120mA
- 3.3V micro driver-able
- 25MHz clock frequency

The data is inputted serially through the serial data input (SDI) pin and outputted in parallel through the out 0 thru 7 pins. The latch-enable (LE) and the output-enable (OE) pins are data control pins. The clock is provided at the clock pin (CLK). Figure 4.3 shows the pin-out of the chip used.

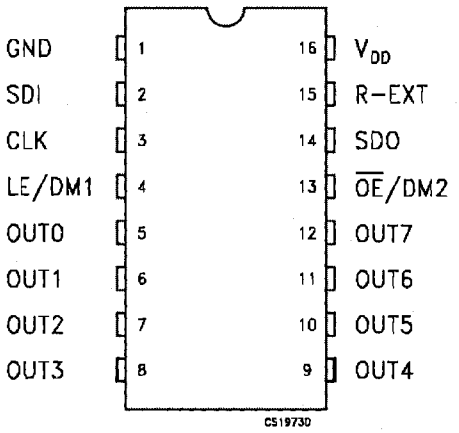

Figure 4.3 A schematic diagram showing the 8-bit constant current LED sink driver (STP08CDC596) [37].

The timing diagram provided in the data-sheet needs to be considered in the software design and is shown in Figure 4.4. In normal mode the OE/DM2 must remain low at least two clock cycles. In case of OE signal enabled (OE is active low) during no clock activity (clock stopped), after the CLK restarts, 3 full CLK cycles are necessary before disabling the OE signal (OE is passive high) [37].

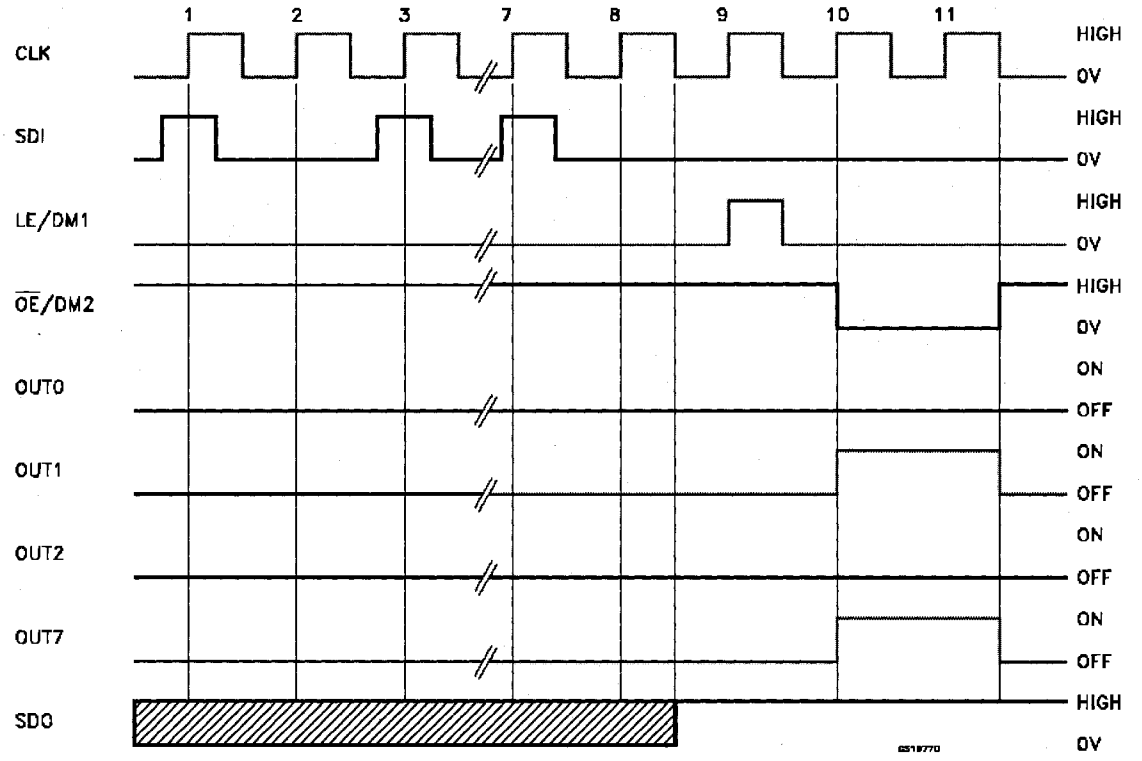

Figure 4.4 A timing diagram showing the pin's statuses of the LED driver chip [37].

There are 32 driver chips used in order to accommodate the number of LEDs, 256 LEDs, required for an 8x8 pixel display. The schematic in Figure 4.5 shows the layout of the circuitry supporting the prototype. In the schematics RW pins represent the data for red and white and the BG represent the blue and green data pins. The rest of the pins are described at the beginning of this section.

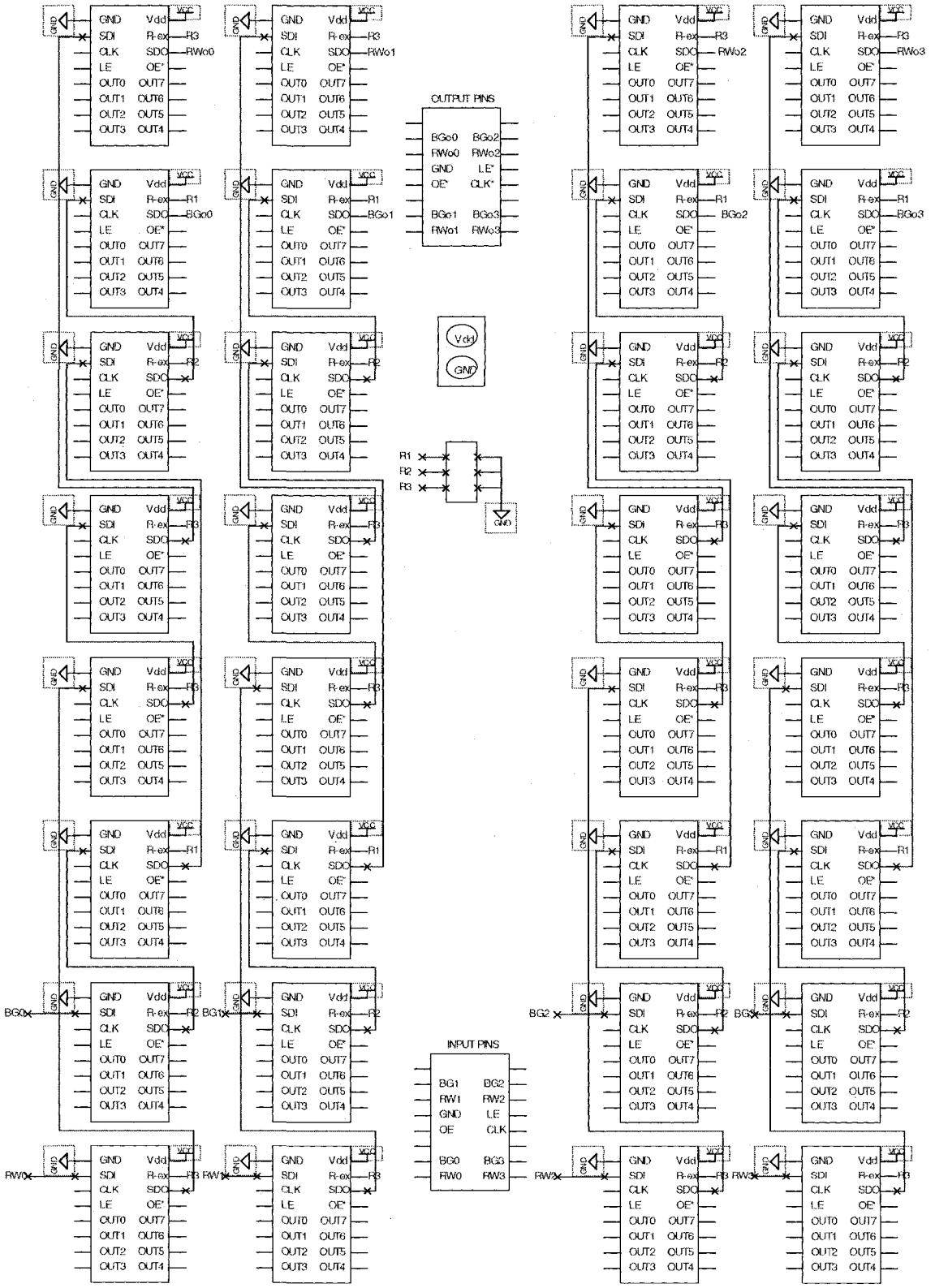

Figure 4.5 A schematic diagram showing the circuit layout of the prototype.

4.4.3 The Display Driver

In order to drive the LED display prototype, the DE2 development and education board is used. The DE2 has many key features and contains the appropriate components for the hardware requirements of the project. The following is a list of the DE2 components and features that are used in the project as listed in the user manual of the DE2 board [38]:

- Altera Cyclone® II 2C35 FPGA device
- Altera Serial Configuration device - EPCS16
- USB Blaster (on board) for programming and user API control; both JTAG and Active Serial
- 512-Kbyte SRAM
- 8-Mbyte SDRAM
- Expansion headers (76 signal pins)
- 4-Mbyte Flash memory
- 18 toggle switches
- 18 red user LEDs
- 50-MHz oscillator and 27-MHz oscillator for clock sources
- VGA DAC (10-bit high-speed triple DACs) with VGA-out connector

4.4.4 Software

As described in the block diagram in Figure 4.8 there are two different RGB sources: Pattern generator (implemented in memory), and real time serial digital input (SDI) video signal (outputted from a scalar board that converts video signal to RGB). In the pattern

generator, the synchronization signals shown in Figures 4.6.a and 4.6.b are also generated.

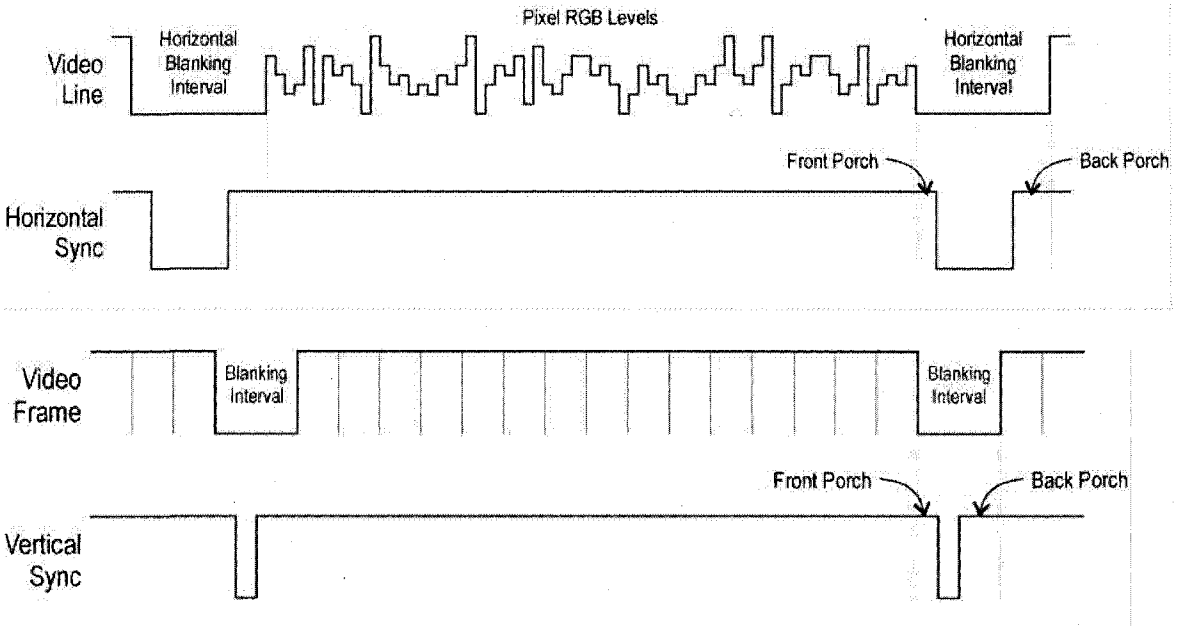

Figure 4.6 A timing diagram showing the (a) horizontal timing (b)vertical timing [39].

Using an FPGA The signals are decoded and fed into the RGB to RGBW converter. Then, the RGBW input data (eight bit data bus for every color) is remapped. Due to the architecture of the display, the input data looses its order when outputted directly to the display as shown in Figure 4.7. For optimal hardware design, such configuration was required.

R27	R26	R25	R24	R11	R10	R9	R8
W19	W18	W17	W16	W3	W2	W1	W0
R28	R29	R30	R31	R12	R13	R14	R15
W20	W21	W22	W23	W4	W5	W6	W7

Figure 4.7 A diagram showing the order of the white and the red of the pixels of the first two rows of the display without reordering

Finally, pulse width modulation (PWM) is used to output to the RGBW data to the display. The color accuracy of the white point will be maintained by reducing the variation in white point if the LEDs are driven using PWM [15]. A 5" x 5"of white plastic diffuser is used in order to properly mix the light of the pixel in order to perceive a uniform color.

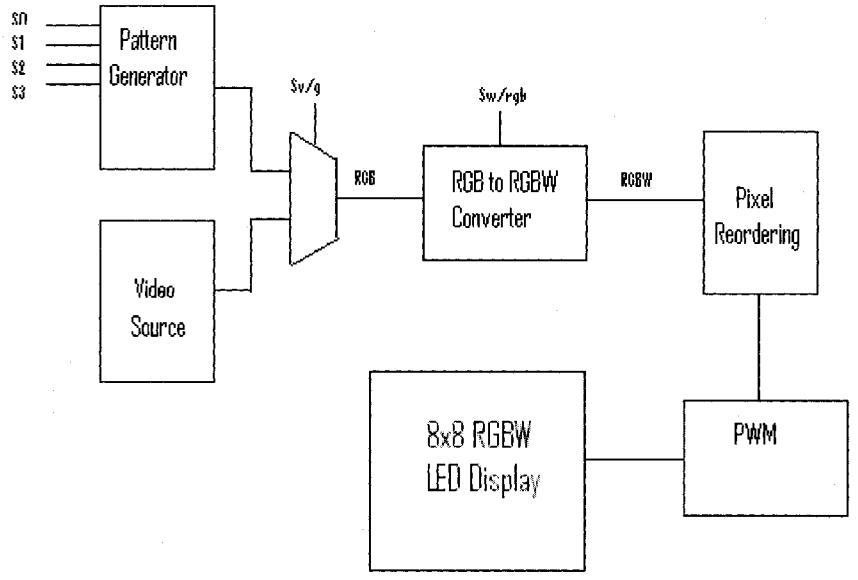

Figure 4.8 A block diagram where S (0-3) allow variety of solid colors to be displayed, S(v/g) selects pattern generator or video, and S(w/rgb) turns the RGB to RGBW conversion on or off.

Using the switches of the development board of the FPGA, one can choose to bypass the conversion so that the display will use the classical RGB pixel instead of RGBW. Using another set of switches, the hardware provides the possibility to choose various solid colors from the pattern generator to be displayed.

The following schematics Figures 4.9 (a thru i) demonstrate the logic implementation in the FPGA of every part described in the block diagram in Figure 4.8. These are selected parts of the schematics file that was split due to its large size.

A 27 MHz clock from the DE2 evaluation board is used for both synchronization of the implemented logic and for the generation of the signals required for image display (compatible with a VGA input connector) as shown in Figure 4.9.a. These signals include the horizontal and vertical syncs (hsync and vsync), horizontal and vertical blanks (hblank and vblank), and the vertical count (Vcnt). The logic was implemented with a 16.6 ms refreshing rate requirement assuming a resolution of 720x 480. Then, an extraction of 8x8 pixels was done to match the size of the prototype.

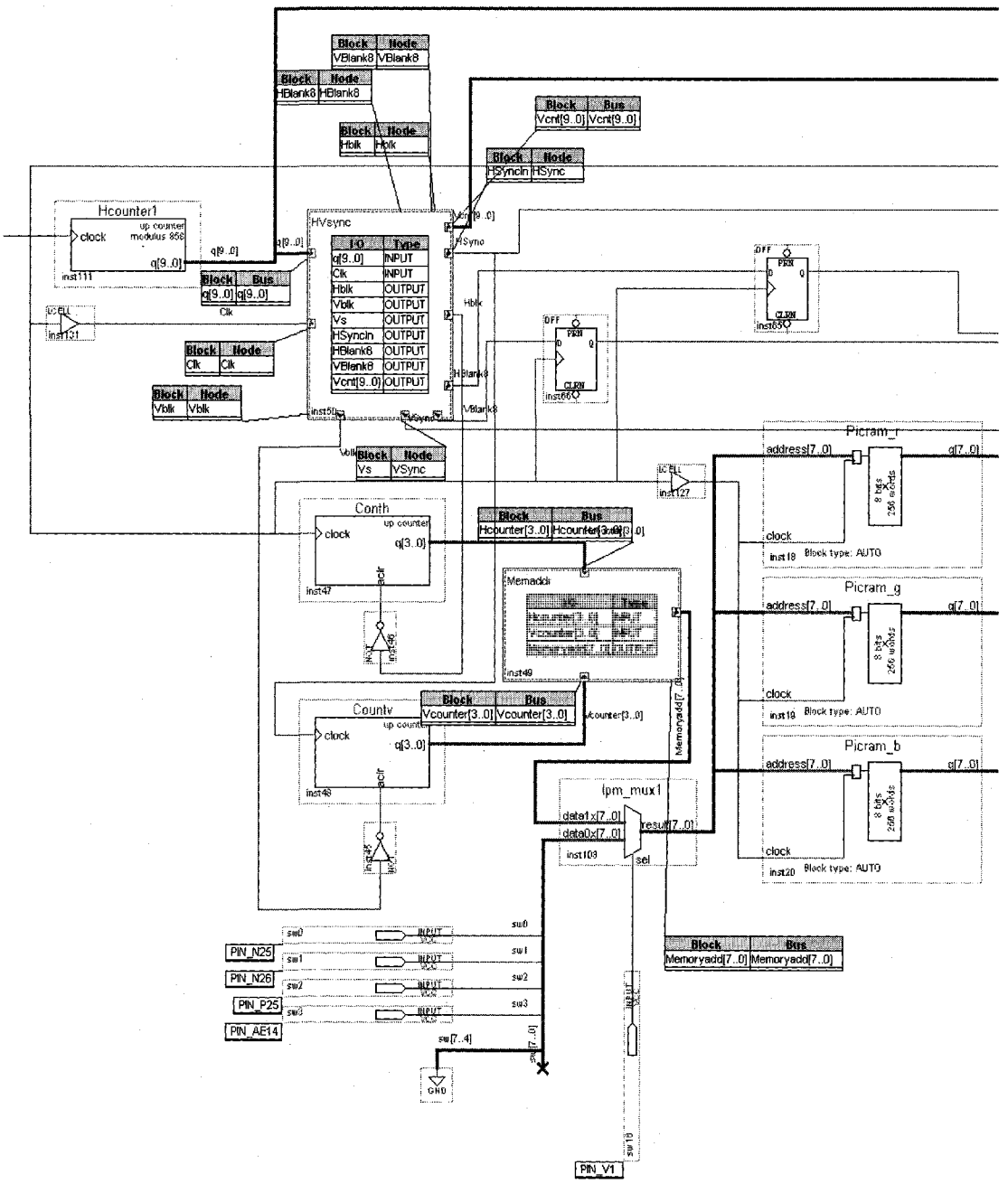

Figure 4.9.a A schematic diagram showing the implementation of the pattern generator.

The hsync and vsync are two of the signals of which a VGA connector consists for RGB video output. They provide the monitor with the timing information necessary to correctly display the pixel RGB data. VGA video output is a stream of frames that are

refreshed at a certain frequency (refreshing rate). Every frame consists of a series of horizontal lines where each of which is made up of a series of pixels [40]. In every frame, the pixel data is transmitted in order from top left corner to bottom right corner. In order to locate the ends of every line and frame, separate horizontal and vertical synchronization signals are required [40]. There are two regions that every horizontal line of the display experiences: active video and blanking region. In the active video region, RGB values are outputted for every pixel in the line. In the blanking region, there is the front porch where black pixels are transmitted. Then, a horizontal sync pulse is transmitted which is an indicator of the end of the line. The blanking interval after the sync pulse is called the back porch where black pixels are also transmitted [40]. In order to display a single frame, all the lines of which the frame consists are transmitted in the active region of the vertical timing. Similar to the horizontal line, black lines will be transmitted in the front porch. Then, a vertical sync pulse is transmitted indicating the end of a frame followed be the back porch. Figure 4.6(a-b) is a timing diagram showing the appropriate timing of the vsync and hsync signals to be outputted with the video signal.

The synchronization signals are also used in order to address the RAM, which contains RGB data which can be manually changed through the software. As shown in Figure 4.9.a, the memory can be addressed either by the counter that is controlled by the horizontal and vertical counters or by the switches that can be manually controlled from the evaluation board by the user. The RGB data is inputted to the other parts of the project units from the data generator along with VGA video output. The interface is shown in Figure 4.9(b-c) where the RGB data from both sources are decoded with 2 to 1 multiplexers that select either source as an input to the next part which is the converter.

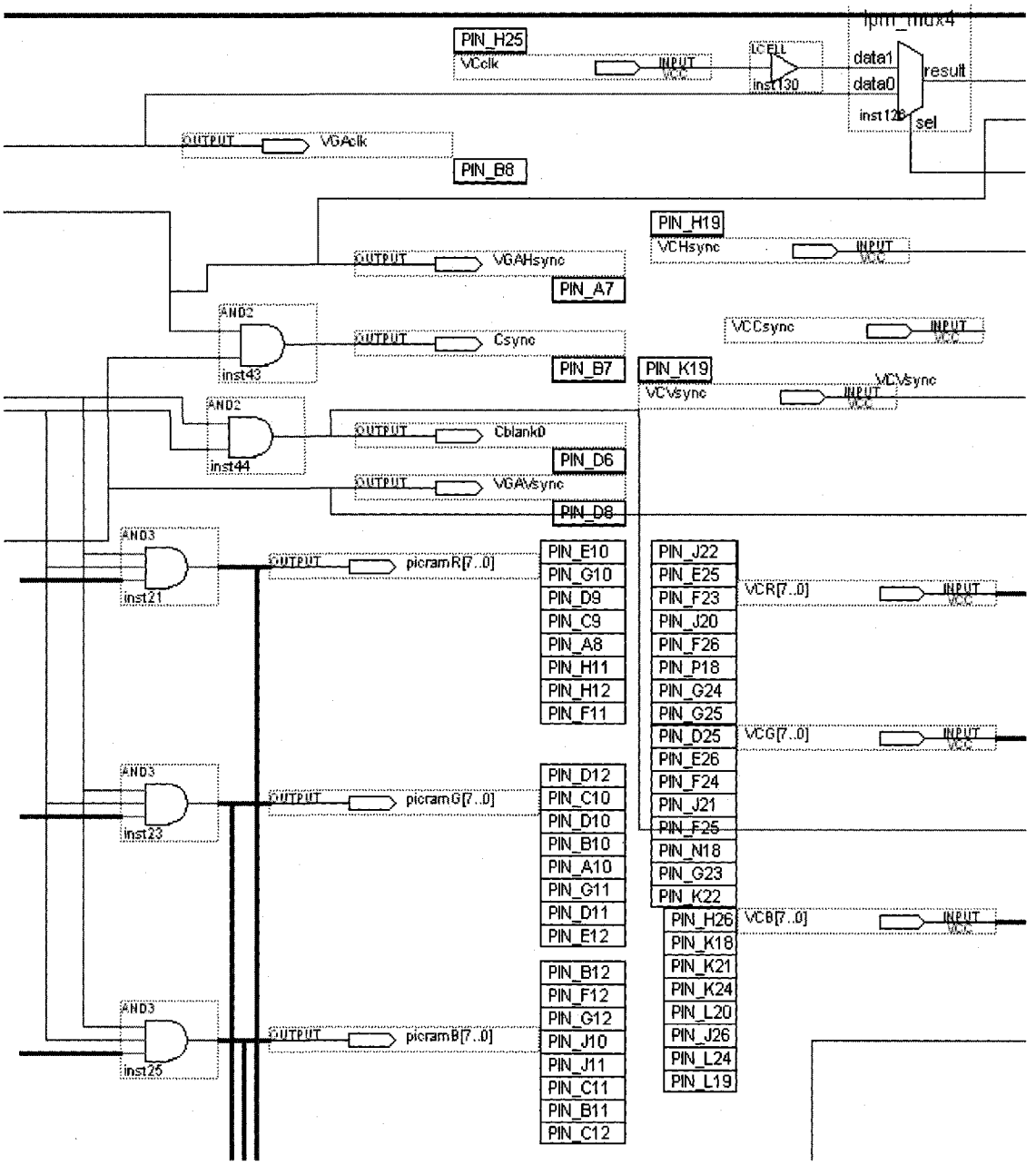

Figure 4.9.b A schematic diagram showing the video input source.

The data of the video input source is taken directly from the SDI which is an 8 bit data stream representing RGB. The desired signal, whether it is the generator or the video is determined by the select line (sel).

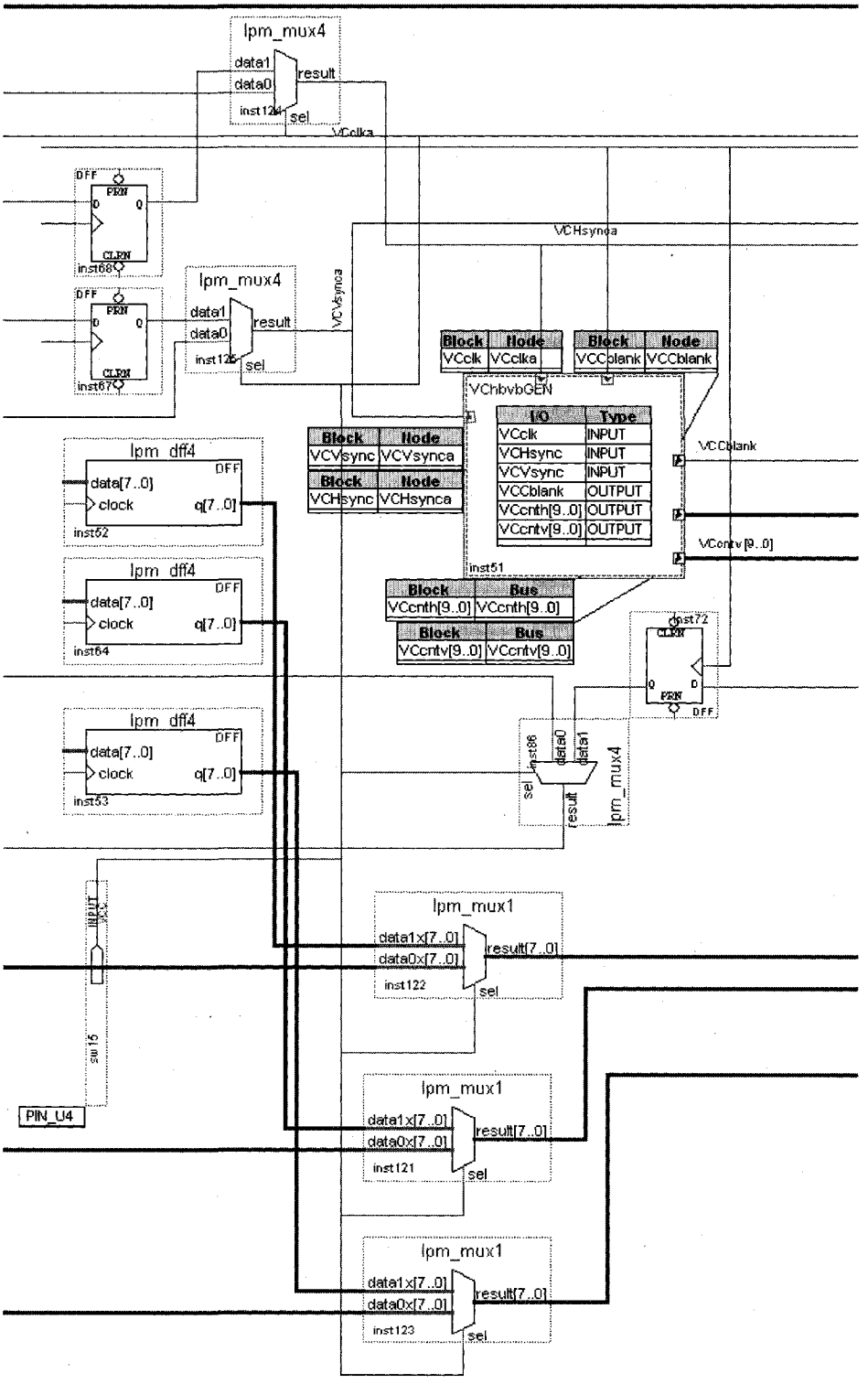

Figure 4.9.c A schematic diagram showing the interface between the input sources and the converter.

After receiving the RGB data from the appropriate source, it is passed to the RGB to RGBW convertor. The data is compared to each other to determine the color with the minimum value as shown in Figure 4.9.d. The logic levels of the comparator's outputs are used along with a lookup table to set the multiplexer to the value that needs to be subtracted from RGB and supplied to the white LED.

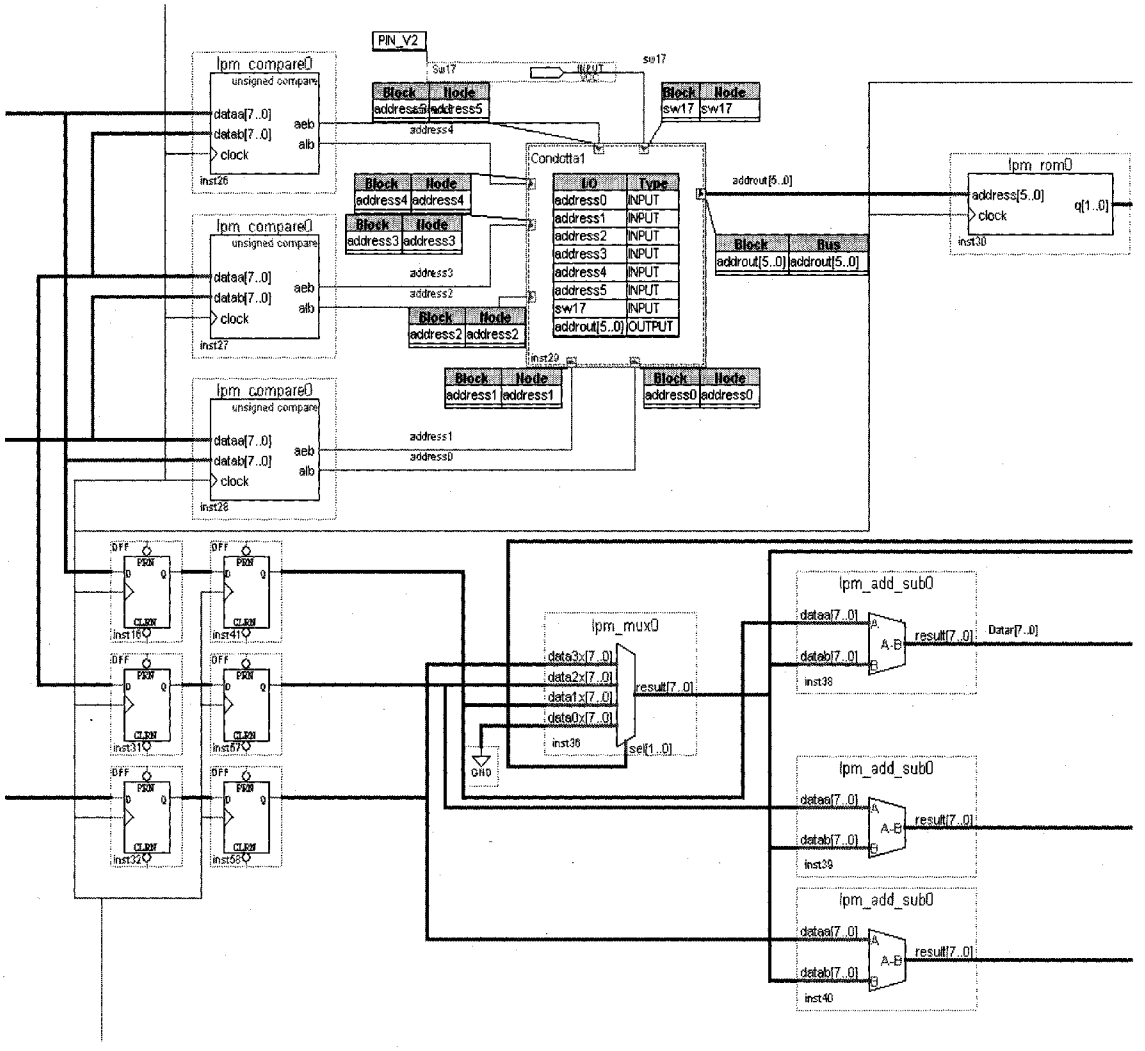

Figure 4.9.d A schematic diagram showing the implementation of the RGB to RGBW converter.

The block in Figure 4.9.e is an implementation of the control signals generation for different parts of the design. These signals include: FIFO memory read enable (FIFOrdEn), dual ported memory stage 1 and 2 read enables, DPst1rdEn and DPst2rdEn, respectively, and the LED display latch and output enables LEDisp and OEDisp, respectively.

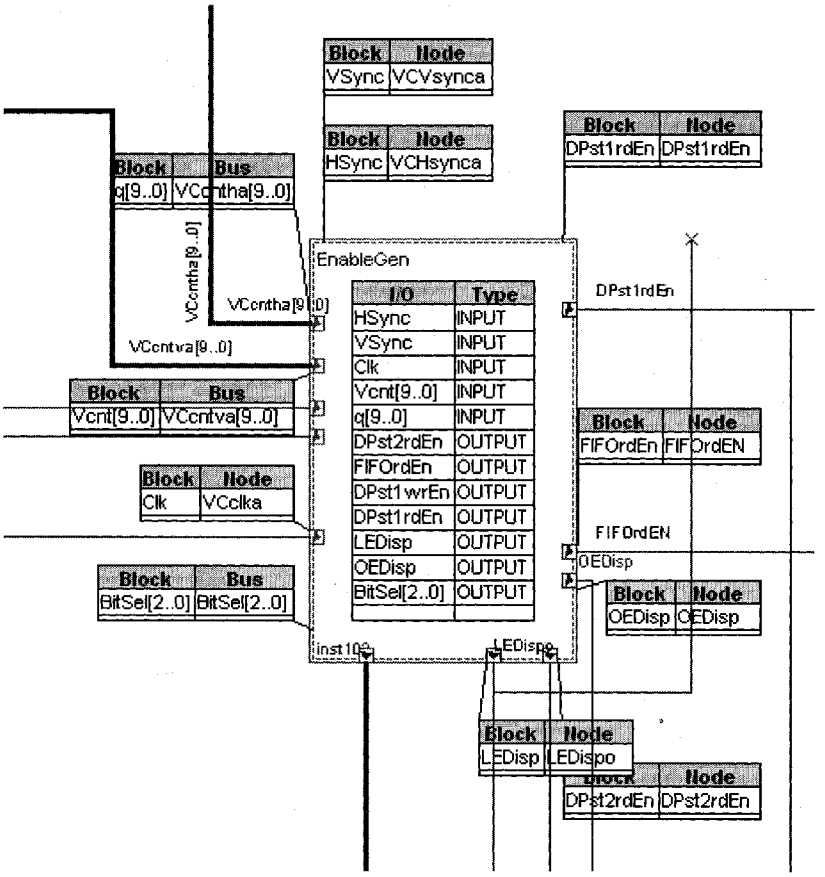

Figure 4.9.e A schematic diagram showing the implementation of the control signals generator.

The order of the data when directly outputted to the prototype the way it is received from the video or generator data stream takes a pattern as shown in Figure 4.8. Therefore,

it was necessary to implement a pixel reordering mechanism.

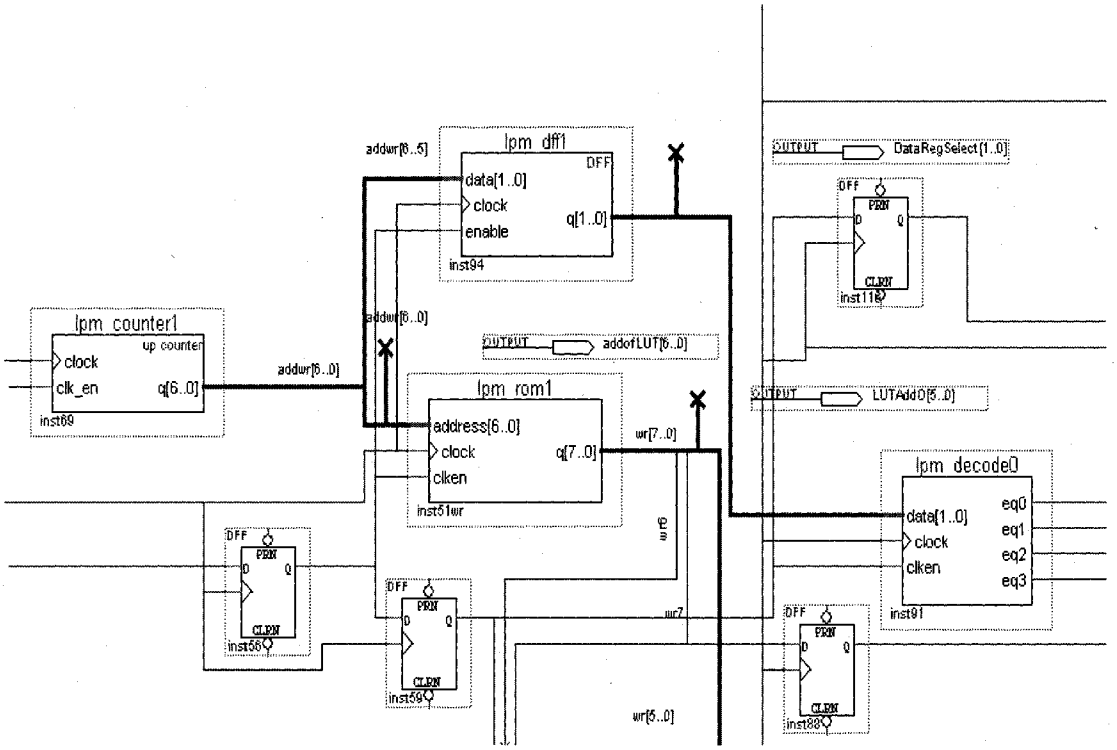

Figure 4.9.f A schematic diagram showing the implementation of the pixel reordering block.

Pixel reordering was done using the enable signals and a lookup table, as shown in Figure 4.9.f. These signals were used to address the dual ported memory shown in Figure 4.9.g. There are three memory stages one is FIFO and the other two stages are dual ported memories. After the RGB to RGBW conversion, the RGBW data is inputted to the FIFO then to the first dual ported memory stage; finally, inputted to the last dual ported memory stage in the desired order, shown in Figure 4.9.h.

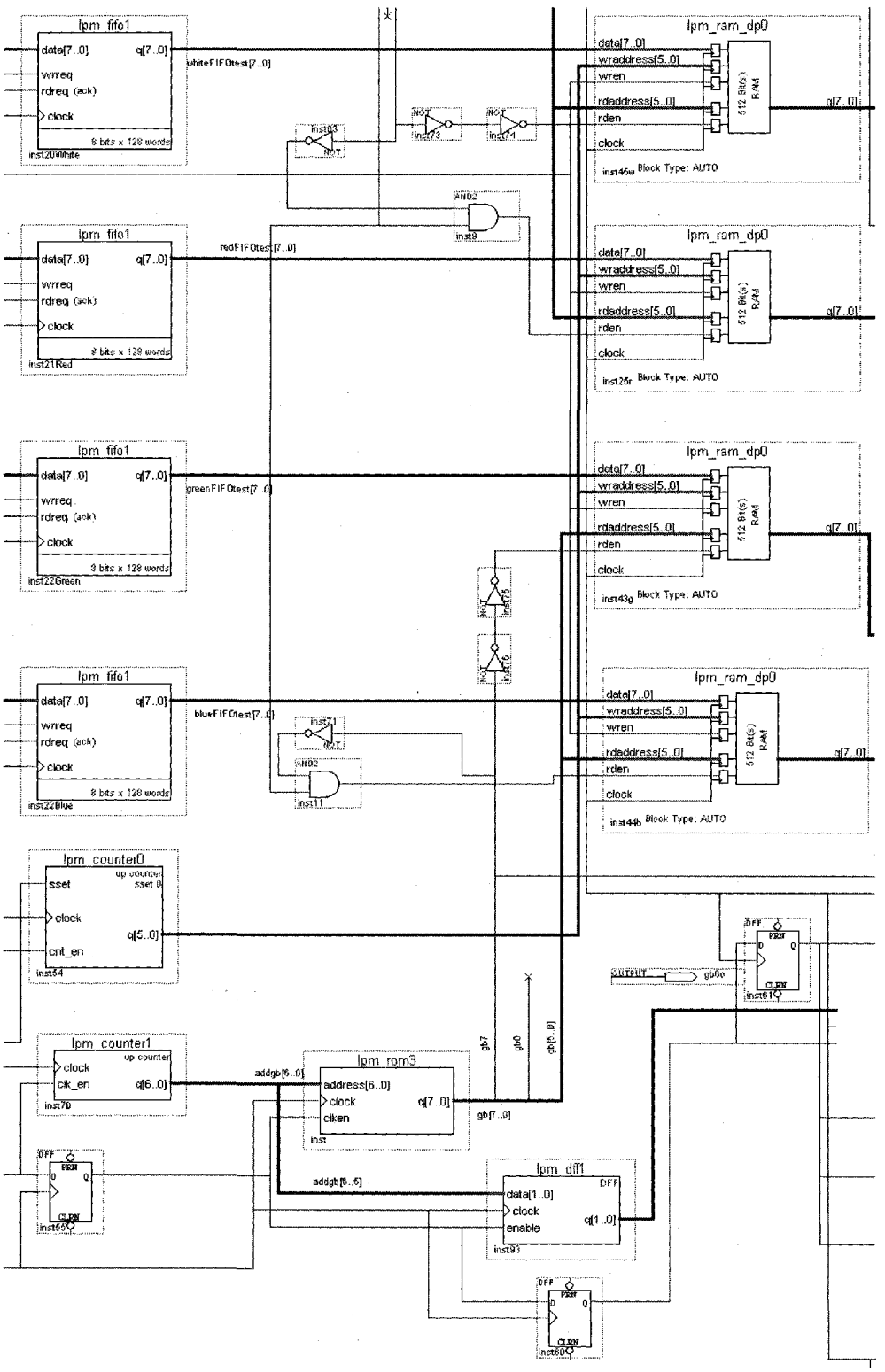

Figure 4.9.g A schematic diagram showing the implementation of the RGBW data processing- stage 1 and 2.

The 8 bit RGBW data lines are pulse width modulated which provides the ability of displaying 256 different intensities. After each bit outputted, latch enable (LE) has to be pulsed once and then output enable (OE) has to be pulsed. The duration of the OE pulse width determines the intensity of the LED; therefore, OE was doubled for every bit so that:

$$OE_{PWbit(x)} = 2 \times OE_{PWbit(x-1)} \tag{4.3}$$

The sample code below shows the settings of the LE, OE, and data output lines for bit 0 (refer to Appendix I for complete code).

```
---------------------------------
DPst2rdv.clk  =     !HSync;
DPst2rdv.j    =     Vcnt[] == 1;
DPst2rdv.k    =     Vcnt[] == 2;
---------------------------------
LEDispdv.clk  =     !HSync;
LEDispdv.j    =     Vcnt[] == 1;
LEDispdv.k    =     Vcnt[] == 2;
---------------------------------
OEDispdv.clk  =     !HSync;
OEDispdv.j    =     Vcnt[] == 2;
OEDispdv.k    =     Vcnt[] == 3;
---------------------------------
```

Figure 4.10 A sample AHDL code showing the settings of the LE, OE, and data output lines for bit 0.

Given that 16.6ms refresh rate has to be maintained, there are access of 431911 clocks in order to complete modulating 8 bit data lines for 64 pixels taking into account a clock period of 0.037μs. the pulse width was increased so that the LEDs will give a linear response with respect to the binary input of the data lines.

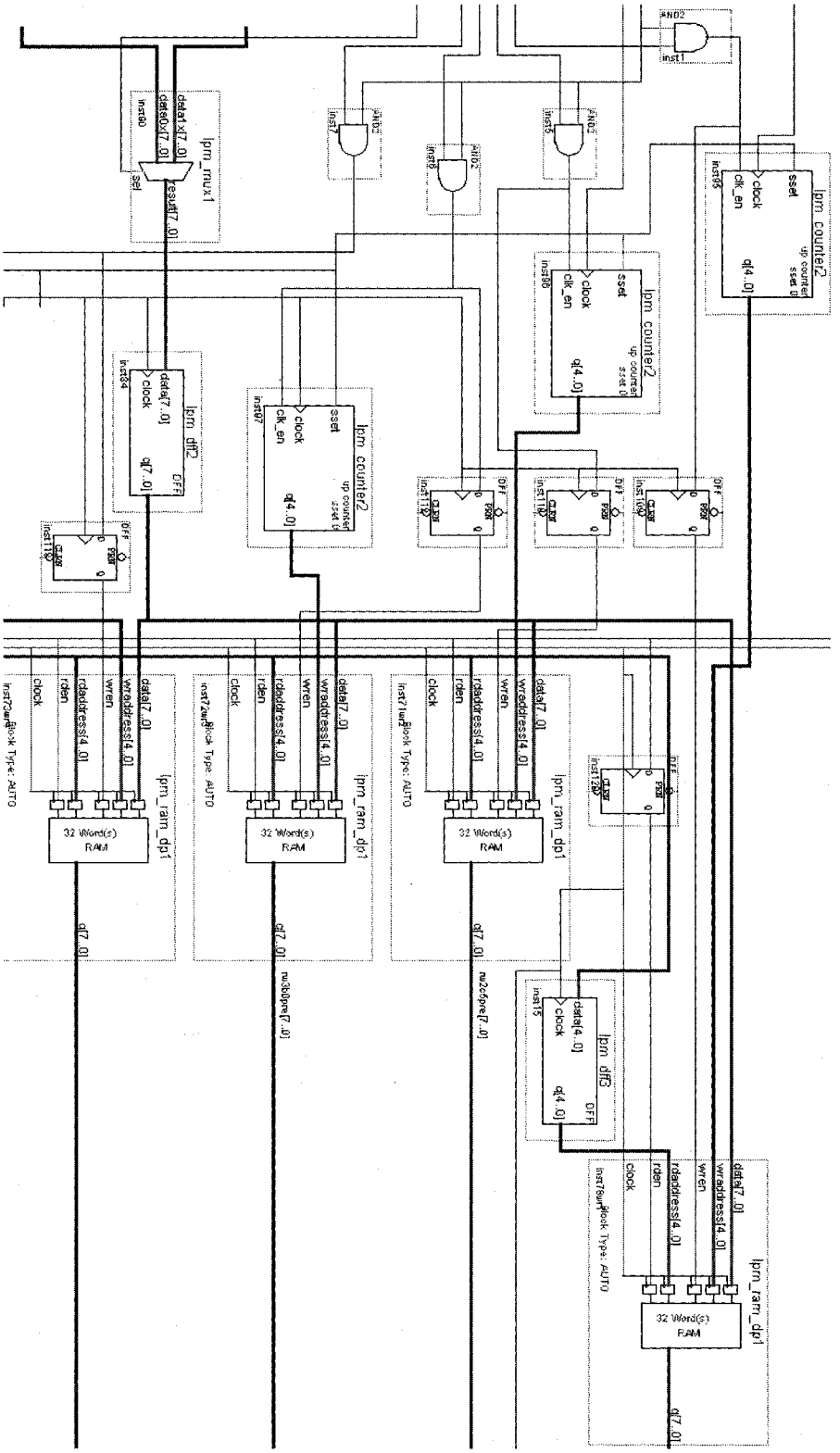

Figure 4.9.h A schematic diagram showing the implementation of the RGBW data processing- stage 3.

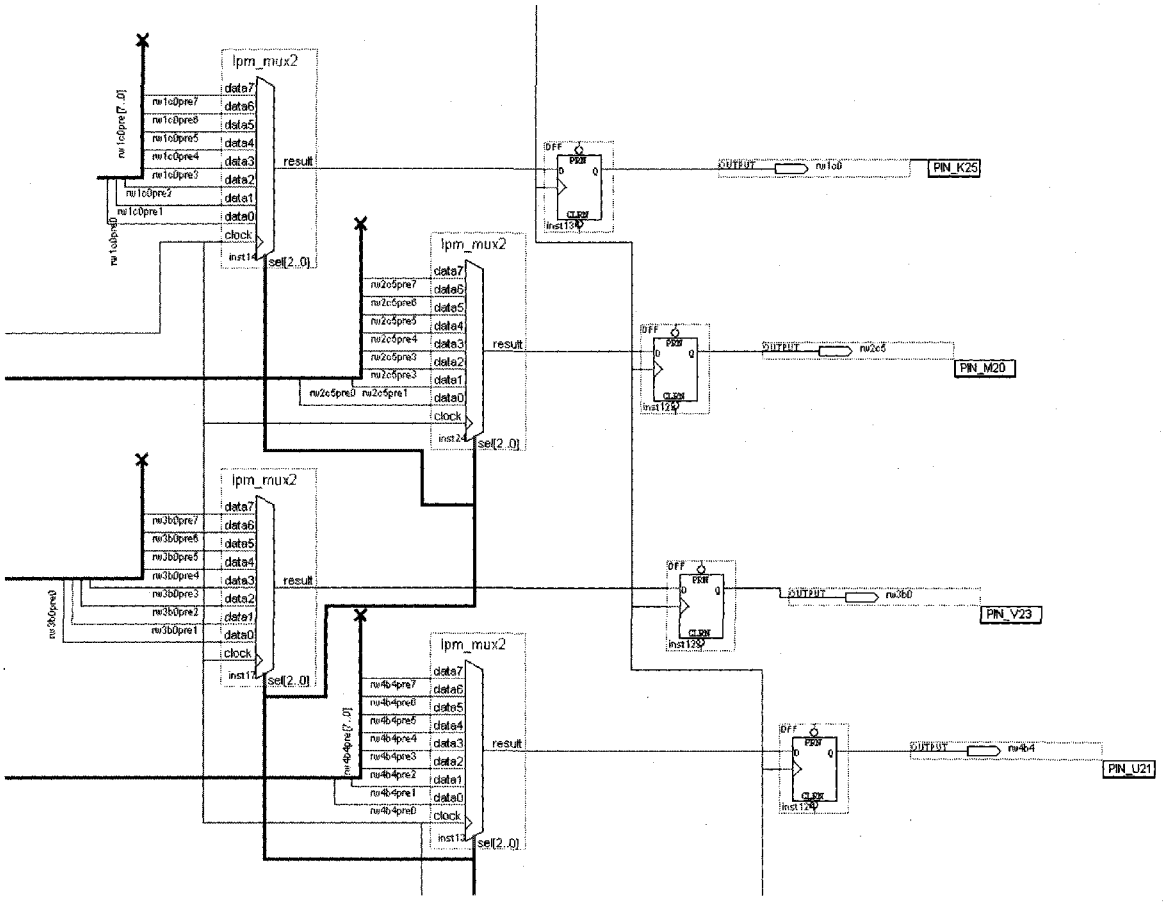

Figure 4.9.i A schematic diagram showing the implementation of the PWM of the RGBW data.

Using an 8 to 1 multiplexer, the appropriate bit is chosen in according to the pulse width of the OE signal, then, finally outputted to the LED display as demonstrated in Figure 4.9.i.

The intensity response was tested for the red, green, blue, and white LEDs using a spectrometer (Ocean Optics USB3000). The spectrometer was placed directly on top of the measured LED where complete stillness was maintained in every part for better accuracy. The results in Figure 4.10(a-d) clearly show a linear response.

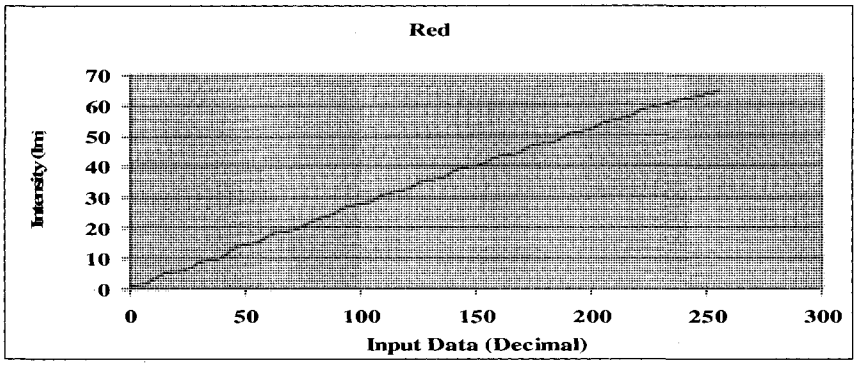

(a)

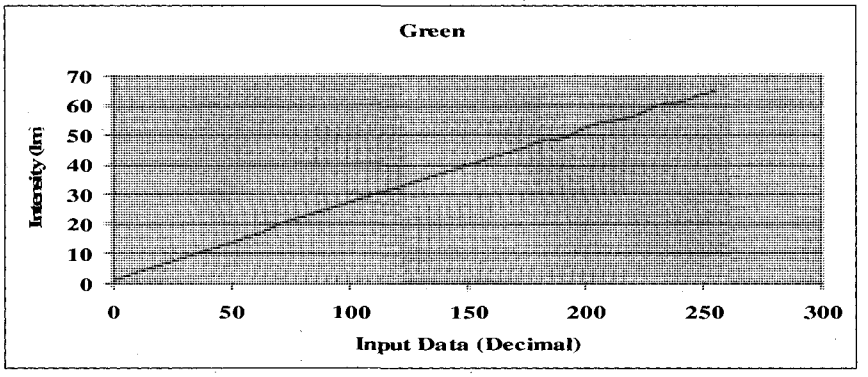

(b)

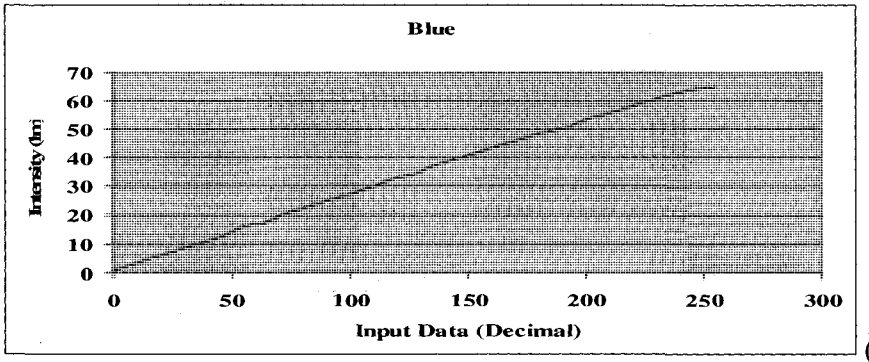

(c)

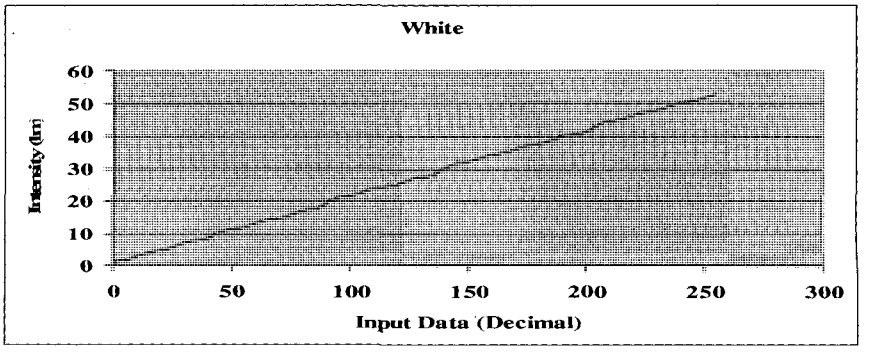

(d)

Figure 4.11 A graph showing the intensity response of the (a) red (b) green (c) blue (d) white LED.

CHAPTER 5

EXPERIMENTS, RESULTS, AND DISCUSSION

In this chapter, results and discussion are presented. Spectroscopic measurements of various colors for RGB and RGBW are shown, compared and contrasted. Details of the experimentation with respect to human perception of color from two different technologies (RGB and RGBW) and energy calculations based on measured currents are presented and discussed.

5.1 Spectroscopic Measurements

Using the spectrometer Ocean Optics USB4000, the spectrum, representing the radiant flux, of the colors generated by RGB is measured and compared to the spectrum of color generated by RGBW. The spectrometer was placed directly after the diffuser attached to the LED display in order to capture the right proportions of the light mixture. A static environment was maintained while measurements were taken. Figure 5.1 shows the spectra of the white light generated using the white LED and RGB LEDs, respectively.

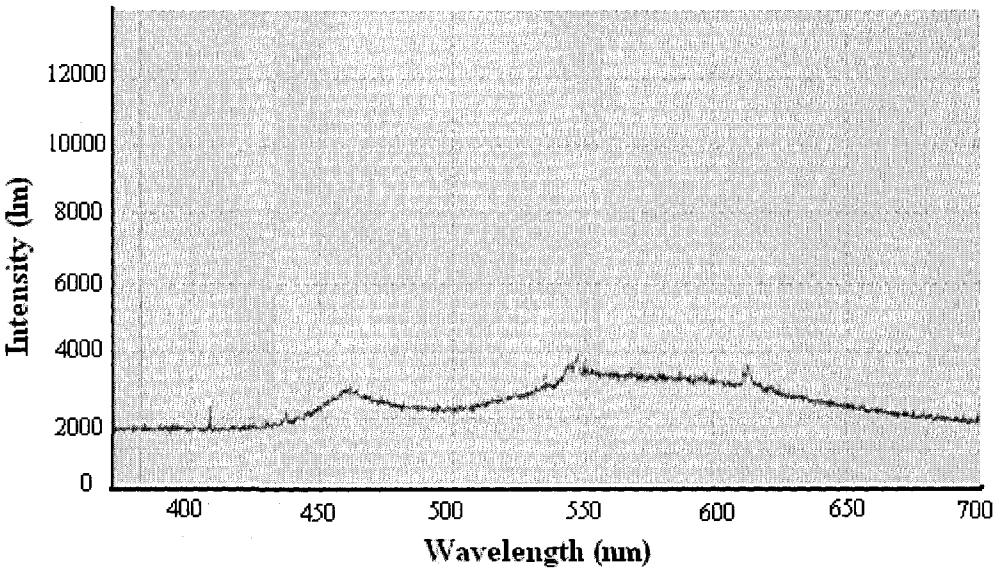

(a)

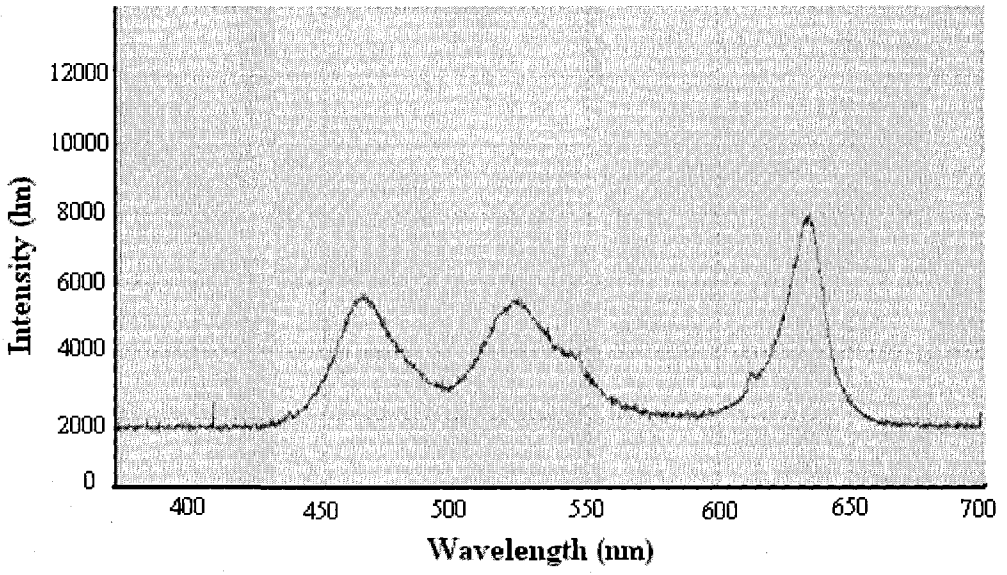

(b)

Figure 5.1. Spectrum of white, intensity with respect to wave length, using (a) RGBW and (b) RGB.

In Figure 5.1 (a), the intensities corresponding to the local maxima wavelengths are as follows: Red (3267 @ 612nm), Green (3647 @ 547nm), and Blue (2911 @ 460nm). On the other hand, the intensities corresponding to the local maxima wavelengths in (b) are: Red (8104 @ 633nm), Green (5297 @ 521nm), and Blue (5729 @ 464nm). The total brightness of white generated by the white LEDs is noticeably on an average less than the total brightness of white generated by RGB since intensity of white in the display prototype used can not be treated as separate from intensity of red LEDs. Furthermore, the intensity distribution among the various wavelengths differs slightly which results in a variation of the white perceived from the two different sources; even though both are perceived as white. This has an effect on the rest of the experimental measurements. The light spectra for three different colors Navy blue, light blue, and Yellow were also measured using RGBW and RGB configuration and are shown in Figures 5.2-4. Also numerical data of peak intensities of the R, G and B with RGBW and RGB configurations are presented in Table 1 confirm our results.

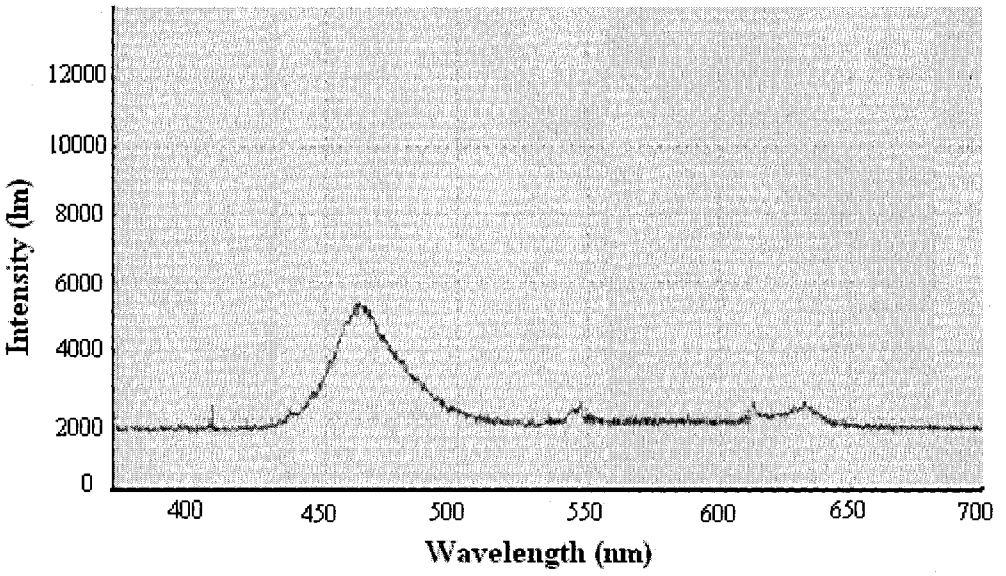

(a)

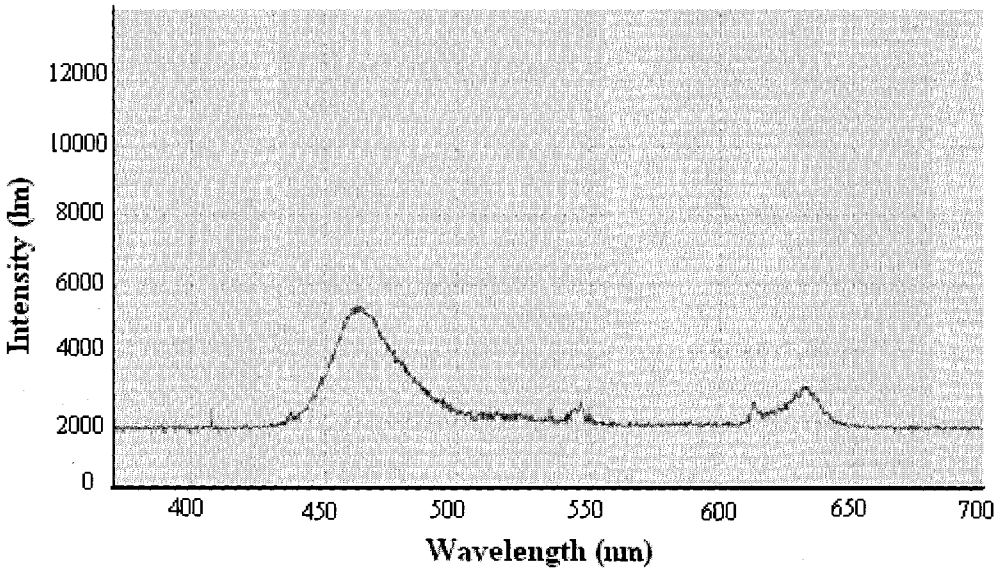

(b)

Figure 5.2. Spectrum of Navy Blue using (a) RGBW and (b) RGB

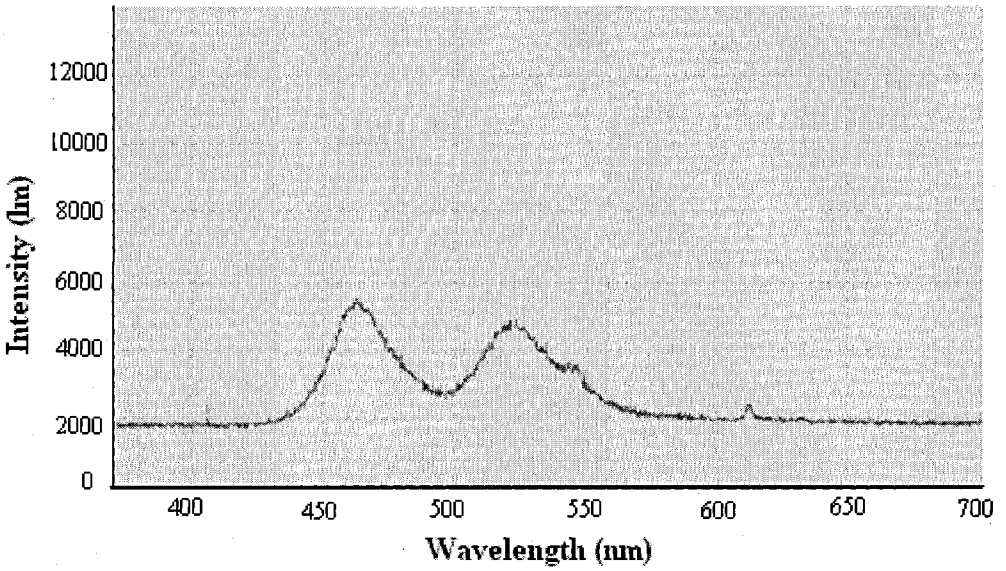

(a)

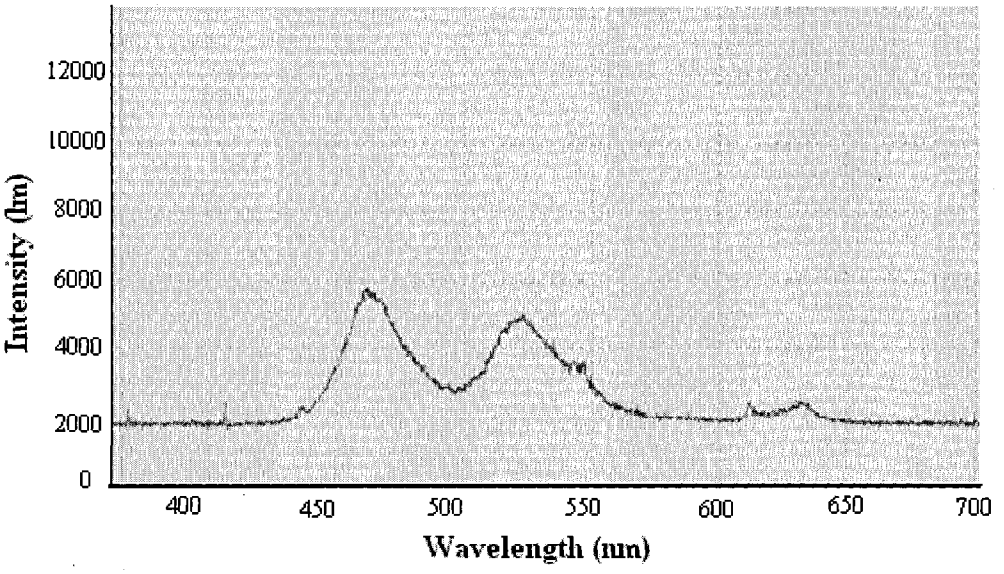

(b)

Figure 5.3. Spectrum of Light Blue using (a) RGBW and (b) RGB

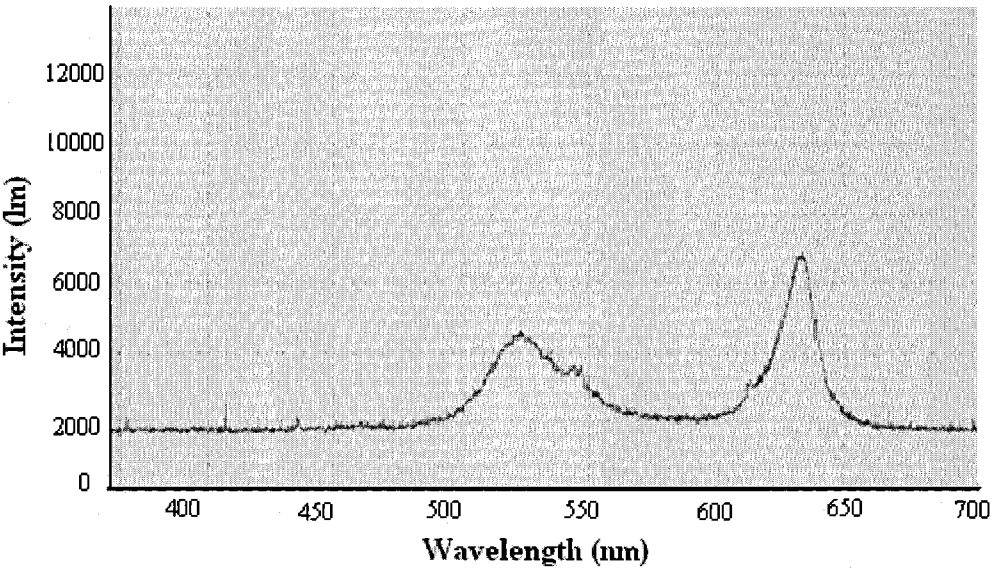

(a)

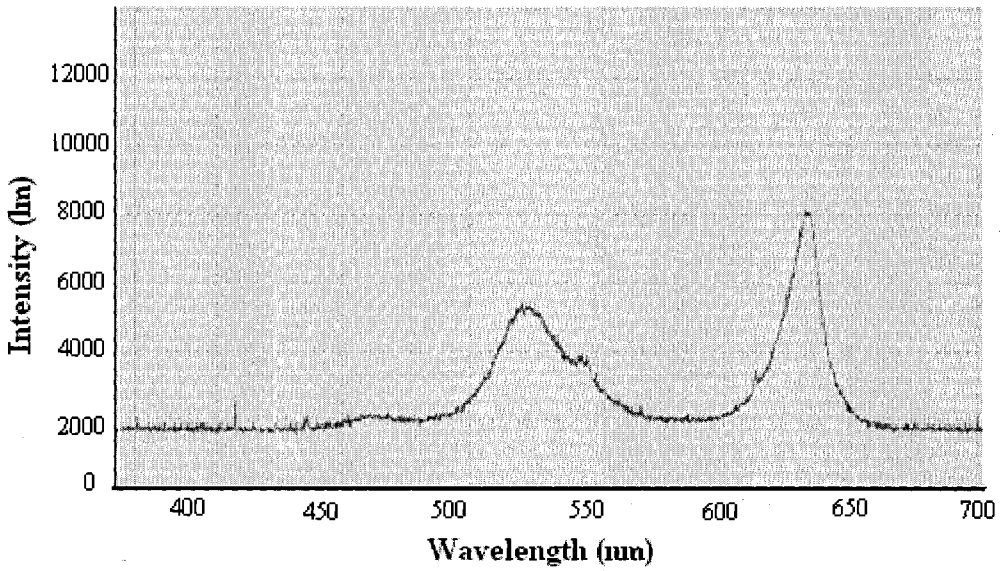

(b)

Figure 5.4. Spectrum of Yellow using (a) RGBW and (b) RGB

Table 5.1. Peak intensities in radiant flux units corresponding to R (612nm), G (547nm) and B(460nm) for RGB and RGBW configurations.

	Navy Blue		**Light Blue**		**Yellow**	
	RGBW	**RGB**	**RGBW**	**RGB**	**RGBW**	**RGB**
R	2471	2910	1742	2330	7018	7621
G	1742	2176	4642	4863	4480	5321
B	5286	5341	5397	5870	1742	2078

Table 5.1 shows the monochromatic intensity measurements at the primary colors for RGB and RGBW. These values are obtained from the spectrometer readings shown in Figures 5.2 - 5.4. From the figures, it is clear that the intensity spectrum distributions of the measured colors are very similar in wave form. The values in Table 5.1 demonstrate the colors to have the same proportions among the monochromatic waves for every primary color (RGB) which shows that the colors displayed using RGB have the same hue as the colors displayed using RGBW; however, it is noticeable that the overall intensity of the spectra exhibits a small difference between the RGB and RGBW. This is due to the architecture of the prototype, which does not allow a separate calibration control for the white LEDs.

5.2 Human Perception Experiments

5.2.1 Experimental Procedure

This part of the study required a special approval (refer to Appendix II) since human subjects were involved. In order to test how people perceive the difference between the old (RGB) and the new (RGBW) LED display architectures, it was necessary to conduct

an experimental survey involving a sample of people. To obtain the approval, the Institutional Review Board (IRB) reviews the research project which involves human subjects to ensure subjects are not at unjustified risk and that test subjects are given informed consent at the time of participation. Furthermore, researches have to undergo IRB training through the collaborative institutional training initiative (CITI) which offers different types of training. This requirement is designed to provide information and guidance to researchers in order to minimize risks.

Subjects were selected at random; recruiting was done at UNLV, an educational institution; therefore, majority of subjects were students between the ages of 18 and 30. Vast majority of students were willing to take the survey directly after briefly explaining to them about the experiment. They were told that they would have to compare colors displayed using an LED display and make a note of differences they notice. Upon their arrival to the laboratory were the experiment was conducted, more detailed instructions were given to them as well as a handout that contains detailed directions (refer to Appendix III for the informed consent), the approval and the survey questions (refer to Appendix IV).

Twelve pairs of different colors were tested. The colors fall into three groups, gray scale, low saturation, and high saturation. Every subject was shown pairs of colors and asked to determine whether the colors are:

(a) Identical = 98% or more similarity

(b) Almost the same = 90% or more similarity (the same hue)

(c) Not the same at all = less than 90%

(d) Unsure

Three different sets of experiments were conducted. In the first set, the experimental group, each color was displayed twice once with RGB and once with RGBW. There were 100 subjects in this category. In the second set, each color was displayed twice with RGB. This set is one of the control groups and had 20 subjects. In the third set, each color was displayed twice with RGBW and it is the second control group which also had 20 subjects. The purpose of the control groups of sets 2 and 3 was to assess the reliability or consistency of the results obtained in set 1.

5.2.2 Results and Discussion

Data of human perception for gray scale, low saturation colors, and high saturation colors are shown in Tables 5.2 – 5.4, respectively.

Table 5.2 Human Perception data for gray scale (i) White (ii) Gray and (iii) Dark Gray where (a) Identical, (b) Almost the same, (c) Not the same, (d) Unsure

White	**a**	**b**	**c**	**d**	**Total**
RGB-RGBW	7	37	56	0	100
RGB	15	5	0	0	20
RGBW	14	6	0	0	20

(i)

Gray	**a**	**b**	**c**	**d**	**Total**
RGB-RGBW	3	31	66	0	100
RGB	13	6	1	0	20
RGBW	11	9	0	0	20

(ii)

Dark Gray	**a**	**b**	**c**	**d**	**Total**
RGB-RGBW	10	55	35	0	100
RGB	10	8	2	0	20
RGBW	12	7	1	0	20

(iii)

In the experiment involving gray scale, it appears that most subjects perceived colors to be not the same. For the same reasons mentioned in section 5.1 which confirms the data obtained from the spectrometer. Due to the architecture of the prototype, which does not allow a separate calibration control for the white LEDs, gray scale shows the most inconsistent data.

Table 5.3 Human Perception data for low saturated colors (i) Purple (ii) Purplish Blue (iii) Medium Green and (iv) Yellow where (a) Identical, (b) Almost the same, (c) Not the same, (d) Unsure.

Purple	**a**	**b**	**c**	**d**	**Total**
RGB-RGBW	10	72	18	0	100
RGB	6	10	4	0	20
RGBW	13	6	1	0	20

(i)

Purplish Blue	**a**	**b**	**c**	**d**	**Total**
RGB-RGBW	16	65	19	0	100
RGB	11	9	0	0	20
RGBW	13	7	0	0	20

(ii)

Medium Green	**A**	**b**	**c**	**d**	**Total**
RGB-RGBW	25	68	7	0	100
RGB	12	8	0	0	20
RGBW	14	6	0	0	20

(iii)

Yellow	**a**	**b**	**c**	**d**	**Total**
RGB-RGBW	15	68	17	0	100
RGB	12	8	0	0	20
RGBW	13	6	1	0	20

(iv)

Most subjects found low saturated colors to be almost the same. Keeping in mind that

low saturation is equivalent to a high white value in the color, it is expected of test subjects to notice a minor difference between the RGB and RGBW colors.

Table 5.4 Human Perception data for high saturated colors (i) Rose (ii) Violet (iii) Cyan (iv) Green and (v) Orange where (a) Identical, (b) Almost the same, (c) Not the same, (d) Unsure

Rose	**a**	**b**	**c**	**d**	**Total**
RGB-RGBW	59	39	2	0	100
RGB	12	8	0	0	20
RGBW	12	8	0	0	20

(i)

Violet	**A**	**b**	**c**	**d**	**Total**
RGB-RGBW	62	36	2	0	100
RGB	10	9	1	0	20
RGBW	15	5	0	0	20

(ii)

Cyan	**A**	**b**	**c**	**d**	**Total**
RGB-RGBW	73	26	1	0	100
RGB	13	7	0	0	20
RGBW	16	4	0	0	20

(iii)

Green	**A**	**b**	**c**	**d**	**Total**
RGB-RGBW	48	52	0	0	100
RGB	15	4	1	0	20
RGBW	16	4	0	0	20

(iv)

Orange	**A**	**b**	**c**	**d**	**Total**
RGB-RGBW	35	61	4	0	100
RGB	10	9	1	0	20
RGBW	17	3	0	0	20

(v)

Most subjects found high saturated colors to be identical or almost the same. On the contrary of low saturation, high saturation means a low white value in the color;

therefore, it is expected of test subjects to hardly notice any difference between the RGB and RGBW colors.

5.2.3 Statistical Analysis

5.2.3.1 Theory of Statistical Analysis

The binomial probability model is appropriate for the data collected from Experiments 1, 2, and 3, as the following will show. Let X denote the number of subjects out of N_j for Experiment j (j = 1, 2, 3) who thought that the colors produced were 'Identical or Almost the Same'. The probability distribution of X then can be modeled by the binomial probability distribution:

$$P(X=x)=\binom{N}{x}p_j^x(1-p_j)^{N-x}, x=1,2,...,N \quad (5.1)$$

where pj is the proportion of subjects in the population who think that the colors produced in two trails are 'identical or almost the same'. The population proportion p_j is estimated by the sample proportion

$$\hat{p}_j=\frac{x_j}{N_j} \quad (5.2)$$

where x_j is the number of subjects who thought the colors in two trials were identical, for experiment j (j = 1, 2, 3). Confidence intervals for p_j can be computed using the following approximate formula for 95% confidence:

$$p_j(95\%Confidence-Intervals)=\hat{p}_j\pm 1.96\times\sqrt{\frac{\hat{p}_j(1-\hat{p}_j)}{N_j}} \quad (5.3)$$

Exact confidence intervals can also be calculated using the software package MINITAB. The later approach is used in this work. The 95% confidence interval for p_j

has the property that the repeated use of the formula for computing the 95% confidence interval, over similar experiments, will contain the true unknown p_j 95% of the time.

5.2.3.2 Data Analysis

Using data presented in Table 5.2 and equation 5.3 the estimate, p_j and the upper and lower 95% confidence intervals were calculated using MINITAB and reported in Table 5.5 for white, gray, and dark gray. The data for "almost the same" and "Identical" were combined to obtain the estimate, p_j. Thus, values of $\hat{p}_j$ indicate that the pair of colors appear the same. The 95% confidence intervals (U95, L95) indicate the spread or the variability of data.

Table 5.5 $\hat{p}$, L95, and U95 values after the statistical analysis of the data for gray scale.

	White			Gray			Dark Gray		
	RGB/W	**RGB**	**W**	**RGB/W**	**RGB**	**W**	**RGB/W**	**RGB**	**W**
L95	0.34	0.86	0.86	0.25	0.75	0.86	0.55	0.68	0.75
$\hat{p}$	0.44	1	1	0.34	0.95	1	0.65	0.9	0.95
U95	0.54	1	1	0.44	0.99	1	0.74	0.99	0.99

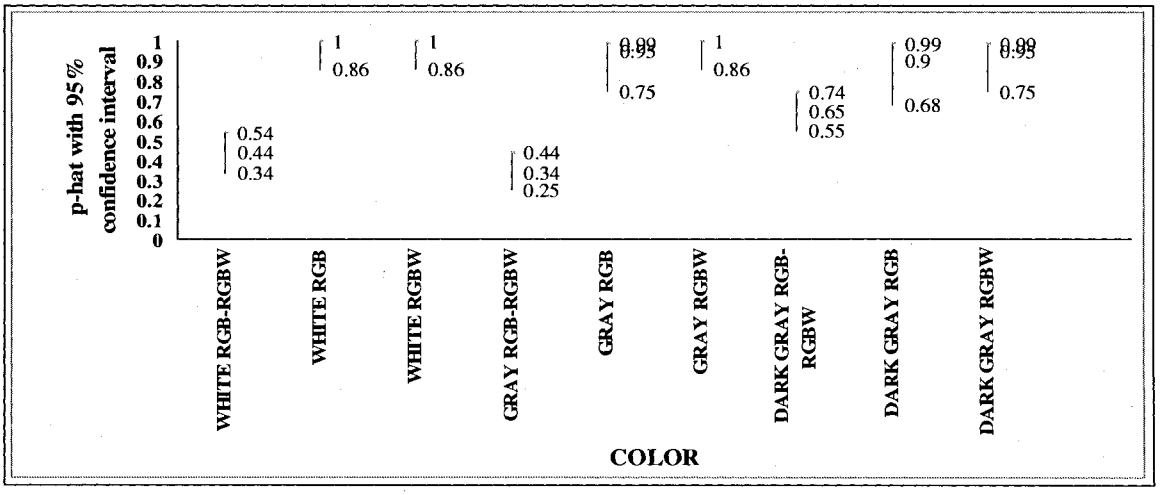

Figure 5.5 Estimate, $\hat{p}$, with 95% confidence interval for White, Gray, and Dark Gray.

It appears that white color created by RGB, as shown in Table and Figure 5.5, is perceived the same as that by RGBW only to 44% ± 10% of the subjects and only 34% ± 10% for gray. The reason for obtaining percentages below 50% stems from the fact that the white LEDs in the prototype that was used for this experiment did not have independent intensity control; thus, maintaining an equivalent intensity between the two whites was a challenge. Since gray has low saturation, the amount of white in it is fairly high, which explains why the data is below 50%. For dark gray, however, the percentage of subjects that found the colors generated by RGB and RGBW to be the same significantly increased to be 65% +9% /-10% since the white level decreases for high saturated colors.

Table 5.6 $\hat{p}$, L95, and U95 values after the statistical analysis of the data for low saturated colors.

	Purple			Purple Blue			Medium Green		
	RGB/W	**RGB**	**W**	**RGB/W**	**RGB**	**W**	**RGB/W**	**RGB**	**W**
L95	0.73	0.56	0.75	0.72	0.86	0.86	0.86	0.86	0.86
$\hat{p}$	0.82	0.8	0.95	0.81	1	1	0.93	1	1
U95	0.89	0.94	0.99	0.88	1	1	0.97	1	1

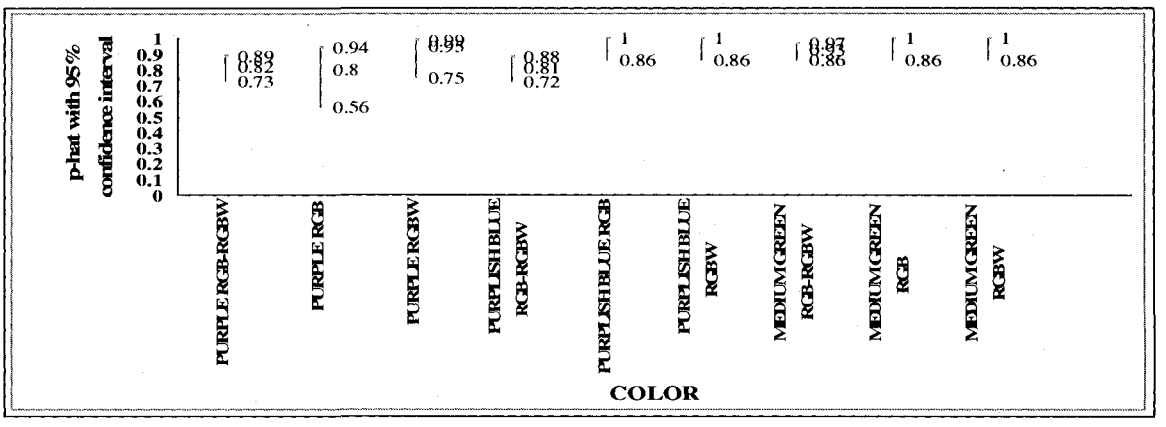

Figure 5.6 Estimate, $\hat{p}$, with 95% confidence interval for Purple, Purplish blue, and Medium Green.

As shown in Figure 5.2 and Figure 5.3, the percentages are dramatically improved compared to the gray scale. 82% (+6% /-9%) of test subjects for purple, 81% (+7% /-9%) for purplish blue, and 93% (+4% /-7%) for medium green found the difference between RGB and RGBW to be "almost the same or identical". This increase in percentage was expected since adding the right amount of white, as it was illustrated in the previous chapter section 4.3, does not change the hue of the perceived color.

Table 5.7 $\hat{p}$, L95, and U95 values after the statistical analysis of the data for yellow and high saturated colors.

	Yellow			Rose			Violet		
	RGB/W	**RGB**	**W**	**RGB/W**	**RGB**	**W**	**RGB/W**	**RGB**	**W**
L95	0.74	0.86	0.75	0.93	0.86	0.86	0.93	0.75	0.86
$\hat{p}$	0.83	1	0.95	0.98	1	1	0.98	0.95	1
U95	0.89	1	0.99	0.99	1	1	0.99	0.99	1

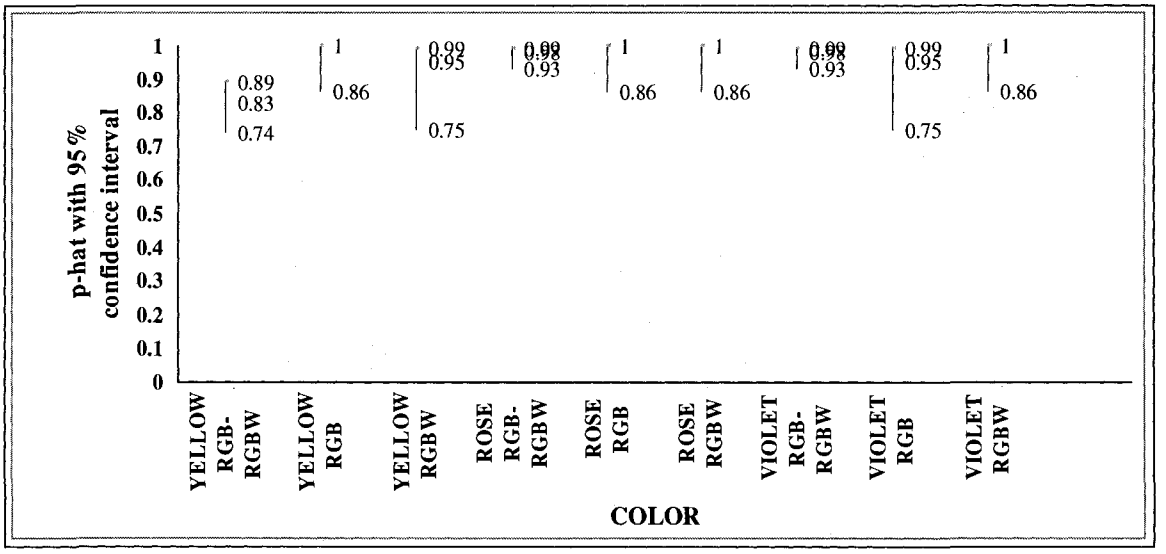

Figure 5.7 Estimate, $\hat{p}$, with 95% confidence interval for Yellow, Rose, and Violet.

The percentages for high saturated colors, as shown in Table 5.7-5.8 and Figure 5.7-

5.8, seem to be very promising obtaining more than 95%. It is shown that 98% (+0% /-5%) of test subjects for rose, 98% (+0% /-5%) for violet, 99% (+0% /-4%) for CYAN, 100% (+0% /-3%) for green, and 96% (+2% /-6%) for orange found almost no difference between the colors when displayed using RGB and RGBW. This indicates that it is very difficult to differentiate between the two architectures (RGB and RGBW) for high saturated colors since the amount of white used in high saturated colors is minimal.

Table 5.8 $\hat{p}$, L95, and U95 values after the statistical analysis of the data for high saturated colors

	Cyan			Green			Orange		
	RGB/W	**RGB**	**W**	**RGB/W**	**RGB**	**W**	**RGB/W**	**RGB**	**W**
L95	0.95	0.86	0.86	0.97	0.75	0.86	0.9	0.75	0.86
$\hat{p}$	0.99	1	1	1	0.95	1	0.96	0.95	1
U95	0.99	1	1	1	0.99	1	0.98	0.99	1

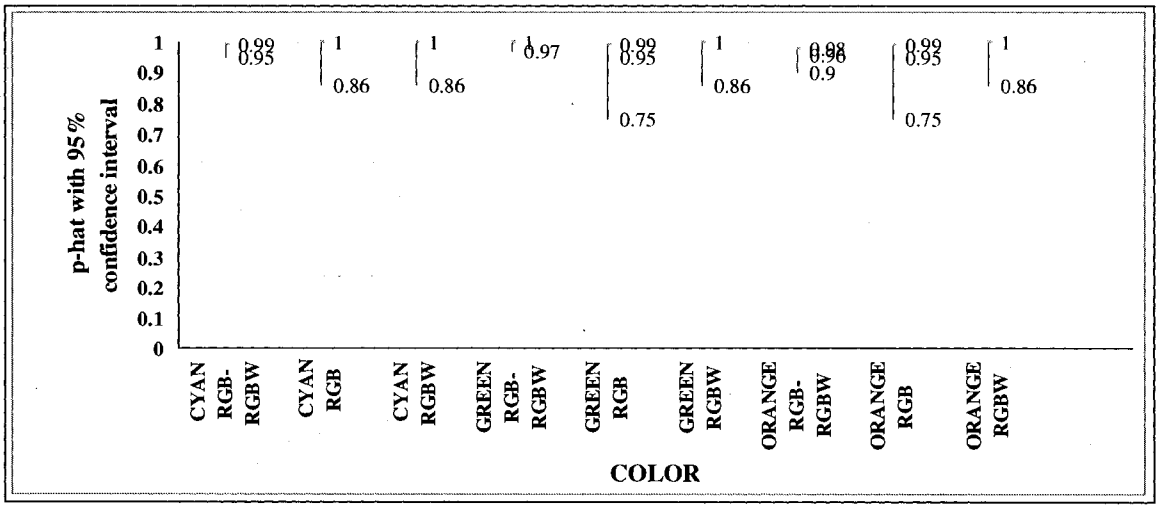

Figure 5.8 Estimate, $\hat{p}$, with 95% confidence interval for Cyan, Green, and Orange.

5.3 Energy Measurements and Calculations

5.3.1 Experimental Procedure

Since the power consumed is directly proportional to current supplied due to constant voltage, twelve pairs of different colors are tested. The colors are divided into three groups gray scale, low saturation, and high saturation. For every pair, the current supplied to the 8x8 pixel display is measured twice once for RGB and once for RGBW.

5.3.2 Results and Discussion

The currents consumed by the 8x8 pixel LED display are measured for the twelve pairs of colors using RGB and RGBW and listed in Table 5.9. It is noted that the current values are in the range of 0.63 - 1.78A where the highest values are consumed by white and the lowest values by dark gray.

Table 5.9 Measured currents for RGB, RGBW

	I (RGB) [A]	**I (RGBW) [A]**
White	1.78	0.91
Gray	1.4	0.93
Dark Gray	0.66	0.39
Purple	1.32	0.88
Purplish Blue	0.92	0.63
Medium Green	1.21	0.7
Yellow	1.27	0.86
Rose	1.06	0.91
Violet	1.16	1.06
Cyan	1.27	1.16
Green	1.15	1
Orange	1.24	1.16

5.3.3 Data Analysis

The power consumed by the LED display, P, is given by:

$$P = V \times I \tag{5.4}$$

where V is the voltage supplied to the device, and I is the Current through the device. In this study, the voltage of operation used was 5v which is the required voltage by the system.

The percentage of power savings as a result of using RGBW instead of RGB, P_s, is given by:

$$\% P_s = (P_{RGB} - P_{RGBW}) / P_{RGB} \times 100 \tag{5.5}$$

Table 5.10 Power consumed by pixels for RGB, RGBW and % power savings of RGBW over RGB.

	P (RGB) [W]	**P(RGBW) [W]**	**P savings %**
White	5.87	3.00	49
Gray	4.62	3.07	34
Dark Gray	2.18	1.29	41
Purple	4.36	2.90	33
Purplish Blue	3.04	2.08	32
Medium Green	3.99	2.31	42
Yellow	4.19	2.84	32
Rose	3.5	3.00	14
Violet	3.83	3.5	9
Cyan	4.19	3.83	9
Green	3.8	3.3	13
Orange	4.09	3.83	6

Using the data reported in table 5.9 and the equations 5.4 and 5.5, P_{RGB}, P_{RGBW}, and $\%P_s$ were calculated and reported in Table 5.10 for twelve colors. % power saving for various colors is plotted in Figure 5.9

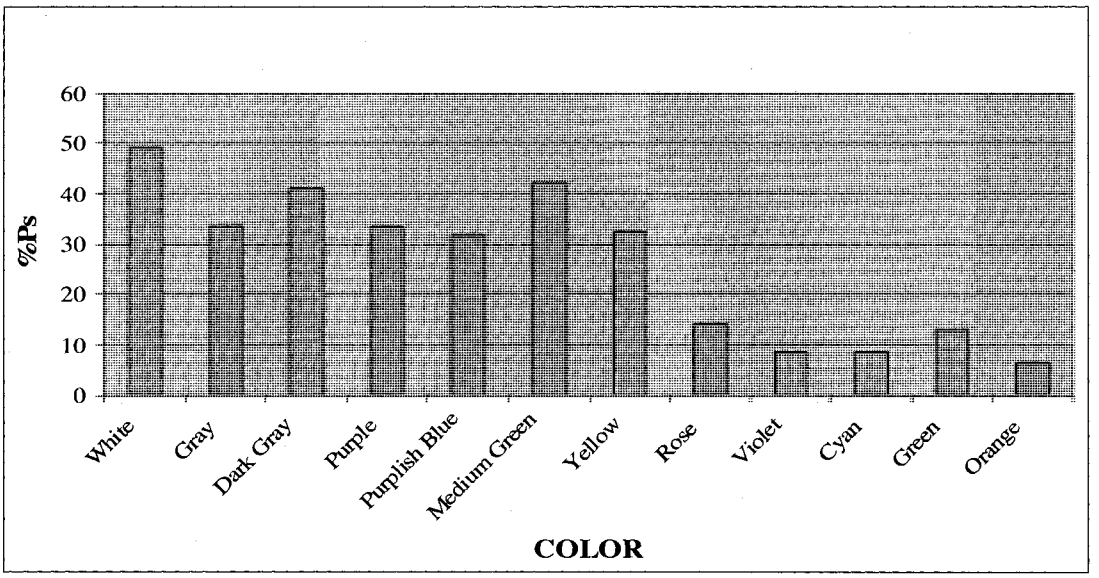

Figure 5.9 The % power savings for twelve colors

The data presented in Figure 5.9 shows power savings that ranges between 30% and 50% for gray scale and low saturated colors (purple, purplish blue, medium green, and yellow). Power savings for high saturated colors, such as rose, violet, cyan, green, and orange, is much lower than power savings for the gray scale and the low saturated colors. The low percentages for high saturated colors stems from the fact that the compensating white level of such colors is minimal. As expected, using the new RGBW pixel architecture saves power in most cases, i.e., gray scale, high saturation, and low saturation colors.

5.4 Colors from Display

Photographs were taken of twelve different colors generated by RGB and RGBW and are displayed next to one another in Figures 5.10-5.12. Photograph in (a) corresponds to

RGB and that in (b) corresponds to RGBW.

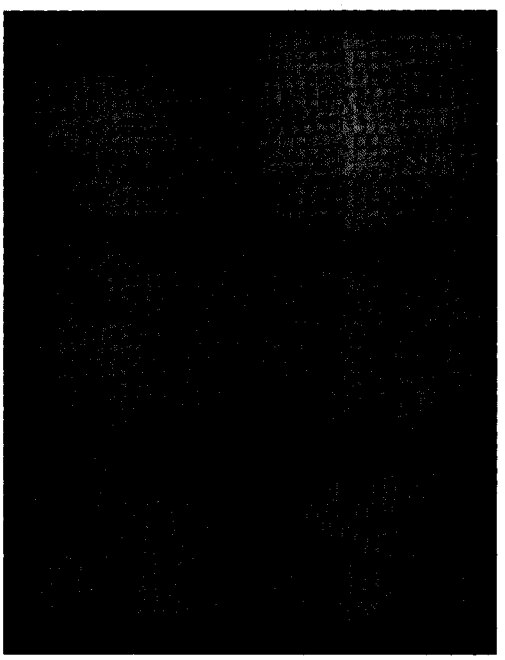

Figure 5.10 A photograph of gray scale colors from (a) RGB (b) RGBW (i) white (ii) gray (iii) dark gray.

For the photograph of gray scale shown in Figure 5.10, it is noted that colors displayed with RGB seem to be slightly brighter than colors displayed with RGBW. This is due to the fact that the white generated from RGB and the white generated from RGBW are some what different as seen in the spectrometer reading in Figure 5.1. Column (a) seems to be brighter than (b).

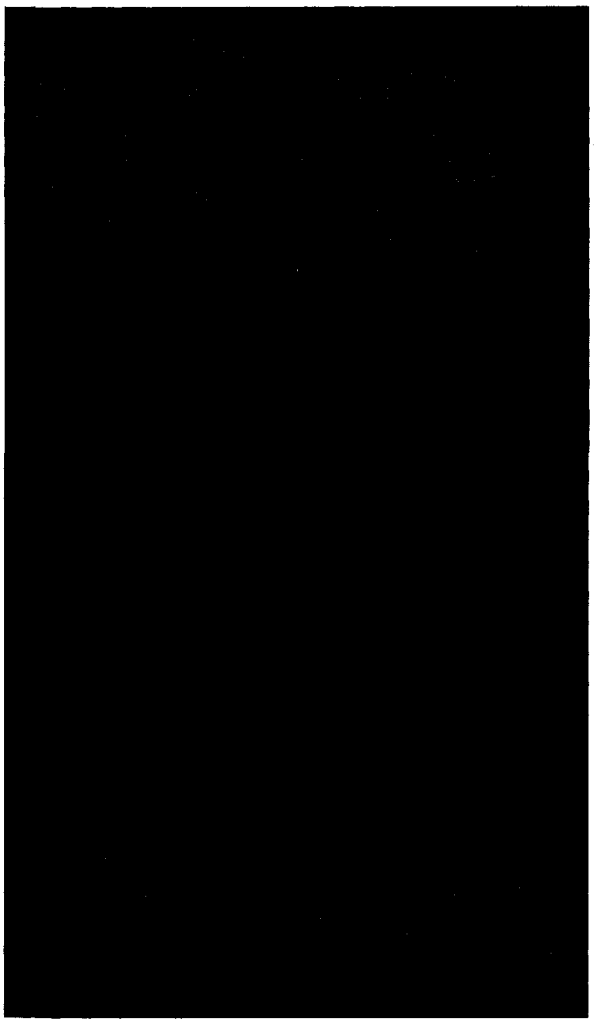

Figure 5.11 A photograph of low saturated colors from (a) RGB (b) RGBW (i) purple (ii) purplish blue (iii) medium green (iv) yellow.

Low saturated colors are shown in Figure 5.11. Photographs for RGB and RGBW for all colors appear to be very close; however, it is noticeable that column (a) is brighter than column (b) since the component of white is high in low saturated colors. A photograph of high saturated colors is shown in Figure 5.12. Colors in this photograph are also indistinguishably similar since the white component is low for this category of

colors.

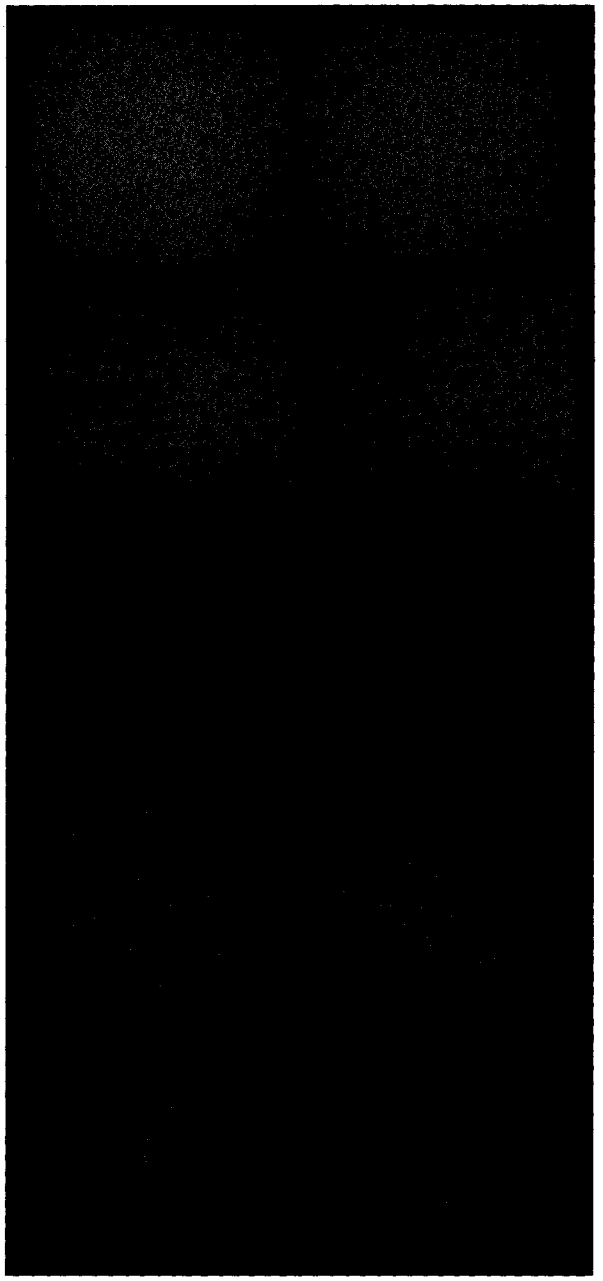

Figure 5.12 A photograph of high saturated colors from (a) RGB (b) RGBW (i) rose (ii) violate (iii) cyan (iv) green (v) orange.

CHAPTER 6

CONCLUSIONS AND RECOMMENDATIONS

In this work, a novel pixel configuration RGBW, consisting of red (R), green (G), blue (B), and white (W) LEDs, was employed and investigated for color generation. Energy consumption and various hues of new pixels were compared to standard pixels consisting of RGB LEDs. Human perception experiments were conducted in order to study the perceptual difference between the two architectures when colors are generated using RGBW vs. RGB. Various experimental approaches were considered such as spectrometric readings, human perception experiment, and theoretical analysis in order to verify that the hue is maintained with the new architecture. The spectrometer reading has shown that the spectrum of the colors generated using RGB and RGBW are similar. Furthermore, statistics has shown that 44% of test subjects found the colors in gray scale to be the same, whereas 82% and 95% of test subject found low saturated colors and high saturated colors, respectively, to be identical. Theoretical analysis of the new RGBW pixel based on fundamentals of color theory has shown that using RGBW will not change the hue when it replaces RGB. Real life captions were included demonstrating that the colors are almost indistinguishable. Power measurements for an 8x8 pixel LED display has demonstrated power savings, in all cases, using RGBW. The percentage of saved power, however, differed from one case to another, for instance using RGBW as an

alternative achieved up to 49% power savings for gray scale, over 30% power savings for low saturated colors, and up to 12% for high saturated colors. Most colors have witnessed over 30% power savings.

Future research may include:

- Using the white LED in the pixel along with the RGB in order to create a brighter and sharper image.
- Testing efficiency and perception of real video using RGB and RGBW.
- The resolution of the RGBW LED display can improve by studying different LED configurations for pixels such as RGB surrounding the white LED.
- Using the centered triangle configuration of RGBW with a white LED at the center of an equilateral triangle and study its performance against square configuration studied in this thesis.

APPENDIX I

AHDL CODE OF THE SOFTWARE IMPLIMENTATION

```
SUBDESIGN HVsync
(

Clk, q[9..0]                                    :INPUT;
HSyncIn, Hblk, Vs, Vblk, Vcnt[9..0], HBlank8 : OUTPUT;
VBlank8             :OUTPUT;

)
variable

Hsff, Hblank, Vsff, Vblank, Shb, Svb, Shb8, Svb8 :JKFF;
vcount[9..0]                                          :DFF;


begin

Hsff.clk        =       Clk;
Hsff.j          =       q[] == 736;
Hsff.k          =       q[] == 781;

Hblank.clk      =       Clk;
Hblank.j        =       q[] == 0;
Hblank.k        =       q[] == 720;

Shb.clk                 =       Clk;
Shb.j           =       q[] == 360;
Shb.k           =       q[] == 376;

Shb8.clk        =       Clk;
Shb8.j          =       q[] == 362;
Shb8.k          =       q[] == 370;


HSyncIn                 =       !Hsff;
%Hblk           =       Hblank;%
```

```
Hblk            =       Shb;
HBlank8                 =       Shb8;

vcount[].clk    =       Hsff;
if vcount[]     == 525 then
vcount[]                = 0;
else vcount[].d = vcount[].q +1;
end if;

Vsff.clk        =       Hsff;
Vsff.j          =       vcount[] == 495;
Vsff.k          =       vcount[] == 498;

Vblank.clk      =       Hsff;
Vblank.j        =       vcount[] == 0;
Vblank.k        =       vcount[] == 479;

Svb.clk                 =       Hsff;
Svb.j           =       vcount[] == 240;
Svb.k           =       vcount[] == 256;

Svb8.clk                =       Hsff;
Svb8.j          =       vcount[] == 244;
Svb8.k          =       vcount[] == 252;

Vs                      =       Vsff;
%Hblk           =       Vblank;%
Vblk            =       Svb;
VBlank8                 =       Svb8;

Vcnt[]          =       Vcount[];

end;


SUBDESIGN VChbvbGEN
(
        -- {{ALTERA_IO_BEGIN}} DO NOT REMOVE THIS LINE!
        VCclk : INPUT;
        VCHsync : INPUT;
        VCVsync : INPUT;
        VCCblank : OUTPUT;
        VCcnth[9..0] : OUTPUT;
        VCcntv[9..0] : OUTPUT;
        -- {{ALTERA_IO_END}} DO NOT REMOVE THIS LINE!
)
```

```
variable

        cnth[9..0]          :dff;
        cntv[9..0]          :dff;
        blankh              :jkff;
        blankv              :jkff;

begin

        cnth[].clk  =  VCclk;
        cnth[].clrn =  VCHsync;
        cnth[].d    =  cnth[].q +1;

        VCcnth[9..0] =  cnth;

        blankh.clk  =  VCclk;
        blankh.j    =  cnth[] == 362;
        blankh.k    =  cnth[] == 370;



        cntv[].clk  =      VCHsync;
        cntv[].d    =  cntv[].q + 1;
        cntv[].clrn =  VCVsync;

        VCcntv[9..0] =  cntv;

        blankv.clk  =  VCHsync;
        blankv.j    =  cntv[] == 244;
        blankv.k    =  cntv[] == 252;

        VCCblank    =  blankv and blankh;

end;

SUBDESIGN Condotta1
(
        -- {{ALTERA_IO_BEGIN}} DO NOT REMOVE THIS LINE!
        address0 : INPUT;
        address1 : INPUT;
        address2 : INPUT;
        address3 : INPUT;
        address4 : INPUT;
        address5 : INPUT;
        sw17 : INPUT;
        addrout[5..0] : OUTPUT;
```

```
        -- {{ALTERA_IO_END}} DO NOT REMOVE THIS LINE!
)

Begin
if sw17 == 1 then
        addrout[5..0] = address[5..0];
else
        addrout[5..0]  =        56;
end;

--if sw17==1 then
--      addrout[5..0]  =        address[5..0];
--end;

End;


SUBDESIGN EnableGen
(
        -- {{ALTERA_IO_BEGIN}} DO NOT REMOVE THIS LINE!
        HSync : INPUT;
        VSync : INPUT;
        Clk : INPUT;
        Vcnt[9..0] : INPUT;
        q[9..0] : INPUT;
        DPst2rdEn : OUTPUT;
        FIFOrdEn : OUTPUT;
        DPst1wrEn : OUTPUT;
        DPst1rdEn : OUTPUT;
        LEDisp : OUTPUT;
        OEDisp : OUTPUT;
        BitSel[2..0] : OUTPUT;
        -- {{ALTERA_IO_END}} DO NOT REMOVE THIS LINE!
)


variable

counth[9..0], countv[9..0], FIFOrd, delay1, DPst1rd, DPst2rd, LEDispd,OEDispd,
BitSelC[2..0]           :dff;
FIFOrdh, FIFOrdv, DPst1rdh, DPst1rdv, DPst2rdh, DPst2rdv, LEDispdh, LEDispdv,
OEDispdh, OEDispdv      :jkff;


begin
--Main counters
```

```
--counth[].clk  =       Clk;
--counth[].clrn =       HSync;
--counth[].d            =       counth[].q + 1;


--countv[].clk  =       HSync;
--countv[].clrn =       !VSync;
--countv[].d            =       countv[].q + 1;

BitSelC[].clk   =       Clk;

if Vcnt[] >= 1 and Vcnt[] < 3  then
BitSelC[].d = 0;

elsif Vcnt[] >= 3 and Vcnt[] < 6 then
BitSelC[].d = 1;

elsif Vcnt[] >= 6 and Vcnt[] < 11 then
BitSelC[].d = 2;

elsif Vcnt[] >= 11 and Vcnt[] < 20 then
BitSelC[].d = 3;

elsif Vcnt[] >= 20 and Vcnt[] < 37 then
BitSelC[].d = 4;

elsif Vcnt[] >= 37 and Vcnt[] < 71 then
BitSelC[].d = 5;

elsif Vcnt[] >= 71 and Vcnt[] < 139 then
BitSelC[].d = 6;

elsif Vcnt[] >= 139 and Vcnt[] < 273 then
BitSelC[].d = 7;

end if;

BitSel = BitSelC;



-----------------------------
FIFOrdh.clk             =       Clk;
--FIFOrdh.clrn=         HSync;
FIFOrdh.j               =       q[] == 400;
FIFOrdh.k               =       q[] == 464;
```

```
FIFOrdv.clk          =      !HSync;
--FIFOrdv.clrn=      !VSync;
FIFOrdv.j            =      Vcnt[] == 255;
FIFOrdv.k            =      Vcnt[] == 256;

FIFOrd.clk           =      Clk;
FIFOrd.d             =      FIFOrdh and FIFOrdv;

FIFOrdEn             =      FIFOrd;

------------------------------

delay1.clk           =      Clk;
delay1.d             =      FIFOrd;

DPst1wrEn            =      delay1;

------------------------------
DPst1rdh.clk  =     Clk;
--DPst1rdh.clrn      =      HSync;
DPst1rdh.j           =      q[] == 471;
DPst1rdh.k           =      q[] == 599;

DPst1rdv.clk  =     !HSync;
--DPst1rdv.clrn      =      !VSync;
DPst1rdv.j           =      Vcnt[] == 256;
DPst1rdv.k           =      Vcnt[] == 257;

DPst1rd.clk          =      Clk;
DPst1rd.d            =      DPst1rdh and DPst1rdv;

DPst1rdEn            =      DPst1rd;

------------------------------
------------------------------
DPst2rdh.clk  =     Clk;
--DPst2rdh.clrn      =      HSync;
DPst2rdh.j           =      q[] == 1;
DPst2rdh.k           =      q[] == 33;
------------------------------
LEDispdh.clk =      Clk;
--LEDispdh.clrn      =      HSync;
LEDispdh.j           =      q[] == 137;
LEDispdh.k           =      q[] == 138;
------------------------------
OEDispdh.clk =      Clk;
```

```
--LEDispdh.clrn      =      HSync;
OEDispdh.j           =      q[] == 0;
OEDispdh.k           =      q[] == 858;
-------------------------------
-------------------------------

-------------------------------
-------------------------------
--Bit0
-------------------------------
DPst2rdv.clk  =      !HSync;
--DPst2rdv.clrn     =      !VSync;
DPst2rdv.j           =      Vcnt[] == 1;
DPst2rdv.k           =      Vcnt[] == 2;
-------------------------------
LEDispdv.clk =       !HSync;
--LEDispdv.clrn     =      !VSync;
LEDispdv.j           =      Vcnt[] == 1;
LEDispdv.k           =      Vcnt[] == 2;
-------------------------------
OEDispdv.clk =       !HSync;
--LEDispdv.clrn     =      !VSync;
OEDispdv.j           =      Vcnt[] == 2;
OEDispdv.k           =      Vcnt[] == 3;
-------------------------------
-------------------------------


-------------------------------
-------------------------------
--Bit1
-------------------------------
DPst2rdv.clk  =      !HSync;
--DPst2rdv.clrn     =      !VSync;
DPst2rdv.j           =      Vcnt[] == 3;
DPst2rdv.k           =      Vcnt[] == 4;
-------------------------------
LEDispdv.clk =       !HSync;
--LEDispdv.clrn     =      !VSync;
LEDispdv.j           =      Vcnt[] == 3;
LEDispdv.k           =      Vcnt[] == 4;
-------------------------------
OEDispdv.clk =       !HSync;
--LEDispdv.clrn     =      !VSync;
OEDispdv.j           =      Vcnt[] == 4;
OEDispdv.k           =      Vcnt[] == 6;
```

```
--------------------------------
--------------------------------
--Bit2
--------------------------------
DPst2rdv.clk  =      !HSync;
--DPst2rdv.clrn     =      !VSync;
DPst2rdv.j         =      Vcnt[] == 6;
DPst2rdv.k         =      Vcnt[] == 7;
--------------------------------
LEDispdv.clk  =      !HSync;
--LEDispdv.clrn     =      !VSync;
LEDispdv.j         =      Vcnt[] == 6;
LEDispdv.k         =      Vcnt[] == 7;
--------------------------------
OEDispdv.clk  =      !HSync;
--LEDispdv.clrn     =      !VSync;
OEDispdv.j         =      Vcnt[] == 7;
OEDispdv.k         =      Vcnt[] == 11;
--------------------------------
--------------------------------


--------------------------------
--------------------------------
--Bit3
--------------------------------
DPst2rdv.clk  =      !HSync;
--DPst2rdv.clrn     =      !VSync;
DPst2rdv.j         =      Vcnt[] == 11;
DPst2rdv.k         =      Vcnt[] == 12;
--------------------------------
LEDispdv.clk  =      !HSync;
--LEDispdv.clrn     =      !VSync;
LEDispdv.j         =      Vcnt[] == 11;
LEDispdv.k         =      Vcnt[] == 12;
--------------------------------
OEDispdv.clk  =      !HSync;
--LEDispdv.clrn     =      !VSync;
OEDispdv.j         =      Vcnt[] == 12;
OEDispdv.k         =      Vcnt[] == 20;
--------------------------------
--------------------------------
--------------------------------
--------------------------------
--Bit4
--------------------------------
```

```
DPst2rdv.clk  =      !HSync;
--DPst2rdv.clrn      =      !VSync;
DPst2rdv.j           =      Vcnt[] == 20;
DPst2rdv.k           =      Vcnt[] == 21;
--------------------------------
LEDispdv.clk =       !HSync;
--LEDispdv.clrn      =      !VSync;
LEDispdv.j           =      Vcnt[] == 20;
LEDispdv.k           =      Vcnt[] == 21;
--------------------------------
OEDispdv.clk =       !HSync;
--LEDispdv.clrn      =      !VSync;
OEDispdv.j           =      Vcnt[] == 21;
OEDispdv.k           =      Vcnt[] == 37;
--------------------------------
--------------------------------


--------------------------------
--------------------------------
--Bit5
--------------------------------
DPst2rdv.clk  =      !HSync;
--DPst2rdv.clrn      =      !VSync;
DPst2rdv.j           =      Vcnt[] == 37;
DPst2rdv.k           =      Vcnt[] == 38;
--------------------------------
LEDispdv.clk =       !HSync;
--LEDispdv.clrn      =      !VSync;
LEDispdv.j           =      Vcnt[] == 37;
LEDispdv.k           =      Vcnt[] == 38;
--------------------------------
OEDispdv.clk =       !HSync;
--LEDispdv.clrn      =      !VSync;
OEDispdv.j           =      Vcnt[] == 38;
OEDispdv.k           =      Vcnt[] == 71;
--------------------------------
--------------------------------


--------------------------------
--------------------------------
--Bit6
--------------------------------
DPst2rdv.clk  =      !HSync;
--DPst2rdv.clrn      =      !VSync;
```

```
DPst2rdv.j          =       Vcnt[] == 71;
DPst2rdv.k          =       Vcnt[] == 72;
--------------------------------
LEDispdv.clk =      !HSync;
--LEDispdv.clrn     =       !VSync;
LEDispdv.j          =       Vcnt[] == 71;
LEDispdv.k          =       Vcnt[] == 72;
--------------------------------
OEDispdv.clk =      !HSync;
--LEDispdv.clrn     =       !VSync;
OEDispdv.j          =       Vcnt[] == 72;
OEDispdv.k          =       Vcnt[] == 139;
--------------------------------
--------------------------------



--------------------------------
--------------------------------
--Bit7
--------------------------------
DPst2rdv.clk  =     !HSync;
--DPst2rdv.clrn     =       !VSync;
DPst2rdv.j          =       Vcnt[] == 139;
DPst2rdv.k          =       Vcnt[] == 140;
--------------------------------
LEDispdv.clk =      !HSync;
--LEDispdv.clrn     =       !VSync;
LEDispdv.j          =       Vcnt[] == 139;
LEDispdv.k          =       Vcnt[] == 140;
--------------------------------
OEDispdv.clk =      !HSync;
--LEDispdv.clrn     =       !VSync;
OEDispdv.j          =       Vcnt[] == 140;
OEDispdv.k          =       Vcnt[] == 273;
--------------------------------
--------------------------------


------------------------------------------------
DPst2rd.clk         =       Clk;
DPst2rd.d           =       DPst2rdh and DPst2rdv;
DPst2rdEn           =       DPst2rd;

LEDispd.clk         =       Clk;
LEDispd.d           =       LEDispdh and LEDispdv;
LEDisp                      =       LEDispd;
OEDispd.clk         =       Clk;
```

```
OEDispd.d       =       OEDispdh and OEDispdv;
OEDisp                  =       OEDispd;


end;
```

APPENDIX II

BIOMEDICAL IRB – EXPEDITED REVIEW
APPROVAL NOTICE

NOTICE TO ALL RESEARCHERS:

Please be aware that a protocol violation (e.g., failure to submit a modification for any change) of an IRB approved protocol may result in mandatory remedial education, additional audits, re-consenting subjects, researcher probation suspension of any research protocol at issue, suspension of additional existing research protocols, invalidation of all research conducted under the research protocol at issue, and further appropriate consequences as determined by the IRB and the Institutional Officer.

DATE: July 9, 2008

TO: Dr. Rama Venkat, Electrical and Computer Engineering

FROM: Office for the Protection of Research Subjects

RE: Notification of IRB Action by Dr. John Mercer, Chair
Protocol Title: University of Nevada Light Emitting Diode Display Engineering (NV)
Protocol #: 0805-2740

This memorandum is notification that the project referenced above has been reviewed by the UNLV Biomedical Institutional Review Board (IRB) as indicated in regulatory statutes 45 CFR 46. The protocol has been reviewed and approved.

The protocol is approved for a period of one year from the date of IRB approval. The expiration date of this protocol is July 6, 2009. Work on the project may begin as soon as you receive written notification from the Office for the Protection of Research Subjects (OPRS).

PLEASE NOTE:
Attached to this approval notice is the official Informed Consent/Assent (IC/IA) Form for this study. The IC/IA contains an official approval stamp. Only copies of this official IC/IA form may be used when obtaining consent. Please keep the original for your records.

Should there be *any* change to the protocol, it will be necessary to submit a Modification Form through OPRS. No changes may be made to the existing protocol until modifications have been approved by the IRB.

Should the use of human subjects described in this protocol continue beyond July 6, 2009 it would be necessary to submit a Continuing Review Request Form *60 days* before the expiration date.

If you have questions or require any assistance, please contact the Office for the Protection of Research Subjects at OPRSHumanSubjects@unlv.edu or call 895-2794.

APPENDIX III

INFORMED CONSENT

INFORMED CONSENT

Department of Electrical and Computer Engineering

TITLE OF STUDY: University of Nevada Light Emitting Diode Display Engineering (NV)

INVESTIGATOR(S): Dr. Rama Venkat

Contact Phone Number: 895-1094

Purpose of the Study

You are invited to participate in a research study. The purpose of this study is to obtain data "how human beings perceive a variety of colors generated by two methods of LED Display lighting (Ref-Green-Blue (RGB) & Red-Green-Blue-White (RGBW))".

Participants

You are being asked to participate in the study because the quality of display is a perceived characteristics and hence data based on human perception is absolutely necessary. If you know that you are color-blind, please let us know as the research involves viewing various colors generated by two different technologies we are comparing.

Procedures

If you volunteer to participate in this study, you will be asked to do the following:

- Sit 5 feet away from a 6 inch x 6 inch white screen where same color from two different technologies and sometimes the same technology will be displayed. Some of you will be assigned to the control group and others to experimental group. You will not know which group you belong to. Only the researcher will know.
- Observe the color and record on a form if the colors are:
  - (i) identical
  - (ii) almost the same
  - (iii) not at all the same.
- If you are not sure, then you can ask the researcher to repeat the procedure for another viewing of

the colors.

- If you are uncomfortable with viewing the colors or any other part of the experimentation, you can withdraw by letting the researcher know.

Benefits of Participation

There may not be direct benefits to you as a participant in this study. However, we hope to learn if the new technology we are developing, which we know saves energy, provides the same quality of colors in a display.

Risks of Participation

There are risks involved in all research studies. This study may include only minimal risks. State the level of anticipated risks (i.e. you may become uncomfortable when answering some questions). Te study involves minimal risk only as the subjects will be viewing colors of same brightness as they see in real life. At any time during the experimentation, if the subject is uncomfortable and does not want to continue, he/she can withdraw by letting the researcher know.

Cost /Compensation

There will not be financial cost to you to participate in this study. The study will take 30 minutes of your time. You will not be compensated for your time.

Contact Information

If you have any questions or concerns about the study, you may contact Dr. Rama Venkat at 895 1094. For questions regarding the rights of research subjects, any complaints or comments regarding the manner in which the study is being conducted you may contact the UNLV Office for the Protection of Research Subjects at 702-895-2794.

Voluntary Participation

Your participation in this study is voluntary. You may refuse to participate in this study or in any part of this study. You may withdraw at any time without prejudice to your relations with the university. You are encouraged to ask questions about this study at the beginning or any time during the research study.

Confidentiality

All information gathered in this study will be kept completely confidential. No reference will be made in written or oral materials that could link you to this study. All records will be stored in a locked facility at UNLV for at least 3 years after completion of the study. After the storage time the information gathered will be deleted.

Participant Consent:

I have read the above information and agree to participate in this study. I am at least 18 years of age. A copy of this form has been given to me.

_____ _____

Signature of Participant Date

_____

Participant Name (Please Print)

Participant Note: Please do not sign this document if the Approval Stamp is missing or is expired.

APPENDIX IV

HUMAN EXPERIMENT QUESTIONNAIRE

Questionnaire for the Subjects

Part 1

Circle "Yes" or "No" for the following questions.

1.	Are you 18 years or older (adult)?	Yes	No
2.	Are you color-blind (if know)?	Yes	No
3.	Are you sensitive to any colors?	Yes	No
4.	Are you sensitive to normal day-to-day light intensity?	Yes	No

Part 2

For each pair of colors that you are asked to view, please circle the appropriate answer of the three choices. If you are not sure, please ask the researcher to repeat the experiment.

Pair 1

Describe color 1: _____

Describe color 2: _____

Compare the colors:

a. Identical
b. Almost the same
c. Not at all the same
d. Unsure

Pair 2

Describe color 1: _____

Describe color 2: _____

Compare the colors:

a. Identical
b. Almost the same
c. Not at all the same
d. Unsure

Pair 3

Describe color 1: _____

Describe color 2: _____

Compare the colors:

a. Identical
b. Almost the same
c. Not at all the same
d. Unsure

Pair 4
Describe color 1: _____
Describe color 2: _____
Compare the colors:
a. Identical
b. Almost the same
c. Not at all the same
d. Unsure

Pair 5
Describe color 1: _____
Describe color 2: _____
Compare the colors:
a. Identical
b. Almost the same
c. Not at all the same
d. Unsure

Pair 6
Describe color 1: _____
Describe color 2: _____
Compare the colors:
a. Identical
b. Almost the same
c. Not at all the same
d. Unsure

Pair 7
Describe color 1: _____
Describe color 2: _____
Compare the colors:
a. Identical
b. Almost the same
c. Not at all the same
d. Unsure

Pair 8
Describe color 1: _____
Describe color 2: _____

Compare the colors:

a. Identical
b. Almost the same
c. Not at all the same
d. Unsure

Pair 9

Describe color 1: _____
Describe color 2: _____
Compare the colors:

a. Identical
b. Almost the same
c. Not at all the same
d. Unsure

Pair 10

Describe color 1: _____
Describe color 2: _____
Compare the colors:

a. Identical
b. Almost the same
c. Not at all the same
d. Unsure

Pair 11

Describe color 1: _____
Describe color 2: _____
Compare the colors:

a. Identical
b. Almost the same
c. Not at all the same
d. Unsure

Pair 12

Describe color 1: _____
Describe color 2: _____
Compare the colors:

a. Identical
b. Almost the same
c. Not at all the same
d. Unsure

BIBLIOGRAPHY

[1] Souk, J.H., Jongseo Lee, "Recent Picture Quality Enhancement Technology Based on Human Visual Perception in LCD TVs", *Journal of Display Technology,* Volume 3, Issue 4, Pages: 371 - 376, Dec,2007.

[2] http://www.audioholics.com/education/display-formatstechnology/displaytechnologiesguide-lcd-plasma-dlp-lcosd-ila-crt

[3] http://www.plasma.com/classroom/LCD_tv_versus_plasma_tv.htm

[4] http://www.unbeatable.co.uk/buyingguides/PlasmaVsLcd-Televisions/32.html

[5] Grantham K. H. Pang, Chi-Ho Chan, and Thomas T. O. Kwan , "Tricolor Light-Emitting Diode Dot Matrix Display System with Audio Output" *IEEE Transaction on Industry Applications*, Volume. 37, No. 2, March/April 2001.

[6] Kohrou Takahashi, Nobuyuki Tadokoro and Satoshi Takeuchi, "High Density LED Display Panel on Silicon Microreflector and Integrated Circuit", *Electronic Manufacturing Technology Symposium18th IEEE/CPMT International,* Page(s): 272-275, December 1995.

[7] R. E. Brown, "LED Displays Past, Present, Future", IEEE Transactions on Consumer Electronics, Vol. CE-24, No. 3, August 1978.

[8] J. Wilson, J.F.B Hawkes, *Optoelectronics*, Prentice Hall, UK, 1989.

[9] http://www.lctecdisplays.com/TN_LCD_technology_side_2.asp

[10] http://www.mc2.chalmers.se/pl/lc/engelska/applications/Displays.html

[11] htpp://www.wtec.org/loyola/dsply_jp/c5_s2.html

[12] Chun-Ho Chen, Han-Ping D. Shieh, "Effects of Backlight Profiles on Perceived Image Quality for High Dynamic Range LCDs", *Journal of Display Technology*, Volume. 4, No. 2, June 2008.

[13] http://compreviews.about.com/od/multimedia/a/LCDSpecs.htm

[14] http://techgage.com/articles/displays/lcd-monitors/

[15] http://www.businessweek.com/magazine/content/08_30/b4093044731823.htm

[16] http://www.ece.uiuc.edu/alumni/w02-03/plasma_history.html

[17] http://www.plasma-display-composition.svg

[18] Y. Kim, S. Park, "Simple driving waveform and circuit for plasma display", *Electronics Letters*, Volume 44, Issue 9, Page(s):572 - 572 April 24, 2008.

[19] Dong-Myung Lee, Dong-Seok Hyun, "A New Driving Scheme for Plasma TVs Using Multi-Functional Gate Driver", *IEEE Transactions on Consumer Electronics,* Volume 53, Issue 4, Page(s):1553 – 1559, November 2007

[20] http://www.consumersearch.com/www/electronics/plasma-tv/

[21] http://palami.eu/screen-adv.html

[22] http://www.neutekled.com/cms/index.php?option=com_content&task=view&id=27-& Itemid =102

[23] http://www.coema.org.cn/E_LEDdisplay.htm

[24] Wyszecki & Stiles, *Color Science*, John Wiley, USA, 1967.

[25] http://www.northdevonhealth.nhs.uk/patientinformation/ophthalmology/understanding_ c ataracts.htm.

[26] http://www.hamwaves.com/antennas/diel-rod.html.

[27] http://www.hyperphysics.phyastr.gsu.edu/hbase/vision/colper.html

[28] http://www.LightEmittingDiodes.org

[29] Williamson, Samuel J., *Light and Color in nature and art*, John Wiley, Canada.

[30] Marko Tkalcic, Jurij F. Tasic, "Colour spaces - perceptual, historical and applicational background", *EUROCON 2003. Computer as a Tool. The IEEE Region 8,*Volume 1, page(s): 304- 308, September 2003

[31] http://www.mathworks.com

[32] Gaurav Sharma, *Digital Color Imaging Handbook*, CRC Press, 2003

[33] http://www.cit.dixie.edu/vt/reading/gamuts.asp

[34] http://www.nichia.com

[35] Muthu, S., Schuurmans, F.J., Pashley, M.D. "Red, green, and blue LED based white light generation: issues and control" *Industry Applications Conference*, Volume 1, Issue Pages: 327 – 333, 2002.

[36] S.Muthu, F. Schuurmans, and M. Pashley, "Red, Green and Blue LEDs for white light illumination", *IEEE journal on selected topics in quatum electronics,*pp. Vol. 8, No. 2, March/April 2002.

[37] STMicroelectronics, STP08CDC596 An 8-bit constant current LED sink driver with full outputs detection datasheet.

[38] Altera Corporation, DE2 Development and Education Board, User Manual version 1.4

[39] http://www.eecg.toronto.edu/~tm4/rgbout.html

[40] http://web.mit.edu/6.111/www/s2004/NEWKIT/vga.shtml

VITA

Graduate College
University of Nevada, Las Vegas

Neveen Shlayan

Local Address:
11101 Calder Ave
Las Vegas, NV 89144

Degrees:
Bachelor of Science, Electrical Engineering, 2006
University of Nevada, Las Vegas

Special Honors and Awards:
Tau Beta Pi, Engineering honor society
Cum Laude, Fall 2006
Best Engineering project award, Fall 2006
Outstanding ECE senior student, Fall 2006
Dean's List award

Publications:
A Novel RGBW Pixel for LED Displays, icseng,pp.407-411, 2008 19th International Conference on Systems Engineering, 2008

Review of Packet Switching Technologies for Future NoC, icseng,pp.306-311, 2008 19th International Conference on Systems Engineering, 2008

Thesis Title: A Novel RGBW Pixel for LED Displays

Thesis Examination Committee:
Chairperson, Dr. Rama Venkat, Ph. D.
Committee Member, Dr. Paolo Ginnobi, Ph. D.
Committee Member, Dr. Emma Regentova, Ph. D.
Graduate Faculty Representative, Dr. Mohamed Trabia, Ph. D.